Identification and Characterization of O-mannosylated Proteins

Inaugural-Dissertation

zur

Erlangung des Doktorgrades

der Mathematisch-Naturwissenschaftlichen Fakultät

der Universität zu Köln

vorgelegt von

Sandra Pacharra

geb. Söte

aus Essen

1. Gutachter: Prof. Dr. M. Paulsson

2. Gutachter: Prof. Dr. A. Berkessel

Prüfungsvorsitzender: Prof. Dr. R. Strey

Tag der mündlichen Prüfung: 17.05.2013

The present research work was carried out under the supervision and the direction of Dr. Isabelle Breloy at the Institute of Biochemistry II, Medical Faculty, University of Cologne, Germany, from November 2009 to March 2013.

I Index of Contents

I INDEX OF CONTENTS I

I.I INDEX OF FIGURES II

I.II INDEX OF TABLES IV

I.III LIST OF ABBREVIATIONS V

I.III.I Monosaccharides – abbreviations and symbols VIII

I.III.II Amino acids – three-letter and one-letter abbreviations IX

II ABSTRACT X

II ZUSAMMENFASSUNG XI

1 INTRODUCTION 1

1.1 PROTEIN GLYCOSYLATION 1

1.1.1 N-Glycosylation 3

1.1.2 O-Glycosylation 4

1.1.3 Glycosaminoglycan modification 5

1.2 *O*-MANNOSYLATION 7

1.2.1 Biosynthesis and structure 7

1.2.2 Elongation of the core mannose 9

1.2.3 O-Mannosylated proteins 9

1.2.4 Initiation of O-mannosylation 10

1.3 PATHOLOGY OF *O*-MANNOSYLATION DEFECTS 10

1.3.1 α-Dystroglycan 10

1.3.2 Dystroglycanopathy 12

1.4 BRAIN EXTRACELLULAR MATRIX 14

1.4.1 Lecticans 15

1.4.2 Neurofascin 17

1.4 AIM OF THIS PROJECT 18

2 MATERIALS AND METHODS 19

2.1 MATERIALS 19

2.1.1 Buffers and Solutions 19

2.1.2 Protein Standards for Electrophoresis 21

2.1.3 Antibodies 21

2.2 METHODS 22

2.2.1 Purification of O-mannosylated proteins 22

2.2.2 Protein identification 24

2.2.3 Analysis of O-glycans and glycopeptides 25

2.2.4 Recombinant expression and purification of neurocan 26

3 RESULTS 27

3.1 Analysis of mouse and calf brain 27
3.1.1 O-Glycome of mouse and calf brain 27
3.1.2 Fractionation of mouse brain proteins 29
3.1.3 Summary 32
3.2 *O*-Mannosylation on neurofascin 34
3.2.1 Purification of neurofascin isoform 186 from mouse brain 34
3.2.2 O-Mannosylation of neurofascin 186 35
3.2.3 Glycopeptide analysis of neurofascin 186 38
3.2.4 Conclusion 42
3.3 *O*-Mannosylation of lecticans 44
3.3.1 O-Glycan analysis of lecticans from mouse brain 44
3.3.2 Recombinant expression of neurocan 46
3.3.3 O-Glycan analysis of calf brain lecticans 47
3.3.4 Conclusion 53

4 DISCUSSION AND OUTLOOK 55

4.1 Comparability of murine and bovine *O*-mannosylation to human protein modification 55
4.2 Implications for dystroglycanopathy 56
4.3 Initiation of mammalian *O*-mannosylation 57
4.4 Unresolved questions 58

5 REFERENCES 61

6 APPENDIX 72

ERKLÄRUNG 90

I.I Index of figures

Figure 1: Major classes of vertebrate glycan structures. 2
Figure 2: Schematic view of the different glycosaminoglycan types. 6
Figure 3: Schematic representation of the *O*-mannosylation pathway of yeast (left) and mammals (right). 8
Figure 4: Schematic diagram of *O*-mannosyl glycans found in mammals. 8
Figure 5: Schematic view of the dystrophin-glycoprotein complex and its interaction partners. 11
Figure 6: Schematic representation of the enzymes involved in the *O*-mannosylation pathway. 13
Figure 7: Schematic representation of the most common CNS CSPGs. 16
Figure 8: Schematic view of the domain composition of neurofascin. 17
Figure 9: *O*-Glycome of mouse brain. 28
Figure 10: Mouse brain glycoprotein fractionation using gel permeation chromatography. 31
Figure 11: Fractionation scheme for mouse brain. 33
Figure 12: BLAST analysis of the *cis*-controlling peptide. 34

FIGURE 13: WESTERN BLOT OF WHOLE MOUSE BRAIN LYSATE (MB). 34
FIGURE 14: *O*-GLYCOME OF SAMPLE F18 (EXPERIMENT A)..... 37
FIGURE 15: FRAGMENTATION SPECTRUM (MS/MS) OF THE *O*-MANNOSE DERIVED SIGNAL AT M/Z = 1099.6.. 38
FIGURE 16: ESI-MS3 OF THE *O*-MANNOSYLATED AND MUCIN-TYPE *O*-GLYCOSYLATED GLYCOPEPTIDE NNSPITD FROM NEUROFASCIN. 41
FIGURE 17: SCHEMATIC VIEW OF THE DOMAIN COMPOSITION OF NEUROFASCIN 186. 43
FIGURE 18: *O*-GLYCOPROFILE OF HYALURONAN AFFINITY-ISOLATED MOUSE BRAIN PROTEINS. 45
FIGURE 19: PURIFICATION OF RECOMBINANT NEUROCAN. 46
FIGURE 20: ANALYSIS OF RECOMBINANT NEUROCAN. 47
FIGURE 21: MALDI-MS OF PERMETHYLATED GLYCAN ALDITOLS DERIVED FROM ISOELECTRIC FOCUSING FRACTION F1 OF CALF BRAIN GLYCOPROTEINS. 48
FIGURE 22: ANALYSIS OF THE LECTICAN-CONTAINING FRACTION F18 FROM EXPERIMENT (B). 51
FIGURE 23: ANALYSIS OF FRACTION F16 FROM EXPERIMENT (B). 53
FIGURE 24: SCHEMATIC VIEW OF THE LOCALIZATION OF *O*-MANNOSYLATED PROTEINS ON A NEURON. 60
FIGURE 25: REACTION SCHEME FOR THE RELEASE OF *O*-GLYCANS BY B-ELIMINATION. 73
FIGURE 26: COMPARISON BETWEEN THE *O*-GLYCOME OF CALF (UPPER PANEL) AND MOUSE BRAIN (LOWER PANEL). 73
FIGURE 27: COMPARISON BETWEEN THE *O*-GLYCANS PRESENT IN THE WGA FLOW-THROUGH (UNBOUND PROTEINS, LOWER PANEL) AND THE ELUTED GLYCOPROTEINS (UPPER PANEL). 74
FIGURE 28: SILVER-STAINED SDS-PAGE GELS OF WGA FLOW-THROUGH (FT) AND ELUATE (E)..... 74
FIGURE 29: SDS-PAGE GEL OF SEVERAL PROTEIN FRACTIONS GENERATED BY PREPARATIVE SDS-PAGE (STAINED WITH COOMASSIE BRILLIANT BLUE). 75
FIGURE 30: GPC FRACTIONATION OF MOUSE BRAIN GLYCOPROTEINS. 77
FIGURE 31: PROTEIN FRACTIONS GENERATED BY PREPARATIVE SDS-PAGE OF MOUSE BRAIN GLYCOPROTEINS AFTER GPC. 77
FIGURE 32: *O*-GLYCAN ANALYSIS OF PERMETHYLATED *O*-GLYCAN ALDITOLS FROM MOUSE NCAM1. 78
FIGURE 33: ESI-MS/MS (CID MODE) OF A GLYCOPEPTIDE FROM NEUROFASCIN. 79
FIGURE 34: ESI-MS/MS OF THE *O*-MANNOSYLATED GLYCOPEPTIDE RSGTLVINFR FROM NEUROFASCIN MODIFIED WITH $NEUACHEX_2HEXNAC$ (M/Z 2048.8). 80
FIGURE 35: SILVER-STAINED SDS-PAGE GELS OF THE MOUSE BRAIN GLYCOPROTEIN FRACTIONATION. 80
FIGURE 36: ANALYSIS OF FRACTION F24 FROM PREPARATIVE GEL ELECTROPHORESIS OF MOUSE BRAIN GLYCOPROTEINS. 81
FIGURE 37: MALDI-MS/MS OF THE PERMETHYLATED OLIGOSACCHARIDE WITH A PRECURSOR MASS OF 1910.0. 81
FIGURE 38: ANALYSIS OF THE ELUATE FROM TENASCIN-R SPECIFIC AFFINITY CHROMATOGRAPHY. 82
FIGURE 39: FRACTIONATION SCHEME FOR CALF BRAIN. 83
FIGURE 40: CALF BRAIN-DERIVED PROTEIN FRACTIONS GENERATED BY PREPARATIVE GEL ELECTROPHORESIS. 84
FIGURE 41: ANALYSIS OF THE MAG-CONTAINING FRACTION F14 FROM EXPERIMENT (A). 85
FIGURE 42: ANALYSIS OF THE LECTICAN-CONTAINING FRACTION F11 FROM EXPERIMENT (A). 86
FIGURE 43: ANALYSIS OF THE LECTICAN-CONTAINING FRACTION F13 FROM EXPERIMENT (A). 87

I.II Index of tables

TABLE 1: SEQUENTIAL EXTRACTION OF MOUSE BRAIN PROTEINS. 30
TABLE 2: PROTEIN IDENTIFICATION BASED ON MASCOT RESULTS OF PROTEIN FRACTION F15 (B). 40
TABLE 3: PROTEIN IDENTIFICATION OF HYALURONAN AFFINITY-ISOLATED MOUSE BRAIN PROTEINS. 45
TABLE 4: PROTEIN IDENTIFICATION OF ISOELECTRIC FOCUSING FRACTION F1 OF CALF BRAIN GLYCOPROTEINS. 49
TABLE 5: PROTEIN IDENTIFICATION BASED ON MASCOT RESULTS OF PROTEIN FRACTION F16 (EXPERIMENT B). 52
TABLE 6: SUMMARY OF ALL MASS-TO-CHARGE (M/Z) VALUES AND THEIR CORRESPONDING *O*-GLYCAN COMPOSITION OBSERVED BY MALDI-MS ANALYSIS OF PERMETHYLATED OLIGOSACCHARIDES. 72
TABLE 7: SUMMARY OF PROTEIN SIZE AND *O*-MANNOSE CONTENT OF THE FRACTIONS GENERATED BY PREPARATIVE SDS-PAGE. 75
TABLE 8: PROTEIN IDENTIFICATION OF THE GEL BAND AT 190 KDA ORIGINATING FROM F21. 76
TABLE 9: BLAST SEARCH FOR PEPTIDES SIMILAR TO THE *CIS*-CONTROLLING PEPTIDE OF A-DG. 76
TABLE 10: PROTEIN IDENTIFICATION OF THE NEUROFASCIN-CONTAINING FRACTION USED FOR ESI-MS/MS OF THE CID MODE. 79
TABLE 11: PROTEIN IDENTIFICATION OF THE ELUATE FROM TENASCIN-R SPECIFIC AFFINITY CHROMATOGRAPHY. 82
TABLE 12: SUMMARY OF LECTICAN-CONTAINING CALF BRAIN FRACTIONS FROM EXPERIMENTS (A) AND (B). .. 84
TABLE 13: PROTEIN IDENTIFICATION BASED ON MASCOT SCORE OF THE LECTICAN-CONTAINING FRACTION F11 FROM EXPERIMENT (A). 86
TABLE 14: SUMMARY OF HUMAN PHENOTYPES OF DYSTROGLYCANOPATHIES AND PHENOTYPES OF THE RESPECTIVE KNOCKOUT IN MICE. 88
TABLE 15: SUMMARY OF CHARACTERISTICS OF PREVIOUSLY KNOWN *O*-MANNOSYLATED PROTEINS. 88
TABLE 16: SUMMARY OF CHARACTERISTICS OF NEWLY IDENTIFIED *O*-MANNOSYLATED PROTEINS. 89

I.III List of Abbreviations

AIS	Axon Initial Segment
ALG	Asparagine-Linked Glycosylation
BLAST	Basic Local Alignment Search Tool
CAM	Cell Adhesion Molecule
CD24	Cluster of Differentiation 24
CDG	Congenital Disorders of Glycosylation
Chase	Chondroitinase ABC
CID	Collision Induced Dissociation
CMD	Congenital Muscular Dystrophy
CNS	Central Nervous System
CS	Chondroitin Sulfate
Da	Dalton
DAG1	Dystrophin-Associated Glycoprotein 1
DG	DystroGlycan
DGC	Dystrophin-Glycoprotein Complex
Dol-P-Man	DolichylPhosphate Mannose
DPM 2/3	Dolichyl-Phosphate Mannosyltransferase polypeptide 2/3
DS	Dermatan Sulfate
EBNA	Epstein Barr virus Nuclear Antigen
ECM	ExtraCellular Matrix
ER	Endoplasmic Reticulum
ESI	ElectroSpray Ionization
FCMD	Fukuyama Congenital Muscular Dystrophy
FKRP	FuKutin-Related Protein
GAG	GlycosAminoGlycan
GPC	Gel Permeation Chromatography

GPI	GlycosylPhosphatidylInositol
HA	Hyaluronan
HEK	Human Embryonic Kidney
HNK-1	Human Natural Killer-1 epitope
HS	Heparan Sulfate
IEF	IsoElectric Focusing
ISPD	IsoPrenoid Synthase Domain containing protein
KS	Keratan Sulfate
LC-MS	Liquid Chromatography coupled Mass Spectrometry
LCMV	Lymphocytic ChorioMeningitis Virus
LFV	Lassa Fever Virus
LGMD	Limb-Girdle Muscular Dystrophy
m/z	mass-to-charge
MAG	Myelin-Associated Glycoprotein
MALDI	Matrix-Assisted Laser Desorption Ionization
MDC1C/D	Merosin-Deficient Congenital muscular dystrophy type 1C/D
MEB	Muscle-Eye-Brain disease
MS	Mass Spectrometry
MS/MS or MS2	Multistage Tandem Mass Spectrometry (2 stages)
MS3	Multistage Tandem Mass Spectrometry (3 stages)
n. d.	not determined
NC	NeuroCan
NCAM	Neural Cell Adhesion Molecule
NF	NeuroFascin
OST	OligoSaccharyl Transferase
P	Phosphate
PAGE	PolyAcrylamid GelElectrophoresis

PBS	Phosphate Buffered Saline
PMT	Protein MannosylTransferase
PNN	PeriNeuronal Net
POMGnT1	Protein *O*-Mannose-β-1,2-*N*-acetylGlucosaminyl Transferase 1
POMT1/2	Protein *O*-MannosylTransferase 1/2
ppGalNAcT	PolyPeptide-*N*-AcetylGalactosaminylTransferase
RNase	RiboNuclease
RPTP	Receptor-type Protein Tyrosine Phosphatase
SDS	Sodium Dodecyl Sulfate
TOF	Time Of Flight
Tris	Tris(hydroxymethyl)aminomethane
TrisHCl	Tris(hydroxymethyl)aminomethane hydrochloride
WGA	Wheat Germ Agglutinin
WWS	Walker-Warburg Syndrome

I.III.I Monosaccharides – abbreviations and symbols

Hexose (general)	Hex	
Galactose	Gal	
Glucose	Glc	
Mannose	Man	
N-Acetylhexosamine (general)	HexNAc	
N-Acetylgalactosamine	GalNAc	
N-Acetylglucosamine	GlcNAc	
Sialic acid (general)	SA	
N-acetylneuraminic acid	NeuAc	
N-glycolylneuraminic acid	NeuGc	
Fucose	Fuc	
Glucuronic acid	GlcA	
Iduronic acid	IdoA	
Xylose	Xyl	

I.III.II Amino acids – three-letter and one-letter abbreviations

Alanine	Ala	A
Arginine	Arg	R
Asparagine	Asn	N
Aspartic acid	Asp	D
Cysteine	Cys	C
Glutamic acid	Glu	E
Glutamine	Gln	Q
Glycine	Gly	G
Histidine	His	H
Isoleucine	Ile	I
Leucine	Leu	L
Lysine	Lys	K
Methionine	Met	M
Phenylalanine	Phe	F
Proline	Pro	P
Serine	Ser	S
Threonine	Thr	T
Tryptophan	Trp	W
Tyrosine	Tyr	Y
Valine	Val	V
Hydroxylysine	Hyl	
Hydroxyproline	Hyp	

II Abstract

In mammals the *O*-mannosylation is a rare protein modification found only on proteins from muscles, brain and peripheral nerves. Although increased levels were detected in brain tissue only a few proteins have been identified to carry *O*-mannosyl glycans so far. However, their *O*-mannosylation does not account for the high amount present in brain. In humans defects in the *O*-mannosylation pathway lead to severe malformations of muscles, eyes and brain revealing the importance of this modification. The pathogenic mechanism of these diseases, called dystroglycanopathies, was only analyzed for α-dystroglycan in more detail whose defective glycosylation can explain the muscle but not the brain phenotype.

In this work new *O*-mannosylated proteins were identified in mammalian brain using an unbiased proteomics approach. Neurofascin isoform 186 from mouse brain was shown to carry *O*-mannosyl glycans as well as the lecticans brevican, neurocan and versican from murine and bovine brain. Thus, the *O*-mannosylation was shown to be similar among different mammalian species. Since the lecticans are highly expressed in brain, finally the high amount of *O*-mannosylation in brain can be explained. In addition, new insights into the pathogenic mechanism of dystroglycanopathies were gained. Because neurofascin and the lecticans play important roles in the stabilization of the extracellular matrix around neurons and in the establishment of specialized microdomains impairment of their functions by a defective *O*-mannosylation might explain the brain-specific symptoms.

II Zusammenfassung

Die *O*-Mannosylierung stellt in Säugetieren eine seltene Proteinmodifikation dar, welche bisher nur auf Proteinen aus Muskeln, Gehirn und peripherem Nervengewebe gefunden wurde. Obwohl im Gehirn größere Mengen der *O*-Mannoseglykane nachgewiesen wurden, konnten bisher nur wenige *O*-mannosylierte Proteine identifiziert werden. Deren *O*-Mannose-Modifikation kann den hohen Anteil im Gehirn nicht erklären. Im Menschen führen Fehler in der Biosynthese der *O*-Mannosylierung zu schwerwiegenden Fehlbildungen der Muskeln, der Augen und des Gehirns, was die Wichtigkeit dieser Modifizierung verdeutlicht. Der genaue Krankheits-mechanismus, welcher den Dystroglykanopathien zugrunde liegt, wurde bisher nur anhand von α-Dystroglykan näher untersucht. Dessen fehlerhafte Glykosylierung kann den Muskel- nicht aber den Gehirn-Phänotyp erklären.

In der vorliegenden Arbeit wurden mittels eines unvoreingenommenen Proteinfraktionierungsverfahrens weitere *O*-mannosylierte Proteine aus Säugetiergehirn identifiziert. Dabei wurde die *O*-Mannosylierung sowohl auf der Neurofaszin-Spleißvariante 186 aus Maushirn als auch auf den Lektikanen Brevikan, Neurokan und Versikan aus Maus- bzw. Rinderhirn gefunden. Auf diese Weise konnte gezeigt werden, dass die *O*-Mannose-Modifikation sich in den verschiedenen Säugetieren ähnelt. Da die Lektikane im Gehirn in großen Mengen exprimiert werden, kann mit deren Modifikation nun auch der insgesamt hohe Anteil der *O*-Mannose-Glykane im Gehirn erklärt werden. Außerdem konnten neue Einblicke in den Mechanismus gewonnen werden, welcher den Dystroglykanopathien zugrunde liegt. Da Neurofaszin und die Lektikane wichtige Funktionen in der Stabilisierung der extrazellulären Matrix rund um Neuronen und in der Etablierung spezialisierter Mikrodomänen spielen könnte eine Beeinträchtigung ihrer Funktion durch eine fehlende *O*-Mannosylierung die Gehirn-spezifischen Krankheitssymptome erklären.

1 Introduction

1.1 Protein glycosylation

Glycosylation is the most common and at the same time the most complex posttranslational modification of proteins (Wopereis *et al.*, 2006). It is thought that over 50 percent of all proteins are modified with a variety of different glycan structures (Apweiler *et al.*, 1999) which vary greatly depending on the species, tissue, developmental state and physiological condition. The importance of glycosylation becomes apparent in the fact that one to two percent of all human genes encode enzymes involved in protein glycosylation (Brooks, 2009).

The glycan moieties are transferred onto the protein by specialized glycosyltransferases which utilize nucleotide or lipid activated sugars as donor substrates (Moremen *et al.*, 2012). Most of these enzymes are located in the rough endoplasmic reticulum (ER) and the Golgi apparatus which is why mainly secretory proteins are glycosylated. These are proteins that are transferred through the secretory pathway to the cell surface where they get exported or anchored to the plasma membrane or the extracellular matrix (ECM) (Lehle *et al.*, 2006).

In mammals ten different monosaccharide building blocks are utilized for the generation of linear or branched glycan chains consisting of two to several hundred sugar units (Brooks, 2004). Not all possible structures occur in nature because of (a) the sequential action of glycosyltransferases during the maturation of a protein on its way from the ER via the Golgi to the cell surface and (b) the competition between multiple enzymes. Still glycans are highly diverse (Spiro, 2002). Since not every potential glycosylation site of a protein is modified and different structures can be attached to the same site of glycoprotein molecules microheterogeneity is observed (Brooks, 2004). With this high grade of diversity glycosylation leads to a further magnitude of complexity in biological macromolecules (Lommel & Strahl, 2009).

The ten monosaccharides used in mammalian glycosylation are fucose (Fuc), galactose (Gal), glucose (Glc), *N*-acetylgalactosamine (GalNAc), *N*-acetyl-glucosamine (GlcNAc), glucuronic acid (GlcA), iduronic acid (IdoA), mannose (Man), sialic acid (SA) and xylose (Xyl). These are linked to the protein by four different linkage types depicted in Figure 1 (Moremen *et al.*, 2012). In *N*-glycosylation (see 1.1.1) the glycan is attached via an amide bond to asparagine (Asn) side chains while in *O*-glycosylation (detailed description in 1.1.2) the saccharides are

glycosidically linked to hydroxyl groups of amino acid side chains. Much more uncommon is the *C*-mannosylation in which Man is bound to tryptophan by a C-C linkage (Löffler *et al.*, 1996). Alternatively, glycans can act as a linker between the protein backbone and the glycosylphosphatidylinositol (GPI) anchor.

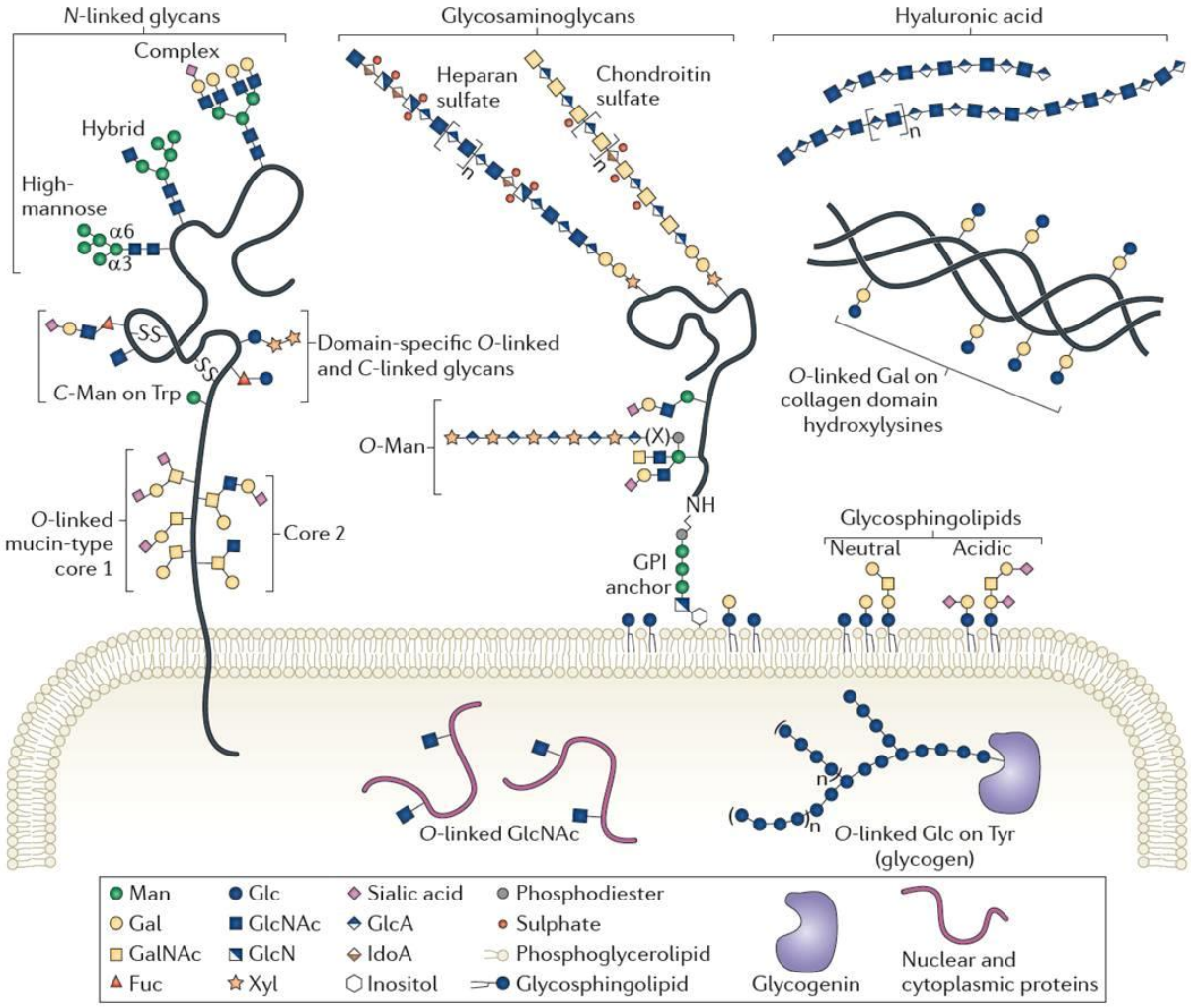

Figure 1: Major classes of vertebrate glycan structures. Depicted are the three classes of *N*-linked glycans: high-mannose-, complex- and hybrid-type and the seven classes of *O*-linked glycans: mucin-type, *O*-Man, *O*-Gal, *O*-GlcNAc, *O*-Glc, *O*-Fuc and the glycosaminoglycan modification. In addition, *C*-mannosylation and GPI-anchor modification are shown. From (Moremen *et al.*, 2012).

For a long time the functional importance of protein glycosylation remained poorly understood but eventually it became evident that the lack of individual glycosyltransferases can cause severe congenital defects (Lehle *et al.*, 2006). Because of their ubiquitous and complex nature the biological functions of glycans are highly diverse and can range from subtle roles to those that are crucial for development, growth and function of an organism (Varki & Lowe, 2009). Glycans have structural and modulatory functions, for example support of protein folding,

protection against degradation and enhancement of hydrophilicity. Also, they act as recognition moieties in protein/protein interactions and thereby they facilitate cell/cell and cell/matrix interactions, fertilization and signaling (Wopereis *et al.*, 2006). Intracellularly, dynamic GlcNAc modification serves as a regulatory switch similar to phosphorylation thereby influencing transcriptional regulation, proteasome-mediated protein degradation and cellular stress signaling. Glycosylation plays a role in viral and bacterial infection since these pathogens sometimes recognize and bind to glycan epitopes (Nizet & Esko, 2009). On the one hand changes in protein glycosylation lead to a variety of diseases, for example to dystroglycanopathies (detailed description in 1.3.2), on the other hand glycosylation changes arise from other diseases, for example from cancer (Brooks, 2009).
All in all the variable and dynamic nature of glycosylation provides a powerful way to generate biological diversity and complexity beyond the genetic code.

1.1.1 *N*-Glycosylation

The Asn-linked glycosylation is the most prevalent form of a glycan-protein bond (Spiro, 2002). Because of its conserved ER and Golgi located biosynthetic pathway *N*-glycosylation is found only on secreted and membrane-bound proteins. Ovalbumin was the first described *N*-glycosylated protein (Johansen *et al.*, 1961) but nowadays many proteins are known including plasma proteins, hormones, enzymes, cell surface receptors and immunoglobulins.
In eukaryotes the synthesis of *N*-glycans starts with the assembly of a glycan core ($Glc_3Man_9GlcNAc_2$) onto a lipid anchor at the cytosolic side of the ER membrane. This process is referred to as the asparagine-linked glycosylation (ALG) pathway (Burda & Aebi, 1999). After the re-orientation to the luminal side of the ER the oligosaccharide is transferred to Asn side chains of the nascent protein by the multi subunit enzyme oligosaccharyl transferase (OST) (Moremen *et al.*, 2012). Mostly Asn residues in the consensus sequence Asn-Xaa-Ser/Thr (with Xaa being any amino acid beside Pro) are modified (Marshall, 1974). Since only about 66 percent of all sequons are glycosylated (Apweiler *et al.*, 1999), further structural requirements have to be fulfilled which are currently not completely understood.
After trimming of the core glycan by different glycosidases it can be elongated into various structures in the Golgi in a protein- and tissue-specific manner. In general, three types of *N*-glycans are discriminated (see Figure 1): high-mannose-type

glycans, complex-type glycans and hybrid-type glycans which show characteristics of both of the two other types.

Special functions of *N*-glycosylation are the sorting of lysosomal proteins via the mannose-6-phosphate pathway and the quality control regarding correct folding of secretory proteins before they are transferred to the Golgi (Lehle *et al.*, 2006).

1.1.2 *O*-Glycosylation

In contrast to *N*-glycans which consist of up to 30 sugar moieties, most *O*-glycans are much smaller. At the same time they are extremely diverse since up to seven different monosaccharides can be attached to all hydroxy amino acids (Ser, Thr, Tyr, Hyl, Hyp) although the most commonly modified are Ser and Thr (Wopereis *et al.*, 2006). Most *O*-glycans are further elongated into linear or branched structures. The initial step, the attachment of the first sugar to a hydroxyl group of a target protein, takes place post-transcriptionally in the late ER or in the Golgi where mostly nucleotide activated monosaccharides are used as donors. Based on the sugar directly attached to the protein *O*-glycans are classified into seven groups (see Figure 1).

In addition to the most common mucin-type *O*-glycosylation (see 1.1.2.1) – which is characterized by a Ser- or Thr-bound GalNAc (Hang & Bertozzi, 2005) – the galactosylation of Hyl in collagens and the reversible *O*-GlcNAc modification of cytosolic and nuclear proteins (Hart, 1997) are described in detail. *O*-Fucosylation which is involved in protein-protein interaction, *O*-glucosylation and *O*-mannosylation (described in detail in 1.2) are less common in mammals. Moreover, the glycosaminoglycan (GAG) modification (see 1.1.3) is often counted among *O*-glycosylation since most types are attached to Ser residues of the target protein.

1.1.2.1 Mucin-type O-glycosylation

A wide variety of glycoproteins are modified by mucin-type *O*-glycosylation (Spiro, 2002). Typically, these glycans occur accumulated in special protein domains called mucin domains (Perez-Vilar & Hill, 1999) and can account for more than 50 percent of the glycoprotein's molecular weight. The first GalNAc moiety is transferred to Ser/Thr residues by polypeptide-*N*-acetylgalactosaminyltransferases (ppGalNAcTs) (Ten Hagen *et al.*, 2003) and is elongated by downstream glycosyltransferases to

generate a series of eight core structures (Hang & Bertozzi, 2005). These core *O*-linked glycans can be further modified to generate complex oligosaccharides whereby the occurrence of the different structures depends mainly on the type of tissue in which they are expressed (Brockhausen *et al.*, 2009). In contrast to *N*-linked glycosylation mucin-type modification lacks a known amino acid consensus sequence (Jensen *et al.*, 2010) which also applies to most of the other *O*-glycosylation types. But it could be shown that the presence of Pro near the glycosylation site is beneficial for the *O*-GalNAc modification (O'Connell *et al.*, 1992).
Mucin-type *O*-glycosylation plays an important role in proteins called mucins. This is why highly O-glycosylated peptide stretches rich in Ser, Thr and Pro are usually called mucin domains. Mucins are highly *O*-glycosylated proteins present at the outer surfaces of the digestive, genital and respiratory systems (Wopereis *et al.*, 2006). The glycans present on mucins are able to bind high amounts of water so that they form a mucous layer which serves as a protective coating with antibacterial properties.

1.1.3 Glycosaminoglycan modification

Glycosaminoglycans are long linear polysaccharides containing a disaccharide repeat of an amino sugar (GalNAc or GlcNAc) and a uronic acid (GlcA or IdoA) or Gal (Esko *et al.*, 2009). Often, they are additionally modified by numerous sulfations which, together with the uronic acid moieties, evoke the polyanionic nature of GAGs and result in a high grade of heterogeneity.
The simplest GAG is hyaluronan (formerly called hyaluronic acid, HA) which is composed of up to 25,000 repeats of GlcNAc and GlcA (depicted in Figure 2) and is not modified any further. HA is not attached to a core protein instead it is released into the extracellular space after its synthesis at the plasma membrane (Hascall & Esko, 2009). With this, HA is the only GAG synthesized in the cytoplasm while the growing polymer is extruded from the cell. Different sizes of HA appear to have distinct physiological functions including hydration of tissues, providing of elasticity and creation of cell free spaces for cell migration (Preston & Sherman, 2011).
Most GAGs are attached to Ser residues of proteoglycan core proteins via the linker glycan Gal-Gal-Xyl (see Figure 2) including chondroitin sulfate (CS), dermatan sulfate (DS), heparan sulfate (HS) and heparin. Only keratan sulfate (KS) is bound in a different manner since it is linked through *N*-glycosylation (type I) or core 2

O-glycosylation (type II) (Wopereis *et al.*, 2006). A large number of core proteins have been identified which can be modified with just one GAG chain or with more than 100 chains (Esko *et al.*, 2009). GAG modification is initiated in the ER by the transfer of Xyl to Ser residues. In the Golgi the core is elongated by the sequential action of highly specialized glycosyltransferases, epimerases and sulfotransferases.

GAGs bind large volumes of water and with this the proteoglycans can provide resilience or resistance to compression. In addition, GAGs also play a role in nonspecific protein interactions. For example they adhere to soluble polypeptide growth factors through electrostatic interactions thereby concentrating the growth factors in a defined space (Wopereis *et al.*, 2006).

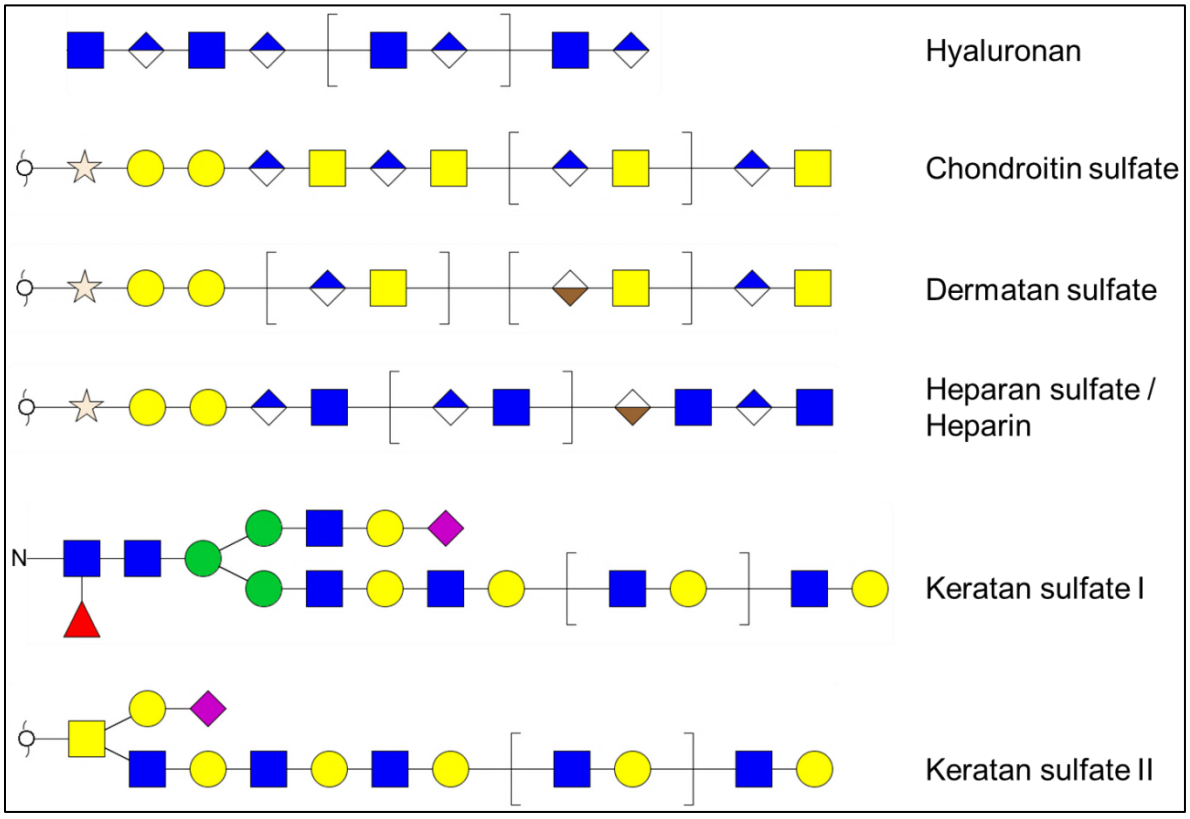

Figure 2: Schematic view of the different glycosaminoglycan types. GAG chains can be modified by epimerization of GlcA to IdoA and by extensive *O*-sulfation (not shown here) or in the case of heparan sulfate and heparin also *N*-sulfation. Brackets indicate disaccharide repeat.

1.2 *O*-Mannosylation

1.2.1 Biosynthesis and structure

O-Mannosylation was discovered in fungi and yeast in which the majority of secreted and cell wall proteins is modified with *O*-mannose (Sentandreu & Northcote, 1968; Lommel & Strahl, 2009). There *O*-mannosylation plays an essential role in cell wall rigidity and cell integrity (Gentzsch & Tanner, 1996). In yeast *O*-mannosylation is initiated in the ER by the transfer of mannose from dolichylphosphate mannose (Dol-P-Man) to Ser or Thr residues of secretory proteins. This transfer is catalyzed by protein mannosyltransferases (PMTs) (see Figure 3) (Haselbeck & Tanner, 1983; Gentzsch *et al.*, 1995b). Several PMT proteins with possibly distinct substrate specificities were identified and found to mostly act as heteroduplexes (Gentzsch *et al.*, 1995a). In the Golgi the core mannose is further elongated by several mannose moieties leading mainly to neutral linear glycans of two to seven saccharides (Endo, 1999).

In mammals, *O*-mannosylation seemed to be an uncommon modification since it was only found on a limited number of glycoproteins present in nerve and muscle tissues so far (Nakamura *et al.*, 2010). The core mannose is transferred to the target protein by a heteroduplex consisting of protein *O*-mannosyltransferases 1 and 2 (POMT1/2) in the ER (Jurado *et al.*, 1999; Willer *et al.*, 2002; Akasaka-Manya *et al.*, 2006) and is further elongated into various linear or branched structures in the Golgi (see Figure 3). The most prevalent *O*-mannosyl glycans in mammals share a common core structure in which the α-linked Man is elongated by GlcNAc and Gal (see Figure 4) (Endo, 1999). This core can additionally be modified by SA or Fuc (Smalheiser *et al.*, 1998). Furthermore, branched structures (Chai *et al.*, 1999) and *O*-mannosyl glycans carrying a sulfated GlcA (called HNK-1 epitope) (Yuen *et al.*, 1997) have been reported. Recently, mannose phosphorylation and further glycan modification forming a phosphodiester have been identified as a completely new glycan modification in mammals (Yoshida-Moriguchi *et al.*, 2010).

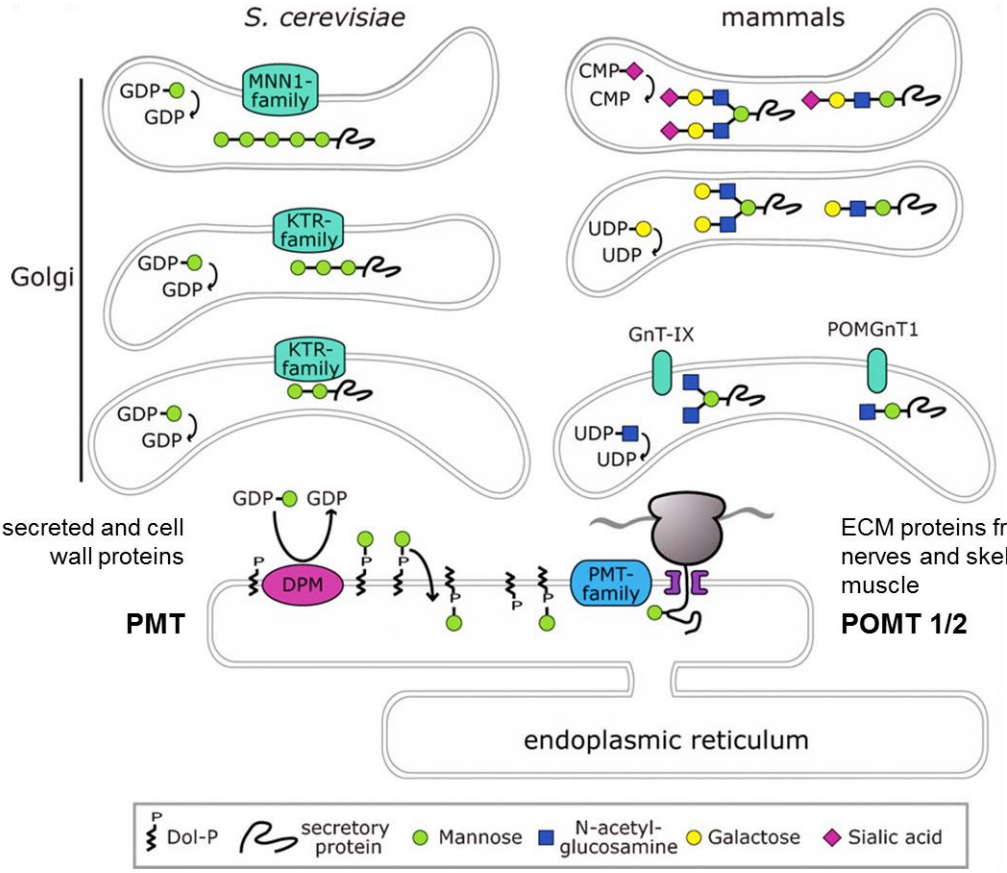

Figure 3: Schematic representation of the *O*-mannosylation pathway of yeast (left) and mammals (right). Dol-P-Man is synthesized on the cytosolic face of the ER membrane and flip-flops into the ER lumen. Mannose is afterwards transferred to proteins entering the secretory pathway by members of the PMT-family. Diversification occurs in the Golgi apparatus where further chain elongation takes place. Modified from (Lommel & Strahl, 2009).

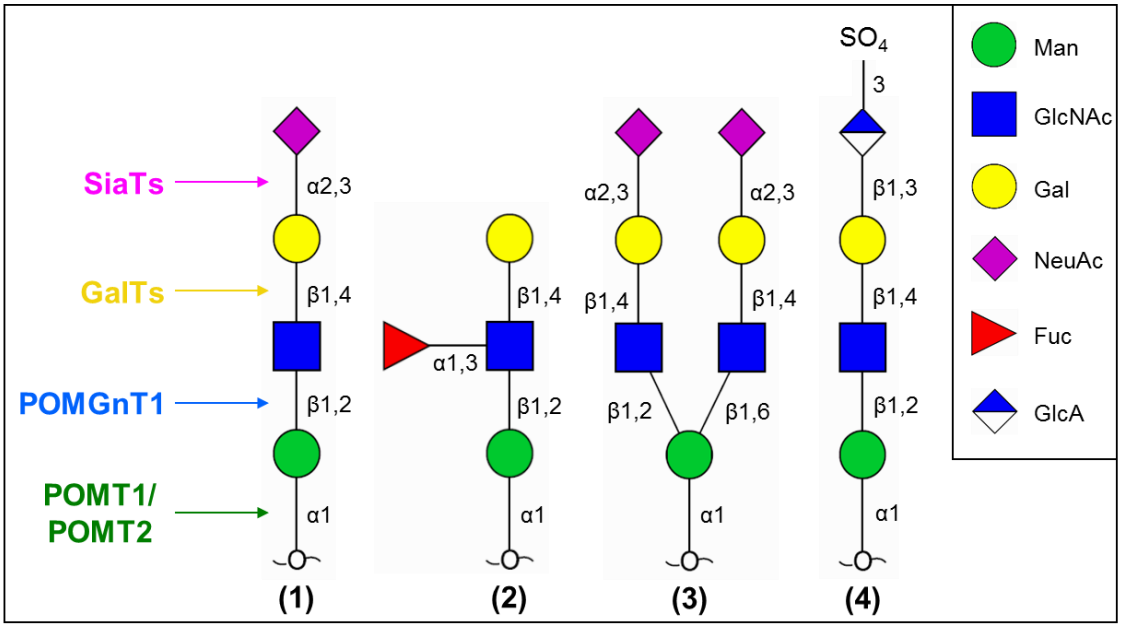

Figure 4: Schematic diagram of *O*-mannosyl glycans found in mammals. The core structure Galβ1-4GlcNAcβ1-2Man-Ser/Thr is common in all *O*-mannosyl glycans and can be sialylated (1) or fucosylated (2). Also, branched structures (3) and *O*-mannosidically linked HNK-1 epitopes (4) have been described.

1.2.2 Elongation of the core mannose

In mammals the extension of the core mannose in the 2-position with a GlcNAc moiety is catalyzed by protein mannose β-1,2-*N*-acetylglucosaminyl-transferase 1 (POMGnT1) (Takahashi *et al.*, 2001). The second GlcNAc in the 6-position which is present in branched structures can only be transferred to the glycan if the core mannose is already modified in the 2-position. This reaction is catalyzed by *N*-acetylglucosaminyltransferase IX which is highly expressed in brain and testes and absent in most other tissues (Inamori *et al.*, 2004). Several potential candidates for enzymes adding SA, Fuc, Gal and GlcA were suggested but the exact identity is not yet known. It is likely that these enzymes are not specific for the *O*-mannosylation pathway but are also used in other *O*- and *N*-glycan syntheses (Nakamura *et al.*, 2010).

As mentioned before the core mannose can be modified by the formation of a phosphodiester-bound glycan but neither the enzyme responsible for the phosphorylation of the core-mannose nor the exact structure of the attached polysaccharide are known. So far, the known or putative glycosyltransferases Large, fukutin and fukutin-related protein (FKRP) were shown to participate in the formation of this newly identified glycan epitope (Yoshida-Moriguchi *et al.*, 2010; Willer *et al.*, 2012). While the enzymatic activity of Large was identified as a bifunctional xylosyl and glucuronyl transferase (Inamori *et al.*, 2012a), the activities of fukutin and FKRP are still unclear.

1.2.3 *O*-Mannosylated proteins

Mammalian *O*-mannosylation was discovered on not otherwise specified chondroitin sulfate proteoglycans from rat brain in 1979 (Finne *et al.*, 1979). However, not much progress in this research area was made until Chai and coworkers found out that 30 percent of the pronase stable glycopeptides from rat brain are based on mannose (Chai *et al.*, 1999). So far, only a few mammalian proteins from nerve and muscle tissues could be identified as *O*-mannosylated – namely α-dystroglycan (α-DG) of nerve and muscle tissues of different species (Chiba *et al.*, 1997; Sasaki *et al.*, 1998; Smalheiser *et al.*, 1998), CD24 (Bleckmann *et al.*, 2009), neuron specific receptor-type protein tyrosine phosphatase β (RPTPβ) (Abbott *et al.*, 2008) and RPTPζ/phosphacan (Dwyer *et al.*, 2012). However, α-DG is the only protein in which

the sites and functions of the *O*-mannose modification were characterized in more detail (see 1.3.1) (Stalnaker *et al.*, 2011b). For a long time it was assumed that α-DG is the main *O*-mannose glycan carrying component in muscle and brain but Stalnaker et al. could show that the conditional knockout of brain α-DG did not lead to altered *O*-mannosylation in mice brains compared to wildtype (Stalnaker *et al.*, 2011a) indicating that other not yet identified *O*-mannosylated proteins are present in the brain.

1.2.4 Initiation of *O*-mannosylation

While some glycosylation types are initiated by a consensus motive within the amino acid chain at or near the glycosylation site the signals leading to *O*-mannosylation of a protein seem to be much more complex and are not fully understood. *In vitro* studies with substrates based on α-DG led to the postulation of a consensus sequence (Manya *et al.*, 2007) but this motif could not be confirmed *in vivo*. In 2008 Breloy *et al.* analyzed the sequential and structural dependence of the *O*-mannosylation of human α-DG on the basis of recombinantly expressed glycosylation probes of the α-DG mucin domain (Breloy *et al.*, 2008). The authors showed that the *O*-mannosylation is controlled by the direct periphery of the mannosylation site (Thr clusters) and by an upstream-located structural element (*cis*-controlling peptide). This peptide region appeared to be necessary but not sufficient.

1.3 Pathology of *O*-mannosylation defects

1.3.1 α-Dystroglycan

As described above α-DG is one of the few identified *O*-mannosylated proteins and it is the only protein in which this modification was analyzed in more detail. Dystroglycan is encoded by the *DAG1* gene whose product is posttranslationally cleaved into the extracellular α-DG and the transmembrane β-DG (Ibraghimov-Beskrovnaya *et al.*, 1992). While β-DG intracellularly binds to dystrophin which in turn attaches to the actin cytoskeleton α-DG stays noncovalently associated to β-DG (see Figure 5) (Barresi & Campbell, 2006). In addition, α-DG binds to various laminin G domain containing ECM proteins such as laminin (Ervasti & Campbell, 1993), agrin (Sugiyama *et al.*, 1994), neurexin (Sugita *et al.*, 2001) or perlecan (Talts *et al.*, 1999; Cohn, 2005). With this DG establishes a link between the actin cytoskeleton and the

ECM which (as part of the dystrophin-glycoprotein complex (DGC)) contributes to the structural stability of the muscle cell membrane during cycles of contraction and relaxation (Campbell, 1995). In fact, disruption of the DGC leads to various types of muscle disorders – the congenital muscular dystrophies (CMDs) (Schachter *et al.*, 2004). In addition α-DG is involved in basement membrane assembly, epithelial polarization, nerve myelination and cell migration.

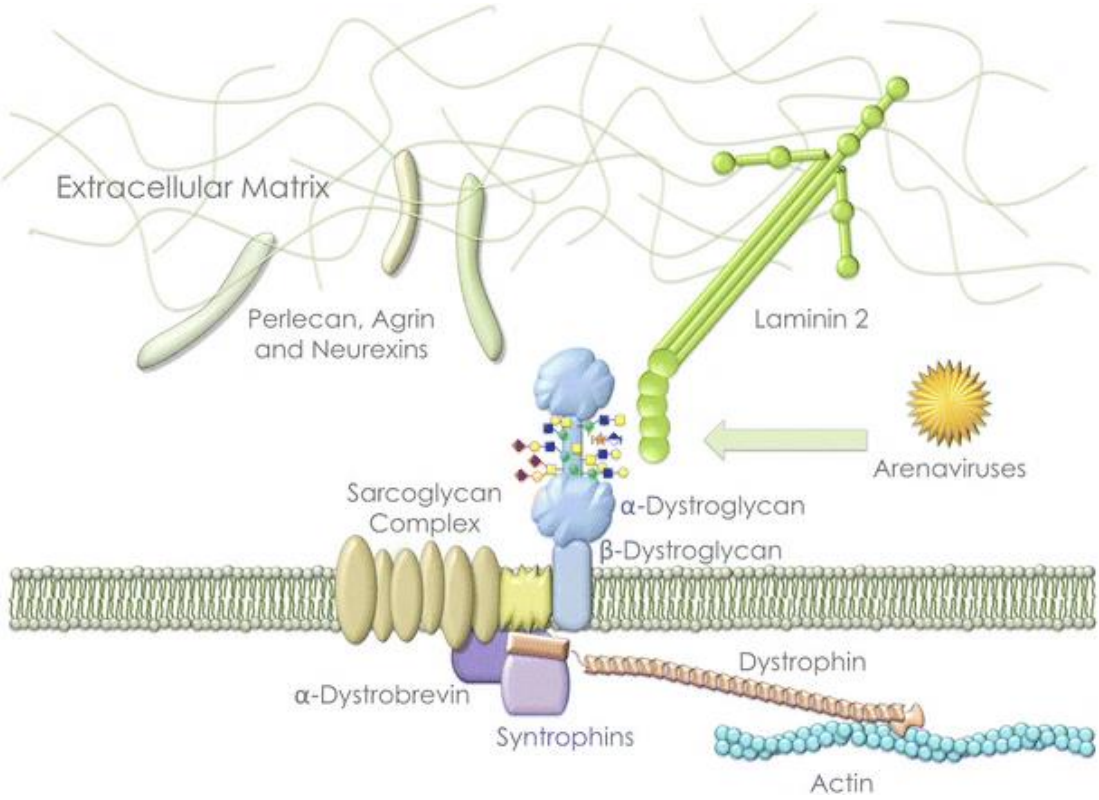

Figure 5: Schematic view of the dystrophin-glycoprotein complex and its interaction partners. *O*-Mannosylated and mucin-type glycosylated α-DG is a central component of the DGC and serves as a binding partner to several ECM proteins (laminin, perlecan, agrin and neurexin) as well as a receptor for members of the arenavirus family (LCMV and LFV). From (Dobson *et al.*, 2012).

DG is widely expressed among all tissue-types but most abundantly in skeletal muscle and heart (Ibraghimov-Beskrovnaya *et al.*, 1993). So far, *O*-mannosylation which is present in the central mucin domain of α-DG was found in nerve and muscle tissues whereby it was first described in bovine peripheral nerve (Chiba *et al.*, 1997) and rabbit skeletal muscle (Sasaki *et al.*, 1998). Chiba *et al.* also found out that intact *O*-mannosylation is a prerequisite for efficient binding to laminin and Michele *et al.* were able to show that hypoglycosylation abolished binding to laminin, agrin and neurexin (Michele *et al.*, 2002). Although no mutations in the dystroglycan gene have been identified in any human disorder (Barresi & Campbell, 2006) the importance of

posttranslational processing of α-DG becomes apparent in the fact that disrupted *O*-mannosylation leads to a group of severe CMDs – called dystroglycanopathies (see 1.3.2 for detailed description).

In addition to its function as ECM binding protein, α-DG also acts as receptor for bacterial and viral infection. Thus, *Mycobacterium leprae* binds laminin 2 and α-DG prior to infection of Schwann cells (Rambukkana *et al.*, 1998). Lymphocytic choriomeningitis virus (LCMV) and Lassa fever virus (LFV) also use α-DG as a receptor (Cao *et al.*, 1998) and Imperiali *et al.* could show that this interaction is also dependent on the *O*-mannosylation present on α-DG (Imperiali *et al.*, 2005).

1.3.2 Dystroglycanopathy

Dystroglycanopathy belongs to the CMDs which is a heterogeneous group of inherited genetic diseases causing progressive weakness and wasting of skeletal muscle (Stalnaker *et al.*, 2011b). CMDs can arise from many genetic mutations in a wide variety of muscle proteins, with laminin α-2 being the most prominent (Schessl *et al.*, 2006). The underlying genetic mutations in dystroglycanopathy are found in genes of known or putative glycosyltransferases of the *O*-mannosylation pathway (Muntoni *et al.*, 2004; Martin, 2007) or in accessory proteins of them (Godfrey *et al.*, 2011). The severe muscle phenotype of dystroglycanopathy can mostly be attributed to hypoglycosylation of α-DG leading to a reduction or a complete loss of its ability to bind laminin (Willer *et al.*, 2003). In addition, dystroglycanopathy patients often exhibit brain malformations and eye abnormalities (Sparks *et al.*, 2001 [Updated 2012]) which are not observed in other CMDs. Until 2007 the defects caused by dystroglycanopathy were commonly attributed solely to the loss of α-DG function (Martin, 2007). But the finding that the expression of the participating glycosyltransferases is not always coincident with DG expression suggests that there might be other glycoproteins that are modified by *O*-mannosylation (Martin, 2007).

So far, mutations in seven known or putative glycosyltransferase genes have been identified to cause dystroglycanopathy (see Figure 6) (Dobson *et al.*, 2012). In addition, mutations in two accessory proteins were found to result in a combined phenotype of dystroglycanopathy and congenital disorders of glycosylation (CDG) (Godfrey *et al.*, 2011). Mutations in POMT1 or POMT2 lead to the severest form of dystroglycanopathy – the Walker-Warburg syndrome (WWS) with life expectancies of only up to twelve months (Beltrán-Valero de Bernabé *et al.*, 2002; van Reeuwijk *et*

al., 2005). Typical symptoms of WWS include type II lissencephaly, muscular dystrophy and structural eye abnormalities. Patients with muscle-eye-brain disease (MEB) which can arise from mutations in the *POMGnT1* gene, exhibit a similar phenotype as observed in WWS only less severe. The life expectancy can be up to twelve years of age (Yoshida *et al.*, 2001).

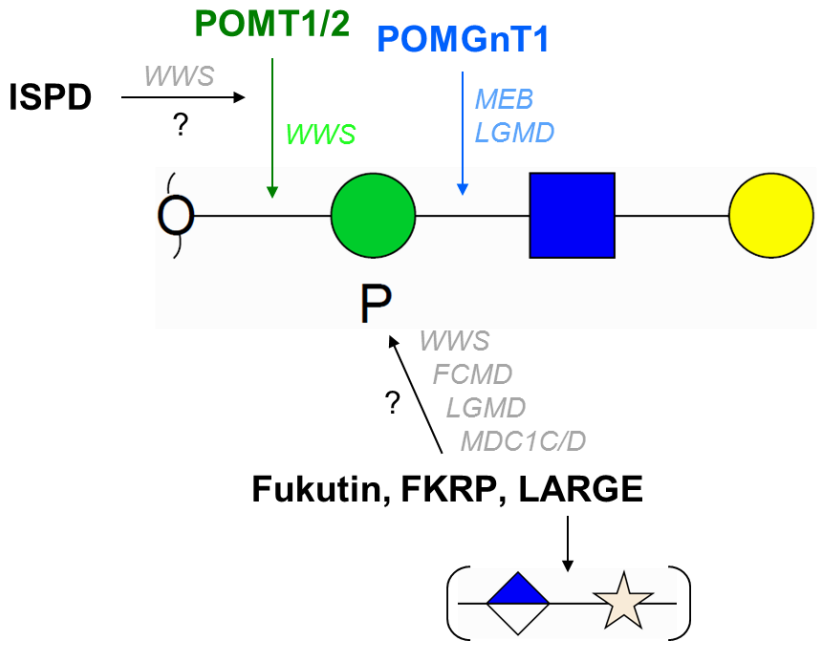

Figure 6: Schematic representation of the enzymes involved in the *O*-mannosylation pathway. Defects of their genes cause different types of dystroglycanopathies. Known or putative glycosyltransferases are shown in bold letters and their catalytic activities are indicated (the question marks indicate that either the enzymatic activity or the linkage type are unknown). The respective disorders caused by genetic defects are shown in italic.

In addition to the mutations in known glycosyltransferases, which are responsible for the core structure synthesis, mutations in enzymes affecting the postphosphoryl modification, namely Large, fukutin and FKRP, also cause dystroglycanopathy. Longman *et al.* could show that mutations in the *LARGE* gene led to MDC1D which presented itself with severe muscular dystrophy and mental retardation (Longman *et al.*, 2003). Humans also harbor the Large2 protein which has a similar activity as Large (Inamori *et al.*, 2012b) but so far no mutations were found in the *LARGE2* gene in dystroglycanopathy patients. Mutations in fukutin and FKRP were found to cause several disorders – namely Fukuyama CMD (FCMD), limb-girdle muscular dystrophy (LGMD), WWS and MDC1C (Dobson *et al.*, 2012). Recently mutations in the *ISPD* gene were identified as a new cause of WWS (Roscioli *et al.*, 2012; Willer *et al.*, 2012). The authors assumed from their tests that ISPD activity is needed for the

transfer of mannose onto the target protein but the exact enzymatic activity of this gene product remains unclear.

In addition to the pure dystroglycanopathies two disorders affecting *O*-mannosylation and *N*-glycosylation were reported. Mutations in *DPM2 (Barone et al., 2012)* and *DPM3* (Lefeber *et al.*, 2009) both affect the activity of dolichyl-phosphate mannosyltransferase (DPM) which catalyzes the synthesis of Dol-P-Man. This in turn is used as substrate in *N*-glycosylation, *O*-mannosylation, *C*-mannosylation and GPI-anchor formation but the authors suspected that *O*-mannosylation is more sensitive to a reduction in Dol-P-Man and was therefore thought to be the main cause of the clinical features (Godfrey *et al.*, 2011).

So far, the underlying mutations of only about half of the patients suffering from dystroglycanopathy were identified and attributed to one of the genes described above (Dobson *et al.*, 2012) indicating that other gene products might also be involved in the *O*-mannosylation pathway.

1.4 Brain extracellular matrix

The central nervous system (CNS) is densely packed with various cells confined by the bony shell of the scull leaving only a small extracellular space (Rauch, 2007). Only about 20 percent of the brain tissue volume is composed of ECM (Nicholson & Syková, 1998), while for example connective tissue consists to over 50 percent of ECM structures. In the brain different forms of ECM structures are present – the most remarkable being perineuronal nets (PNNs) of mature neurons and a basal lamina-like ECM that localizes to the blood-brain barrier (Dityatev *et al.*, 2010). The main components of the CNS matrix were found to be members of the lectican (detailed description in 1.4.1), link protein and tenascin families in addition to the GAG hyaluronan (Zimmermann & Dours-Zimmermann, 2008), but various other proteins are also present – many of them unique to the CNS.

Due to the different types of specialized structures a high grade of heterogeneity throughout the brain is observed. Nonetheless, the ECM serves a rather universal role as a barrier for soluble and membrane associated molecules and therefore contributes to the clustering of these molecules in functional microdomains (Dityatev *et al.*, 2010). Two examples of the ECM barrier function are the accumulation of cations at the nodes of Ranvier thereby ensuring proper conduction of action

potentials along the axon (Bekku *et al.*, 2010) and the clustering of receptors at the postsynapse of synaptic contacts. Dityatev *et al.* could show that the interneuron exciting activity is regulated by the ECM present at the axon initial segment (AIS) (Dityatev *et al.*, 2007). Hedstrom and colleagues found out that the cell adhesion molecule (CAM) neurofascin 186 (see 1.4.2) assembles the ECM at the AIS and links it to the cytoskeleton (Hedstrom *et al.*, 2007). Other functions of the brain ECM are the protection against oxidative stress (Morawski *et al.*, 2004) and the regulation of neuronal plasticity (Galtrey & Fawcett, 2007). Plasticity – the adaptability of the mammalian CNS (Bandtlow & Zimmermann, 2000) – plays a key role in the refinement of connections during development and continues to be important in the response to experience, age or injury in the adult CNS.

1.4.1 Lecticans

The lecticans are a family of four high molecular weight, chondroitin sulfate-bearing proteoglycans (see 1.1.3) which are the most abundant proteins of the ECM in the CNS (Howell & Gottschall, 2012). The core proteins of aggrecan, brevican, neurocan and versican range in size from 95 kDa to more than 300 kDa and share a common domain structure (see Figure 7A). Between the globular domains at the termini a central region of varying length is present that contains attachment sites for CS-GAG chains and also *N*- and *O*-glycosylation sites (Zimmermann & Dours-Zimmermann, 2008). The high grade of glycosylation confers a rather rigid mucin-like structure to this domain (Bandtlow & Zimmermann, 2000). The N-terminal region, called G1, contains a hyaluronan and link protein binding site while the C-terminal domain, G3, can bind to sulfoglycolipids (Miura *et al.*, 1999), tenascins (Aspberg *et al.*, 1997) or fibulins (Olin *et al.*, 2001). The lecticans are expressed in different isoforms and secreted into the extracellular space with one exception, a GPI-anchored splice variant of brevican (Bandtlow & Zimmermann, 2000).

Phosphacan and RPTPβ, which were shown to be *O*-mannosylated, share some structural similarities with the lecticans (see Figure 7B). They have a globular N-terminal domain and a central domain that is modified by CS-GAG chains and *O*-glycosylation (Bartus *et al.*, 2012). While RPTPβ is anchored to the plasma membrane phosphacan which is a splice variant of the former is released into the extracellular space.

Together the above mentioned molecules form complex networks among which the PNNs are the most important. These are mesh-like structures that surround the cell bodies and proximal dendrites of some classes of neurons (Galtrey & Fawcett, 2007) and mainly consist of lecticans, HA, tenascin-R and link proteins. Hyaluronan provides the scaffold for PNNs since it is attached to the neuronal cell surface and extends far into the extracellular space. Many lecticans bind to a single HA molecule while this interaction is stabilized by link proteins. Lecticans can be interconnected by tenascin-R trimers thereby crosslinking the different HA chains. There are variations to the basic organization due to the distinctive distribution of individual members of the lecticans and link proteins. At the nodes of Ranvier for example, versican splice variant V2 was shown to be the principal organizer (Dours-Zimmermann *et al.*, 2009) while the AIS matrix is mainly dependent on brevican (Dityatev *et al.*, 2007).
In addition to the high amount of lecticans integrated into structural matrices, Rauch described the presence of free neurocan (Rauch, 2007). The author proposed that neurocan might act as an interaction modulator for different cell adhesion molecules.

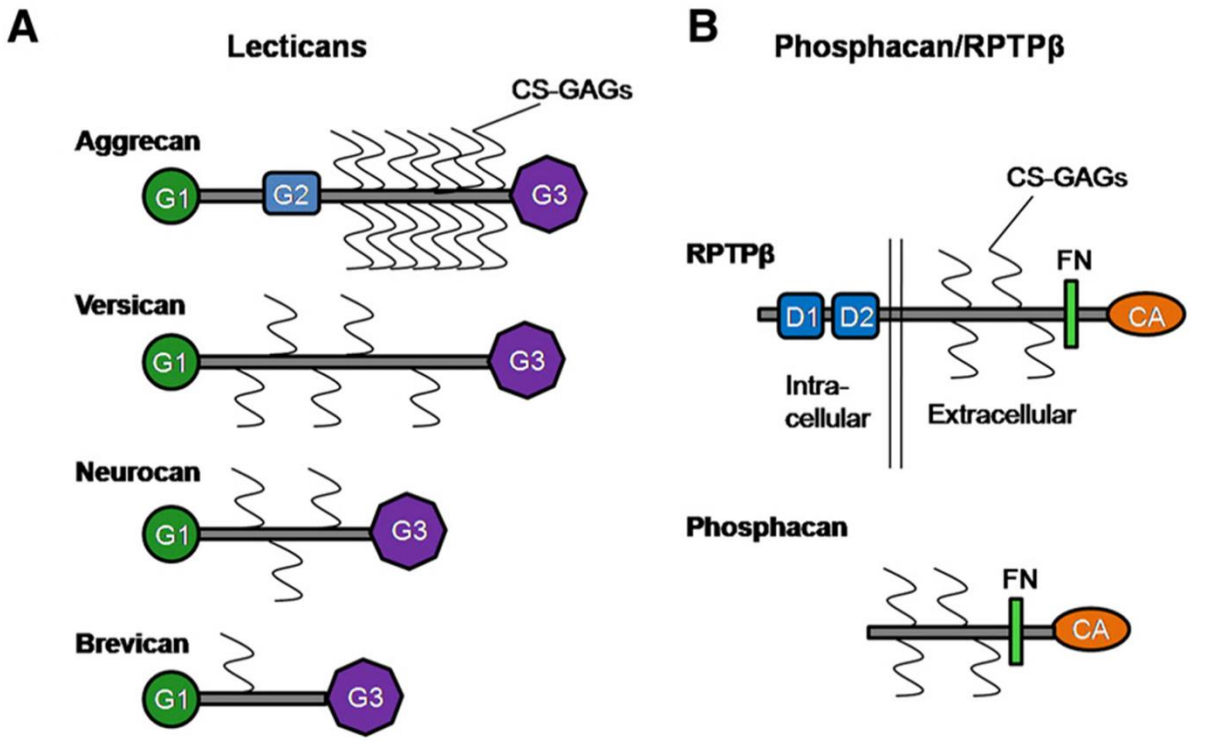

Figure 7: Schematic representation of the most common CNS CSPGs. (A) Lecticans are composed of two globular domains (G1 and G3) flanking a core protein region with GAG attachment sites. Aggrecan has an additional G2 domain adjacent to G1. (B) Phosphacan is a splice variant of RPTPβ. They both have globular N-terminal domains (CA), a CS-GAG-modified central region and a fibronectin type-III domain. Modified from (Bartus *et al.*, 2012).

1.4.2 Neurofascin

Neurofascin (NF) is a cell surface protein of the immunoglobulin superfamily which is only expressed in nervous tissue (Kriebel *et al.*, 2012). Several splice variants of NF have been identified with NF155 and NF186 being the predominant ones. The 155 kDa isoform is expressed by glia cells while NF186 is produced by neurons (Kriebel *et al.*, 2011). They both consist of a short cytoplasmic tail, a single transmembrane intersection and a large extracellular part (see Figure 8) which is mainly composed of immunglobulin-like (Ig) and fibronectintype-III domains (Liu *et al.*, 2011). The main difference between the two isoforms is an additional mucin-like domain present in NF186.

Both variants play crucial roles in the compartmentalization of axonal proteins. While NF155 is required for paranodal junction assembly at the glial interface, NF186 is essential for the accumulation of the nodal protein complex needed for axonal conduction at nodes of Ranvier (Susuki & Rasband, 2008). In addition NF186 assembles the ECM of the AIS and links it to the cytoskeleton. From their experiments Hedstrom *et al.* assume that NF186 directly binds to brevican and thereby assembles a specialized brevican-based ECM at the AIS (Hedstrom *et al.*, 2007). Intracellularly, only ankyrin G was identified as an interaction partner of NF186 so far (Susuki & Rasband, 2008) which in turn recruits specialized sodium channels to the nodes of Ranvier.

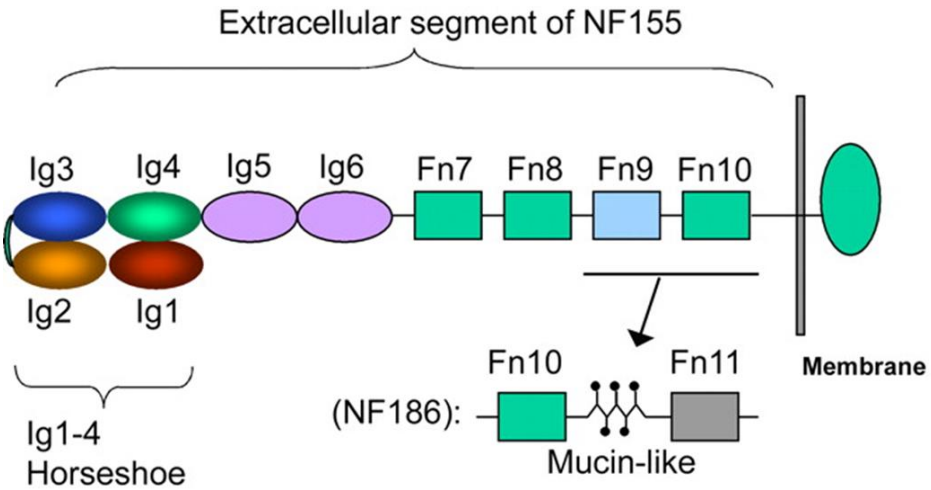

Figure 8: Schematic view of the domain composition of neurofascin. NF harbors six immunoglobulin-like domains (Ig) which form a horseshoe-like structure and four fibronectin type-III domains (Fn). In addition, NF186 comprises a highly glycosylated mucin-like domain (Liu *et al.*, 2011).

1.4 Aim of this project

Protein *O*-mannosylation is a rare posttranslational modification in mammals in general but was found in about one third of all *O*-glycosidically bound glycans in the brain. So far, only very few proteins have been identified to carry this modification and their *O*-mannosyl glycans alone cannot account for the high amount present in nervous tissues. In addition, patients suffering from genetic mutations of enzymes involved in the *O*-mannosylation pathway exhibit a severe neurological phenotype which indicates a still unknown but important role for *O*-mannosylation in the brain. Therefore, the aim of this study was the identification of new *O*-mannosylated proteins of the mammalian brain leading to new insights into the mechanism of initiation and the pathology of *O*-mannosylation defects.

The isolation of *O*-mannosylated proteins ought to be accomplished from mouse and calf brains by means of general proteomics. Since the exposed glycan epitopes of mannose-based glycans are very similar to other *N*- and *O*-glycan epitopes immune affinity purification of *O*-mannosylated proteins was not possible. Therefore, a broad, unbiased proteomics approach was chosen in which mouse or calf brain lysates were to be fractionated via a newly developed sequence of preparative fractionation methods. The generated protein fractions should be analyzed regarding their *O*-glycan content by MALDI mass spectrometry of released *O*-glycans and proteins ought to be identified by LC-MS of tryptic peptides. Further information about the *O*-mannosylation sites was to be gained from glycopeptide analysis via LC-ESI-MS.

2 Materials and methods

2.1 Materials

All chemicals were purchased from Sigma-Aldrich or Carl Roth and were of analytical grade. Exceptions are marked in the text. Proteins were handled at 4°C, long time storage was at -20°C.

2.1.1 Buffers and Solutions

2.1.1.1 Purchased buffers

Buffer	Manufacturer
Dulbecco's PBS	PAA

2.1.1.2 Self-made buffers

SDS-PAGE

Electrophoresis buffer (10×)	1.92 M glycine 0.25 M Tris 1 % (w/v) SDS
Sample Buffer (reducing, 10×)	0.5 M TrisHCl pH = 6.8 10 % (w/v) SDS 50 % (v/v) glycerin 10 % (v/v) 2-mercaptoethanol 0.0025 % (w/v) bromphenol blue
Stacking gel buffer (4×)	0.5 M TrisHCl pH = 6.8
Running gel buffer (4×)	1.5 M TrisHCl pH = 8.8

Western blot

TBS (10×)	0.2 M TrisHCl pH = 7.4 1.5 M NaCl
TBST buffer	1× TBS for Western Blot 0.1 % (v/v) TWEEN 20
Towbin buffer (2×)	0.39 M glycine 48 mM Tris
Blotting buffer	1× Towbin buffer 20 % (v/v) methanol 0.05 % (w/v) SDS

Lysis and WGA affinity chromatography

Solubilization buffer	10 mM TrisHCl pH = 7.5 150 mM NaCl 1 % (w/v) CHAPS or Triton X-100
Washing buffer	10 mM TrisHCl pH = 7.5 0.5 M NaCl 1 % (w/v) CHAPS or Triton X-100
Elution buffer 1	10 mM TrisHCl pH = 7.5 150 mM NaCl 1 % (w/v) CHAPS or Triton X-100 0.2 M GlcNAc
Elution buffer 2	10 mM TrisHCl pH = 3 150 mM NaCl 1 % (w/v) CHAPS or Triton X-100 0.2 M GlcNAc

Differential solubilization

Aqueous extraction buffer	40 mM TrisHCl pH = 9.5 1 mM DTT 1 mM ascorbic acid 5 mM $MgCl_2$
Urea/CHAPS buffer	40 mM TrisHCl pH = 9.5 1 mM DTT 8 M urea 4 % (w/v) CHAPS
Enhanced solubilization buffer	40 mM TrisHCl pH = 9.5 1 mM DTT 5 M urea 2 M thiourea 2 % (w/v) CHAPS 2 % (w/v) SB 3-10
SDS buffer	40 mM TrisHCl pH = 9.5 1 % (w/v) SDS

GPC

GPC buffer	50 mM TrisHCl pH = 7.4 150 mM NaCl 0.5 % (w/v) SDS 50 µg/ml Pefabloc SC (Merck)

HA affinity chromatography

HA buffer	20 mM TrisHCl pH = 8.0 0.5 M NaCl 10 mM EDTA 0.25 % (w/v) CHAPS
Sodium acetate buffer	0.1 M NaAc pH = 4.0 0.5 M NaCl

TrisHCl buffer	0.1 M TrisHCl pH = 8.3 0.5 M NaCl
Chase buffer	50 mM TrisHCl pH = 8.0 60 mM NaAc

IEF

IEF solution	2 % (w/v) CHAPS 2 M thiourea 7 M urea

2.1.2 Protein Standards for Electrophoresis

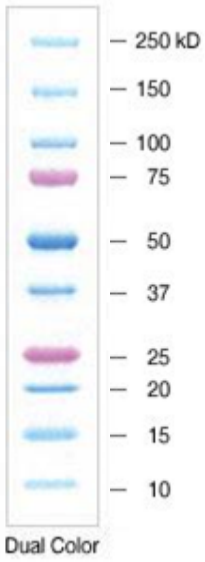

Precision Plus Dual Color Protein Standard (Bio-Rad)

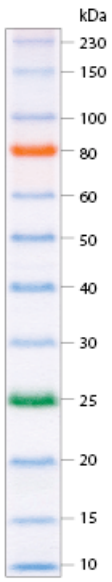

ColorPlus Prestained Protein Ladder, Broad Range (NEB)

2.1.3 Antibodies

2.1.3.1 Primary antibodies

Antibody	Manufacturer
anti-neurofascin P-19	Santa Cruz
anti-neurocan C-12	Santa Cruz
anti-neurocan HPA036814	Sigma

2.1.3.2 Secondary antibodies

Antibody	Manufacturer
HRP-conjugated swine anti-rabbit IgG P0399	DAKO
HRP-conjugated donkey anti-goat IgG sc-2020	Santa Cruz

2.2 Methods

2.2.1 Purification of *O*-mannosylated proteins

2.2.1.1 Lysis of mouse and calf brain

Mouse brains from C57BL/6 wild type mice and calf brain pieces were homogenized on ice in a glass tissue grinder in solubilization buffer containing protease inhibitor cocktail (cOmplete Mini EDTA-free Protease Inhibitor Cocktail Tablets, Roche). Crude lysate was incubated at 4°C on a rotary shaker for 30 min, sonicated on ice followed by centrifugation at 16,100 g for 30 min (mouse) or 1 h (calf). The supernatant (brain lysate) was used for WGA affinity chromatography.

2.2.1.2 WGA-agarose affinity chromatography

The brain lysate was conveyed to an equilibrated WGA-agarose (Vector Laboratories) column in a circular pump driven system. On the next day the column was washed with solubilization buffer and with washing buffer and WGA-bound proteins (glycoproteins) were eluted from the lectin column with elution buffer 1 and elution buffer 2. Eluates were combined and the protein concentration was determined using the DC Protein Assay (Bio-Rad) according to the manufacturer's protocol.

2.2.1.3 Differential solubilization of mouse brain proteins

Mouse brains were homogenized on ice in a glass tissue grinder in aqueous extraction buffer containing protease inhibitor cocktail, sonicated on ice followed by centrifugation at 16,100 g for 60 min. The supernatant was subjected to a fresh tube and the pellet was washed and then homogenized in urea/CHAPS buffer with protease inhibitor cocktail by sonication on ice. After centrifugation the supernatant was transferred to a fresh tube and the pellet was washed and then homogenized in enhanced solubilization buffer (+ protease inhibitor cocktail) by sonication on ice. The remaining centrifugal pellet was solubilized in SDS buffer

by sonication. Supernatant concentrations were determined using the DC Protein Assay (Bio-Rad). Protocol modified from (Molloy *et al.*, 1998).

2.2.1.4 Fractionation of glycoproteins by GPC

Mouse brain glycoproteins were applied to a gel permeation column (Superdex 200 HR10/30, GE Healthcare) equilibrated with GPC buffer. Proteins were separated by size using a flow rate of 0.7 ml GPC buffer per min and fractionated into 9-ml fractions. After analysis via SDS-PAGE (see 2.2.2.1) protein-containing fractions were concentrated in AMICON Ultra-15 Centrifugal Filter Units (Millipore) with a molecular weight cut-off of 10 kDa.

2.2.1.5 Fractionation of glycoproteins by preparative SDS-PAGE

Up to 5 mg protein was mixed with sample buffer (10×), subjected to a gel column with a 3.5 % stacking and a 5 % separation gel (Bio-Rad Miniprep Cell) and separated according to manufacturer's protocol. Eluted proteins were fractionated into 30 fractions of 2.5 ml volume. After analysis via SDS-PAGE (see 2.2.2.1) protein-containing fractions were concentrated in AMICON Ultra-15 Centrifugal Filter Units (Millipore) with a molecular weight cut-off of 10 kDa or desalted using PD-10 desalting columns (GE Healthcare).

2.2.1.6 Hyaluronan affinity chromatography

EAH-sepharose 4B (GE Healthcare) was equilibrated in ddH_2O pH 4.5 (with HCl) and hyaluronic acid (Sigma, sodium salt from *Streptococcus equi*) dissolved in ddH_2O pH 4.5 was added. The coupling reaction was started by the addition of solid N-ethyl-N′-(3-dimethylaminopropyl)carbodiimide (EDC) and incubation at RT for 2 h under regular pH adjustment. After incubation at 4°C over night the reaction was stopped by the addition of 1 M acetic acid and incubation at RT for 6 h. The HA-sepharose was extensively washed with sodium acetate buffer and TrisHCl buffer and equilibrated with HA buffer.

A 3-ml Mobicol column was packed with 600 µl of a 50 % HA-sepharose slurry and washed with HA buffer. The sample (in HA buffer) was applied to the column and the flow-through was reapplied twice. After washing with HA buffer and HA buffer with 1 M NaCl bound proteins were eluted by the addition of HA buffer containing 4 M guanidine HCl. After incubation for 15 min the eluate was recovered.

For chondroitinase ABC (Chase) digestion of glycosaminoglycan chains present on proteoglycans the proteins were precipitated by methanol/chloroform precipitation, resuspended in Chase buffer and incubated with Chase ABC (Sigma) at 37°C over night.

2.2.1.7 Fractionation of glycoproteins by IEF

WGA-bound glycoproteins were eluted directly with IEF solution containing 0.2 M GlcNAc. Approximately 2 mg glycoproteins were subjected to a preparative gel-free isoelectric focusing on the MicroRotofor Liquid-Phase IEF Cell (Bio-Rad) according to the manufacturer's instructions in 3 % BioLyte 3/10 (Bio-Rad) in IEF solution. Concentration and buffer exchange were achieved using ultrafiltration.

2.2.2 Protein identification

2.2.2.1 Gel electrophoresis and Western Blot

SDS-PAGE was done according to Laemmli (Laemmli, 1970) (3 % stacking gel and 3.5 % to 10 % or 5 % to 15 % gradient running gel) on a Mini-Protean II Electrophoresis system (Bio-Rad). Samples were mixed with sample buffer (10×) and electrophoresis was operated in electrophoresis buffer (1×). SDS gels were either stained with silver according to (Vorum *et al.*, 2004) or Coomassie Brilliant Blue G250.

For mass-spectrometry compatible silver-staining according to Vorum the gel was fixated over night in 50 % methanol, 12 % acetic acid and 0.05 % formaldehyde. After washing with 35 % ethanol the gel was pretreated with 0.02 % $Na_2S_2O_3$ and stained in 0.2 % $AgNO_3$ contaning 0.076 % formaldehyde. After washing with water the staining was developed using 6 % Na_2CO_3, 0.05 % formaldehyde, 0.0004 % $Na_2S_2O_3$ and stopped with 50 % methanol, 12 % acetic acid.

Western blots were operated in a tank transfer cell (Mini Trans-Blot Cell, Bio-Rad) onto nitrocellulose or PVDF membranes. Membranes were blocked with 1 to 5 % milk powder in TBST buffer. Neurofascin was detected with anti-neurofascin P-19 (1:100 in 5 % milk powder in TBST). Mouse and rat neurocan were detected with anti-neurocan C-12 (1:200 in 1 % milk powder in TBST) and cow neurocan with anti-neurocan HPA036814 (1:500 in 5 % milk powder in TBST). Horseradish peroxidase (HRP)-conjugated donkey anti-goat IgG (1:5000 in 0.5 % milk powder in TBST) or HRP-conjugated swine anti-rabbit IgG (1:2000 in 5 % milk powder in TBST) were used as secondary antibodies and protein-antibody conjugates were visualized by enhanced chemiluminescence (Roche) on X-ray films (Fuji).

2.2.2.2 Protein identification by LC-MS analysis

Protein identification by LC-MS was performed either on distinct SDS gel bands or proteins in solution. Proteins in solution were precipitated by methanol/chloroform precipitation as follows: 1 Vol of sample was mixed with 4 Vol methanol, 1 Vol chloroform and 3 Vol bidistilled water (ddH_2O). After centrifugation at 16,100 g for 10 min the aqueous phase was removed without disturbing the protein containing interphase. 4 Vol methanol were added,

the sample was mixed thoroughly and again centrifuged at 16,100 g for 10 min. The supernatant was removed, the pellet resuspended in 4 Vol methanol and again centrifuged. Finally, the pellet was allowed to dry. In samples containing calf brain lecticans the buffer was exchanged to 20 % methanol using AMICON Ultra-15 Centrifugal Filter Units (Millipore) and subsequently the sample was dried in a SpeedVac concentrator.

Proteins were reduced with 2.5-5 mM DL-dithiothreitol (DTT) and alkylated with iodoacetamide (IAA) followed by digestion with trypsin. LC-MS analysis of the peptides was done on an HCTultra PTM discovery system (Bruker) coupled with an online nano-LC system (Proxeon) with a C18 column (75 µm x 10 cm). Proteins were identified using Mascot search engine. For murine proteins the SwissProt database was used, for bovine proteins the NCBI database.

2.2.3 Analysis of *O*-glycans and glycopeptides

2.2.3.1 O-Glycan analysis

Proteins were precipitated by methanol/chloroform precipitation (see 2.2.2.2) in order to remove salts and detergents. Calf brain proteoglycans were instead subjected to buffer exchange followed by drying of the sample as described in 2.2.2.2. The *O*-glycan chains were released from precipitated proteins by reductive β-elimination. For this purpose the glycoproteins were incubated with 1 M $NaBH_4$ in 50 mM NaOH for 18 h at 50°C. The reaction was stopped on ice by adding 1 µl of acetic acid. Salt was removed with 100 µl of Dowex 50W-X8 (Bio-Rad) in a batch procedure and excessive borate was eliminated in a stream of nitrogen by washing with ethanol and 1 % acetic acid in methanol.

Permethylation of the glycan chains was done as described by Ciucanu and Kerek (Ciucanu & Kerek, 1984). Released glycans were dried by applying a vacuum and the exsiccator was flooded with argon in order to prevent water contamination. Glycans were resuspended in DMSO by vigorous mixing, NaOH/DMSO suspension was added and the samples were incubated for 30 minutes at room temperature (RT) and then frozen at -20°C. Permethylation was achieved by the addition of 25 µl iodomethane and incubation for 30 min. Salts were removed by chloroform/water extraction. Dried samples were dissolved in methanol, applied to a MALDI target using 2,5-dihydroxybenzoic acid (DHB) or α-cyano-4-hydroxycinnamic acid (HCCA) as matrix and analyzed on the ultrafleXtreme MALDI-TOF/TOF mass spectrometer (Bruker). Spectra were analyzed with the software Flex Analysis.

2.2.3.2 Glycopeptide analysis by CID mass spectrometry

Proteins were precipitated by methanol/chloroform precipitation (see 2.2.2.2) in order to remove salts and detergents. Then, proteins were reduced and alkylated as described above

(see 2.2.2.2) followed by digestion with trypsin and GluC. LC-MS analysis of the peptides was done on a PTMDiscover-System (Bruker) coupled with an online nano-LC system (Proxeon) and a C18 column (75 µm x 10 cm). The gradient ran from 0 – 35 % acetonitrile in 0.1 % TFA during 30 min. Ions were scanned in a range of m/z 300 – 2,500 in MS mode and m/z 200 – 3,000 in MS/MS mode whereby MS/MS spectra were generated by CID fragmentation. Glycopeptide spectra were analyzed in detail with the Data Analysis software (Bruker).

2.2.3.3 Glycopeptide analysis by LC-MS3 mass spectrometry

ESI−MS3 analysis of peptides from neurofascin (generation see 2.2.3.2) was done on an LTQ Orbitrap Discovery system (Thermo Scientific) equipped with a Proxeon nano ESI-source and coupled to a Proxeon Easy nLC II system. The sample was separated on an analytical C18 column (75 µm × 10 cm, Thermo Scientific) using gradient runs from 0 to 35 % acetonitrile in 0.1 % TFA during 74 min. Glycopeptide spectra were analyzed in detail with the Xcalibur software (Thermo Scientific).

2.2.4 Recombinant expression and purification of neurocan

2.2.4.1 Cultivation of HEK293 cells

HEK293-EBNA cells recombinantly expressing full length rat neurocan (kindly provided by U. Rauch of Lund University) were cultivated in DMEM supplemented with 10 % FCS, 100 U/ml penicillin, 100 µg/ml streptomycin and 5 µg/ml puromycin at 37°C with 5 % CO_2. For the collection of neurocan containing supernatant the medium was changed to FCS-free DMEM containing penicillin, streptomycin and puromycin, cells were incubated for 3 days and the supernatant was collected. Detached cells were removed by filtration through a 0.22 µm syringe filter and proteins were concentrated by ultrafiltration using AMICON Ultra-15 Centrifugal Filter Units.

2.2.4.2 Purification of recombinantly expressed neurocan

The concentrated supernatant was applied to hyaluronan affinity chromatography as described in 2.2.1.6.

3 Results

3.1 Analysis of mouse and calf brain

3.1.1 *O*-Glycome of mouse and calf brain

Although glycosylation in general is species- and tissue-specific, the *O*-mannose modification was shown to be similar among all mammals analyzed so far (Endo, 1999). For the identification of new *O*-mannosylated proteins from mammalian brain, mouse and cow were chosen since *O*-mannosylation had been found in these animals before (Chiba *et al.*, 1997; Grewal *et al.*, 2001).

In order to get an overview of the *O*-glycans present in murine and bovine brain the glycoproteins were enriched from crude lysates using wheat germ agglutinin (WGA) affinity chromatography. WGA is a lectin (sugar binding protein) which specifically binds GlcNAc and SA. Since brain proteins are highly sialylated on *O*- and *N*-glycans they can effectively be enriched with this lectin (see below for the efficiency of WGA affinity chromatography). The enriched glycoproteins were precipitated in order to remove salts and detergents that could interfere with the subsequent *O*-glycan analysis. Then, the *O*-glycans were released as glycan alditols using β-elimination, permethylated and analyzed via MALDI mass spectrometry (reaction scheme see appendix Figure 25).

In the spectrum of the *O*-glycome of mouse brain (see Figure 9) the observed mass-to-charge (m/z) values correspond to the sodium ion adducts (Na^+) with a single positive charge. In addition, signals with an m/z difference of 36 to the regular signals were often observed. These may arise during the chemical glycan release or the permethylation reaction and represent the loss of sodium methylate. All glycan signals observed in this study are summarized in appendix Table 6. The *O*-glycans of mouse brain mainly showed the typical masses of mucin-type *O*-glycans. The mono- and disialylated core 1 glycans at m/z values of 895.5 and 1256.6 were confirmed by MS/MS as well as the sialylated core 2 structure at m/z 1344.7. Some signals were also found to correspond to masses of *O*-mannosyl glycans. By fragmentation analysis the signals at m/z ratios of 912.5, 1099.6 and 1910.0 were proven to resemble the fucosylated, sialylated and branched *O*-mannosyl glycans, respectively. A rough estimation of the relative amounts of mannose-based oligosaccharides in comparison to mucin-type glycans revealed that in mouse brain about 30 percent of the *O*-glycans are *O*-mannosyl glycans.

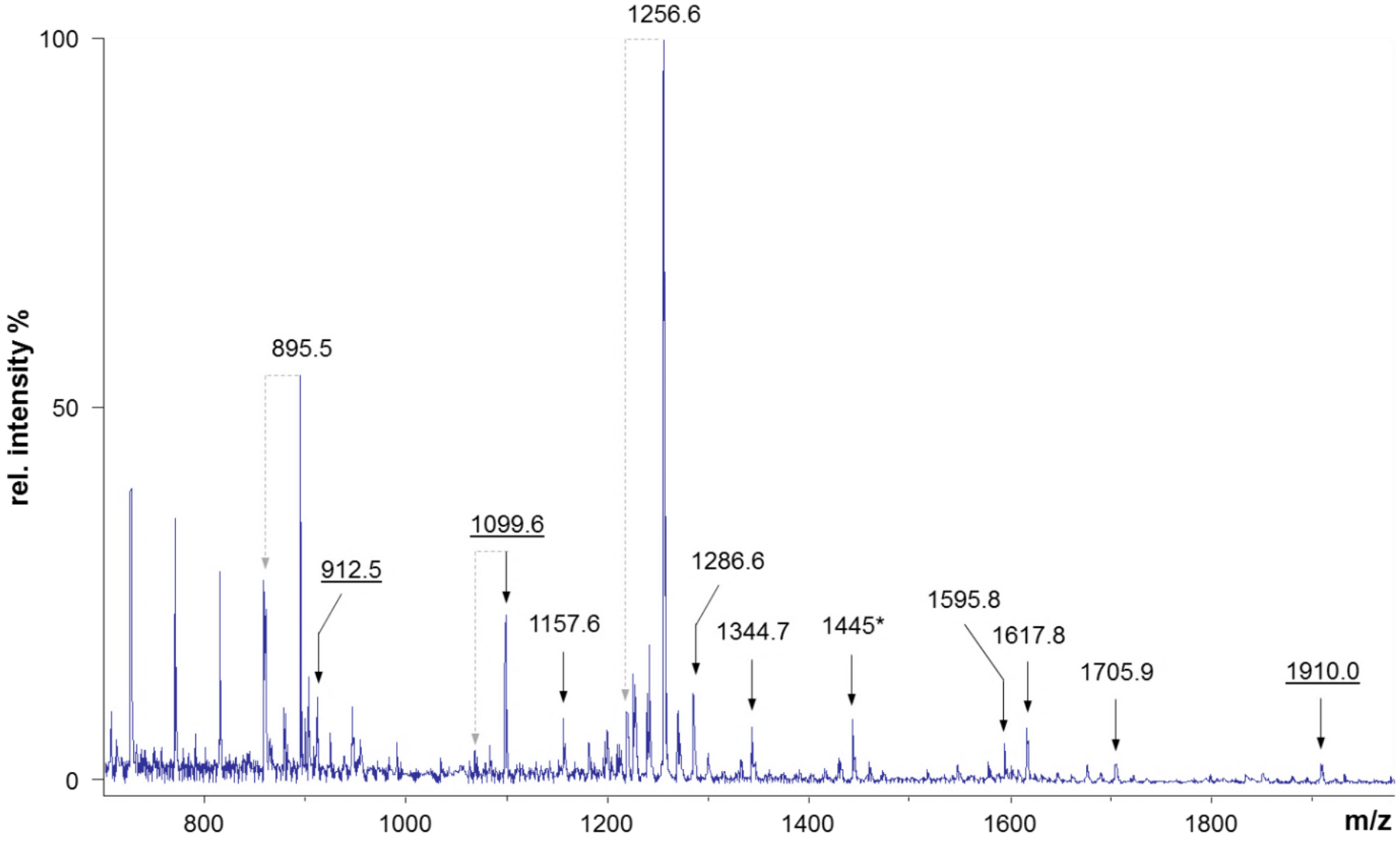

Figure 9: *O*-Glycome of mouse brain. MALDI-TOF spectrum of permethylated *O*-glycan alditols derived from mouse brain after WGA enrichment of glycoproteins. Signals indicated with an asterisk are derived from *N*- or *O*-glycan fragments generated by in-source fragmentation. Monoisotopic masses corresponding to *O*-mannosyl glycans are underlined. Dashed arrows indicate signals derived by a loss of a methyl group and sodium (-36).

The *O*-glycome of calf brain showed mostly identical signals as were observed in the mass spectrum of mouse brain *O*-glycans (see appendix Figure 26 for a comparison between the *O*-glycans from mouse and calf brain). Apart from several mucin-type glycans, the sialylated *O*-mannose structure at an m/z value of 1099.6 was observed in calf brain.

3.1.2 Fractionation of mouse brain proteins

For the isolation of *O*-mannosylated proteins an unbiased fractionation approach was to be used since a purposive isolation, for example by immune purification, was not possible. Because of the similarity of the exposed glycan epitopes of *O*-mannose-based glycans with other *O*- and *N*-glycans until now no antibody has been generated that specifically recognizes *O*-mannose glycans. Therefore, a suitable enrichment scheme consisting of different consecutive fractionation steps was to be developed. With this objective in mind different techniques were tested regarding their ability to enrich and fractionate *O*-mannosylated proteins from mouse brain.
First, the solubility of *O*-mannosylated proteins was analyzed using sequential protein extraction. During sequential solubilization the proteins are partitioned by applying reagents with different solubilization power. Beginning with a buffered aqueous solution that does not affect membranes, the solubilization efficiency is increased stepwise through the addition of chaotropic agents and detergents (see Table 1). Mouse brain proteins were sequentially extracted into four fractions, the protein yield was determined and the *O*-glycans were analyzed as described before. The gentler extractions, namely the aqueous (1) and the urea/CHAPS extraction (2), together were already able to solubilize nearly 90 percent of the total proteins compared to an extract completely solubilized with SDS. Also, only in these fractions *O*-mannosyl glycans were observed which indicates that mainly ECM proteins and proteins which are lightly attached to the membrane are *O*-mannosylated. Hence, a mild solubilization using the detergents CHAPS or Triton X-100 was chosen for all subsequent analyses.

Table 1: Sequential extraction of mouse brain proteins. Extraction steps are shown with their expected protein content according to (Chan *et al.*, 2002). Protein yield in percent of total protein content (n. d.: not determined) and results of the *O*-glycan analysis (+: *O*-mannose glycans present; -: *O*-mannose glycans not observed).

Extraction step	Proteins extracted	Protein yield	*O*-man glycans
1. aqueous extraction	easily soluble proteins (cytosolic and secreted proteins)	64 %	+
2. urea/CHAPS extraction	moderately soluble proteins (membrane-, cytoskeleton- or ECM-associated proteins)	23 %	+
3. enhanced solubilization	badly soluble proteins (membrane proteins)	n. d.	-
4. SDS solubilization	residual proteins		-

After the solubilization the glycoproteins were to be enriched using WGA affinity chromatography as described above. The efficacy of this glycoprotein enrichment was tracked via the *O*-glycan analysis of flow-through and eluate (see appendix Figure 27). In comparison to the WGA eluate (glycoprotein fraction) the flow-through (unbound proteins) showed no measureable glycan signals indicating that most glycoproteins were effectively enriched in the eluate. The silver-stained SDS-PAGE gel (see appendix Figure 28) demonstrates that both fractions contained a multitude of proteins although the glycoprotein fraction (E) harbored only proteins with molecular weights greater than 40 kDa.

The mouse brain glycoproteins were then subjected to gel permeation chromatography (GPC) in which proteins can be fractionated by size. Bigger proteins are not well retained by the gel matrix and therefore they elute prior to smaller proteins. In this case four protein containing fractions were generated from the mouse brain glycoproteins. As can be seen in the silver-stained gel in Figure 10B a size dependent division was achieved. *O*-Glycan analysis of each GPC fraction revealed that the *O*-mannosylation was present in high amounts in the first two fractions (F1 and F2) which contained proteins of all sizes while it was absent in the two fractions with smaller proteins (F3 and F4) showing that almost all *O*-mannosylated proteins can be found in the high mass range.

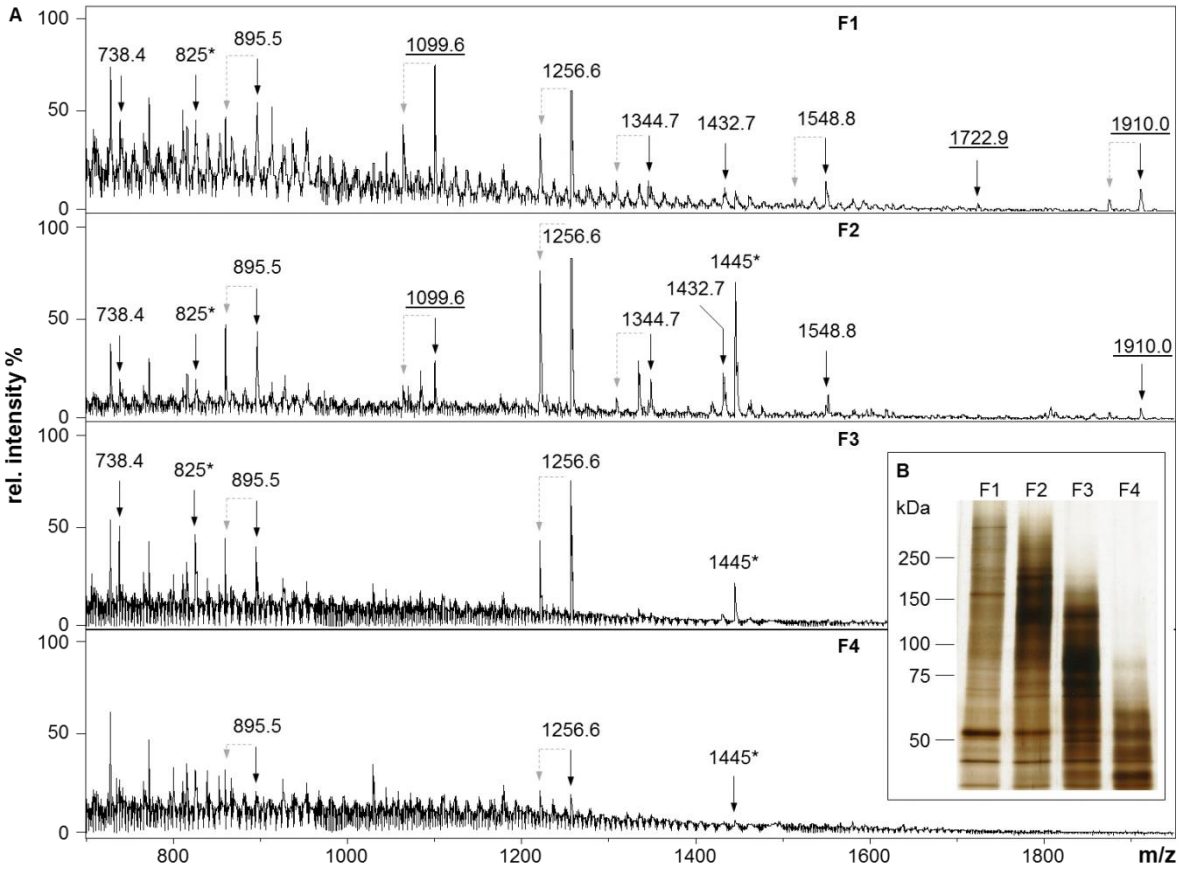

Figure 10: Mouse brain glycoprotein fractionation using gel permeation chromatography. (A) MALDI-TOF spectra of permethylated *O*-glycan alditols derived from the generated GPC fractions F1 to F4. Signals indicated with an asterisk are derived from *N*- or *O*-glycan fragments generated by in-source fragmentation. Monoisotopic masses corresponding to *O*-mannosyl glycans are underlined. Dashed arrows indicate signals derived by a loss of a methyl group and sodium (-36). (B) Silver-stained SDS-PAGE gel of the GPC fractions.

In another approach the mouse brain glycoproteins were fractionated by size using preparative SDS-PAGE. In this case twenty protein-containing fractions were generated (see appendix Figure 29 for an SDS-PAGE gel) and analyzed regarding their respective *O*-glycan content (summary in appendix Table 7). Only fractions containing proteins with SDS-PAGE mobilities greater than 100 kDa showed detectable *O*-mannosylation which is in accordance with the results of the GPC fractionation. Fractions F19 to F21 all showed high amounts of *O*-mannosyl glycans. Since they share a common gel band at about 190 kDa protein identification was performed with fraction F21. The distinct band at 190 kDa was excised and the tryptic peptides were analyzed via ESI-MS. The resulting Mascot scores for the mouse proteins are shown in Table 8 (appendix). In all Mascot results shown in this thesis the significance threshold for protein scores was set to 90. Contaminating keratin and trypsin fragments are not shown since these are not relevant in the *O*-mannose context. The predominant protein in the sample from F21 was neurofascin indicating

that this protein might be *O*-mannosylated. But other secreted proteins such as tenascin-R or neural cell adhesion molecule 1 (NCAM1) were also detected and could be modified with *O*-mannose. All in all, the fractions resulting from preparative SDS-PAGE after WGA enrichment of glycoproteins were still too complex for a further analysis of the fractions and a definite identification of the *O*-mannosylated proteins.

3.1.3 Summary

During the first part of this thesis the course for the actual examination was set. I was able to show that mouse and calf brain contain significant amounts of *O*-mannosylated proteins with the sialylated *O*-mannosyl tetrasaccharide being the prevalent *O*-mannose-based structure. In accordance with Chai *et al.*, who found that about 30 percent of the pronase-stable glycopeptides of rabbit brain are initiated by mannose (Chai *et al.*, 1999), mouse brain proteins also harbor about 30 percent of *O*-mannose oligosaccharides. Calf brain proteins contain the *O*-mannose modification to a lesser extent (20-25 percent). Still, both species seem suitable for the purification of *O*-mannosylated proteins.

The evaluation of different fractionation methods for the efficient enrichment of proteins modified by *O*-mannosylation showed that mainly easily accessible proteins carry this kind of modification since they could be solubilized by mildly denaturing conditions. These are mainly secreted proteins and proteins weakly associated to the membrane. The proteins known to be *O*-mannosylated are consistent with this finding. α-DG and phosphacan both are secreted proteins whereby α-DG is attached to the transmembrane protein β-DG via a non-covalent linkage. CD24 is bound via a single GPI-anchor while RPTPβ has a single transmembrane-spanning region. All of these anchors can be easily solubilized.

It has been shown that the glycoproteins of mouse brain can effectively be enriched using WGA affinity chromatography while no glycoproteins were detected in the unbound protein fraction. The GPC resulted in four protein-containing fractions of which the two fractions containing only small proteins did not show any *O*-mannosylation. Therefore, this technique was chosen as a prefractionation method in order to reduce the content of glycosylated but not *O*-mannose modified proteins in the sample applied to preparative SDS-PAGE. During preparative gel electrophoresis the glycoproteins were fractionated by size into twenty fractions but these fractions

mostly were still too complex to be suitable for further analysis. Therefore all of the above mentioned methods were combined. The complete fractionation scheme used as an unbiased approach to isolate *O*-mannosylated proteins is depicted in Figure 11.

Similar to GPC, no *O*-mannosylation was detected in preparative SDS-PAGE fractions containing proteins with apparent molecular weight below 100 kDa. These findings suggest that only high molecular weight proteins and highly glycosylated proteins are modified with *O*-mannose. This is also supported by the fact that the known *O*-mannosylated proteins all are highly glycosylated. Therefore they show low electrophoretic mobilities during SDS-PAGE.

In these first experiments a candidate protein which might carry *O*-mannosyl glycans was identified – neurofascin. Therefore, this protein was to be purified and analyzed regarding potential *O*-mannosylation in the second part of this study.

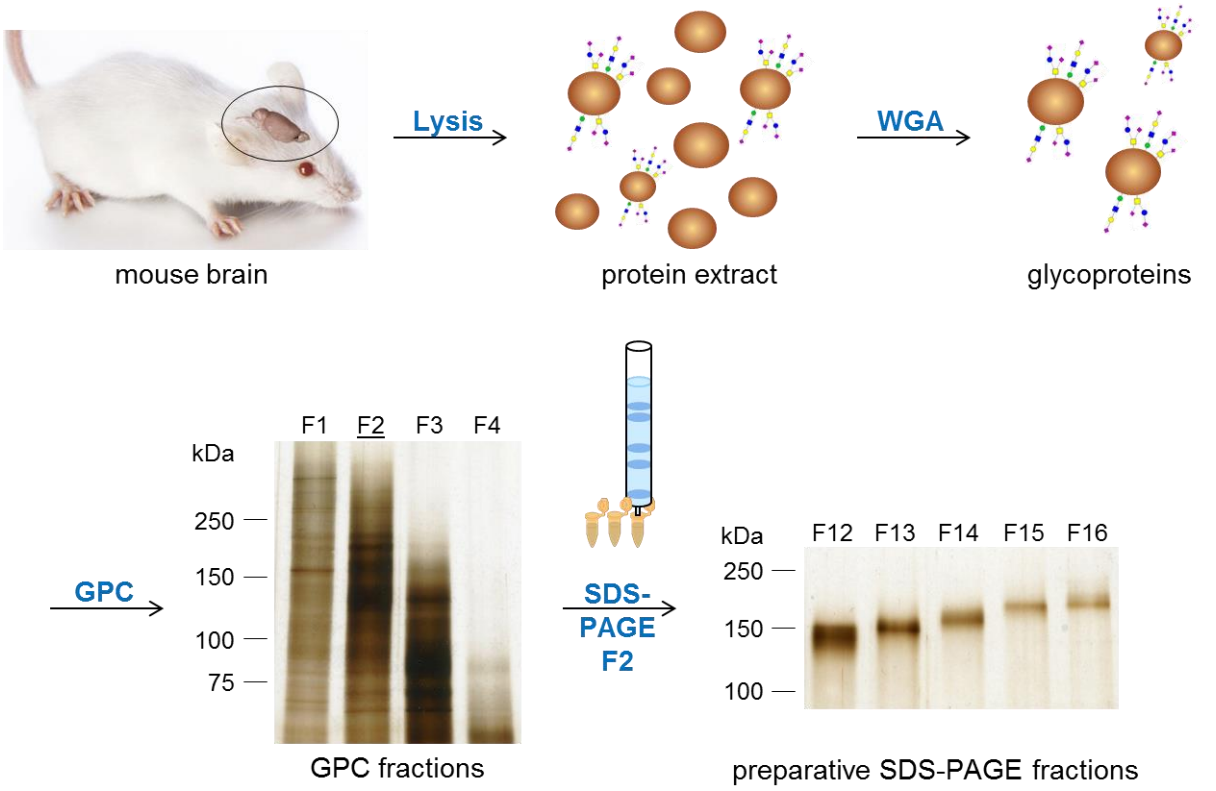

Figure 11: Fractionation scheme for mouse brain. After the lysis of mouse brain the glycoproteins are enriched using WGA affinity chromatography. These are prefractionated using gel permeation chromatography and the proteins from GPC fraction F2 are further fractionated by preparative SDS-PAGE. Exemplary SDS-PAGE gels of the four GPC fractions and some preparative SDS-PAGE fractions are shown.

3.2 *O*-Mannosylation on neurofascin

In the search for novel *O*-mannosylated proteins a BLAST analysis based on the *cis*-controlling peptide needed for the initiation of the *O*-mannose modification on α-DG (Breloy *et al.*, 2008) was performed. This analysis, optimized for short peptides, revealed several mammalian proteins which harbor a peptide region similar to the determinant in α-DG. One protein among these hits also sharing other features with α-DG was the neurofascin splice variant 186 (see Figure 12 for BLAST result for neurofascin, see appendix Table 9 for the other results): Both proteins are anchored to the membrane, harbor large mucin domains and were shown to establish a link between the cytoskeleton and the extracellular matrix. In addition, neurofascin had been identified as a possible *O*-mannosylated protein during the fractionation experiments (see 3.1.2). Therefore, neurofascin was chosen as a first candidate to be isolated from mouse brain and analyzed regarding potential *O*-mannosylation.

neurofascin [Homo sapiens]	Query 16 EAGTTVPGQIRPTMTIPGYVEPTAVAT 42 EA TTVP I PT V PT +AT Sbjct 1062 EA·TTVP··IIPT·····VAPTTIAT 1080

Figure 12: BLAST analysis of the *cis*-controlling peptide. Depicted here are the homologies of the primary sequence between the peptide region of human α-DG (Query) and human neurofascin (Sbjct).

3.2.1 Purification of neurofascin isoform 186 from mouse brain

To check mouse brain for the presence of neurofascin isoform 186 Western blot analysis was performed (see Figure 13). As can be seen the main splice variant occurring in mouse brain was NF186 (about 75 percent according to imageJ analysis) while the other isoforms were only present in minor amounts. This shows that mouse brain is suitable for the purification of NF186.

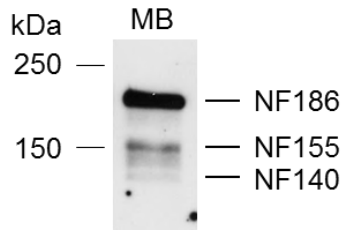

Figure 13: Western blot of whole mouse brain lysate (MB). With the anti-neurofascin antibody different splice variants can be observed. NF186 is the main isoform present in mouse brain (about 75 percent) and NF155 (2 bands) and NF140 are present in minor amounts.

For the isolation of NF186 the glycoproteins from mouse brain lysates were enriched using WGA affinity chromatography and fractionated via GPC and preparative gel electrophoresis as depicted in the fractionation scheme in Figure 11. The fractionation process was performed twice (experiment (A) and experiment (B)). During GPC the glycoproteins were fractionated into four protein-containing fractions, F1 to F4 (silver-stained SDS-PAGE gels for (A) and (B) shown in appendix Figure 30). Fraction F2 was subjected to preparative gel electrophoresis since it harbored proteins in the desired molecular weight range of 100 to 200 kDa. The preparative SDS-PAGE generated 25 protein containing fractions (see appendix Figure 31 for silver-stained SDS-PAGE gels (A) and (B)). Proteins with an apparent molecular mass of about 186 kDa were observed in the fractions F18 to F22 (A) and F15 and F16 (B). The gel also showed that with this fractionation protocol defined fractions were generated which contained only a few proteins per fraction and thus were suitable for further analysis.

In order to confirm the presence of neurofascin Western blot analysis was applied to fraction F19 (A) and F15 to F18 (B) (see appendix Figure 31). As you can see positive signals were observed in fractions F19 (A) and F15 to F17 (B) so these fractions were analyzed in more detail.

3.2.2 *O*-Mannosylation of neurofascin 186

Fraction F18 of experiment (A) which showed a similar pattern in the SDS-PAGE gel as F19 was subjected to protein identification by LC-MS analysis of tryptic peptides (see insert in Figure 14 for Mascot results). The most abundant protein was neurofascin with a Mascot score of 921 while contaminating proteins had scores less than 445. Sodium/potassium-transporting ATPase and excitatory amino acid transporter are transmembrane proteins not relevant in the *O*-mannosylation context. The only secreted protein occurring with considerable amount in the fraction which was known to be glycosylated but had not yet been analyzed for potential *O*-mannosylation was NCAM1. Mouse brain NCAM1 purified by immunoprecipitation was kindly provided by Dr. Mühlenhoff from the Hannover Medical School. The protein identification of the sample revealed that NCAM1 indeed was the only component of the sample in addition to the immunoglobulins used for purification (see insert in appendix Figure 32). The *O*-glycan analysis showed only the core 1 mucin-type glycan at an m/z ratio of 1256.6 and fragments of polysialic acid,

identified by several 361 increments which correspond to the mass of one neuraminic acid residue (see appendix Figure 32). The monoisotopic signal at 1098.8 corresponds to three neuraminic acid residues without a reduced end as can be seen in the fragmentation analysis. Thus, NCAM1 does not carry an *O*-mannosyl modification.

The O-glycan analysis of fraction F18 (A) (see Figure 14) showed the presence of *O*-mannosylation in the form of the fucosylated (m/z = 912.5), the sialylated (m/z = 1099.6) and the branched (m/z = 1910.0) structures. The *O*-glycan structures were confirmed by fragmentation analysis (see Figure 15 for MS/MS of m/z = 1099.6). The fragmentation mainly led to ions of the B and Y series according to the nomenclature of Domon and Costello (Domon & Costello, 1988). While ions of the Y-series were mainly observed as sodium adducts the B-ions occurred primarily as proton adducts. All relevant signals of the *O*-mannose based glycan chain (NeuAcα2-3Galβ1-4GlcNAcβ1-2Man-ol) were present for example the characteristic signal at m/z of 724.4 of the oligosaccharide without the terminal sialic acid ($Hex_2HexNAc + Na^+$). The Y_1-signal at m/z 275.1 corresponds to a permethylated Hexol which shows that the observed glycan harbors a core hexose and not a core *N*-acetylhexosamine. Thus, the glycan structure was identified as a mannose-based glycan.

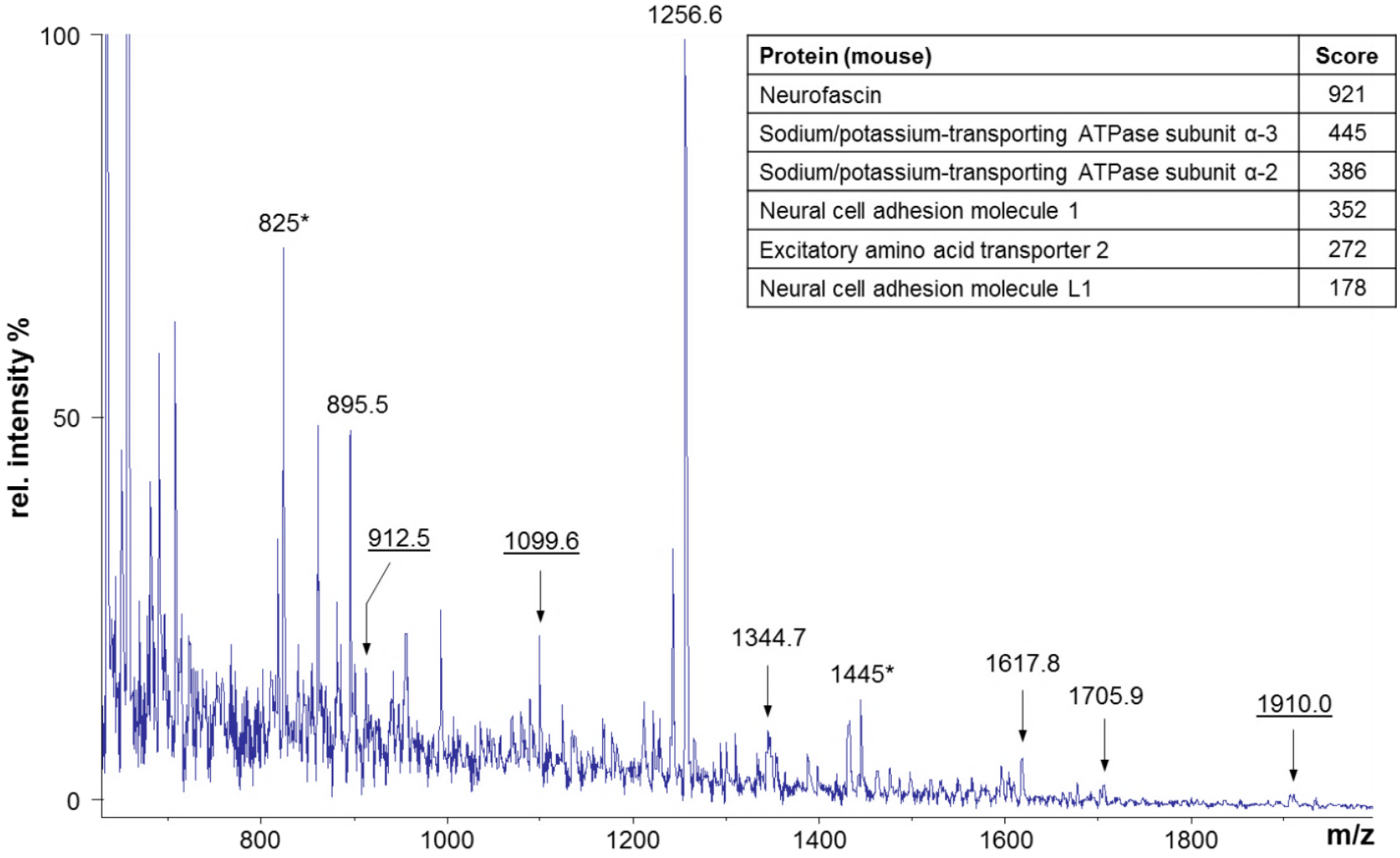

Figure 14: *O*-glycome of sample F18 (experiment A). MALDI-TOF spectrum of permethylated glycan alditols originating from fraction F18. Signals indicated with an asterisk are derived from *N*- or *O*-glycan fragments generated by in-source fragmentation. Monoisotopic masses corresponding to *O*-mannosyl glycans are underlined. The proteins identified by LC-MS of tryptic peptides are depicted in the insert (together with their respective Mascot score).

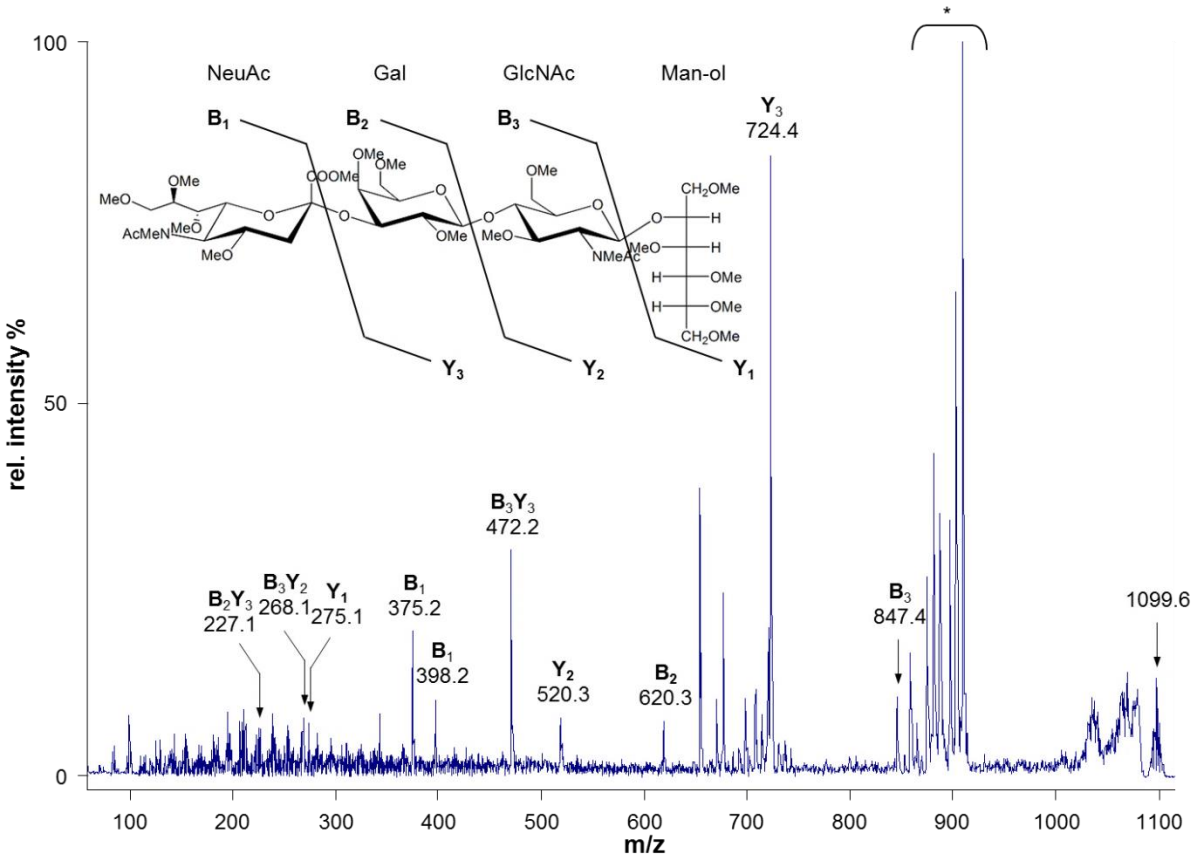

Figure 15: Fragmentation spectrum (MS/MS) of the *O*-mannose derived signal at m/z = 1099.6. Y-ions were detected as sodium adducts, B-ions as proton adducts. The asterisk indicates matrix derived signals. In the fragmentation scheme of the permethylated glycan alditol NeuAcα2-3Galβ1-4GlcNAcβ1-2Man-ol the fragmentation is indicated.

3.2.3 Glycopeptide analysis of neurofascin 186

In order to localize the *O*-mannosylation sites on neurofascin a suitable fraction (Mascot results see appendix Table 10) was digested with trypsin and GluC in order to generate small peptides which can be analyzed by LC-MS. These peptides were subjected to CID fragmentation after liquid chromatography and the generated mass spectra (MS/MS) were searched for glycopeptides with potential *O*-mannosylation by looking for oxonium ions with an m/z value of 528 ($Hex_2HexNAc + H^+$). Spectra with an additional signal at m/z 690 ($Hex_3HexNAc + H^+$) were identified as *N*-glycosylated peptides and not analyzed further. By CID fragmentation mainly the glycan chains are fractionated while not much information can be obtained regarding the peptide backbone. Therefore, glycopeptide spectra were discarded if the peptide mass could also correspond to one of the contaminating proteins. One glycopeptide originating from neurofascin could be identified as *O*-mannosylated (see appendix Figure 33). The peptide sequence could be identified by the mass of the naked peptide

(m/z = 2312.2) and the partial peptide fragmentation. The peptide LYFSNVMLQDMQTDYSCNAR has three potential *O*-glycosylation sites and was found to be modified with two *O*-glycans: an *O*-mannose glycan ($NeuAcHex_2HexNAc$) and a mucin-type glycan (NeuAcHexHexNAc). These were assigned based on the oxonium ions of the free glycans (for example the complete *O*-mannose glycan at m/z of 819) and the glycan fragmentation ions of the glycopeptides.

However, the finding of the above mentioned glycopeptide is the only result obtained using the CID fragmentation approach. Therefore, protein fraction F15 from experiment (B) which showed a high amount of neurofascin based on the Western blot analysis was subjected to a glycopeptide analysis using the Orbitrap system. This LC-ESI system allows further fragmentation of the highest MS/MS signals thereby generating spectra with glycan fragmentation as well as peptide fragmentation (MS3). The proteins of F15 were digested with trypsin and GluC and the resulting peptides and glycopeptides were analyzed by LC-ESI-MS/MS. The Mascot search of these peptides (see Table 2) revealed that neurofascin was the predominant component. NCAM1 which also was present in the sample had already been shown not to carry the *O*-mannosyl modification. In addition, a few other proteins such as neurexin and tenascin-R were present which had not yet been analyzed for potential *O*-mannosylation. Therefore, glycopeptide spectra were discarded if the peptide mass could also correspond to one of these proteins in case no conclusive MS3 data were available.

Table 2: Protein identification based on Mascot results of protein fraction F15 (B).

Protein (mouse)	Score
Neurofascin	443
Neural cell adhesion molecule 1	373
Neurexin-1-α	325
Sodium/potassium-transporting ATPase subunit α-1	297
Sodium/potassium-transporting ATPase subunit α-3	254
Tenascin-R	206
Neurexin-3-α	164
Neurocan core protein	161
Neural cell adhesion molecule L1-like protein	140
Seizure protein 6	104

Many identified peptides were highly modified, almost all were carbamylated and several dehydrated possibly due to the multistep purification procedure under harsh conditions. Several peptides modified with *O*-mannosyl glycans were found by searching for MS/MS spectra containing an m/z signal of 528. The peptide NNSPITD (amino acids 654–660 of NF, m/z = 760.4, modified by carbamylation and dehydration) was found to be *O*-mannosylated with an appropriate MS3 spectrum showing the unequivocal amino acid assignment (see Figure 16). The peptide was modified with $Hex_4HexNAc_4Fuc$ and despite the presence of a consensus sequence not *N*-glycosylated since no typical fragmentation of core HexNAc could be observed. The fragmentation pattern instead revealed a modification with a mucin-type glycan ($FucHex_2HexNAc_3$) at the serine residue and an *O*-mannosyl glycan ($Hex_2HexNAc$) at the threonine residue as retrieved from the MS3 spectrum.

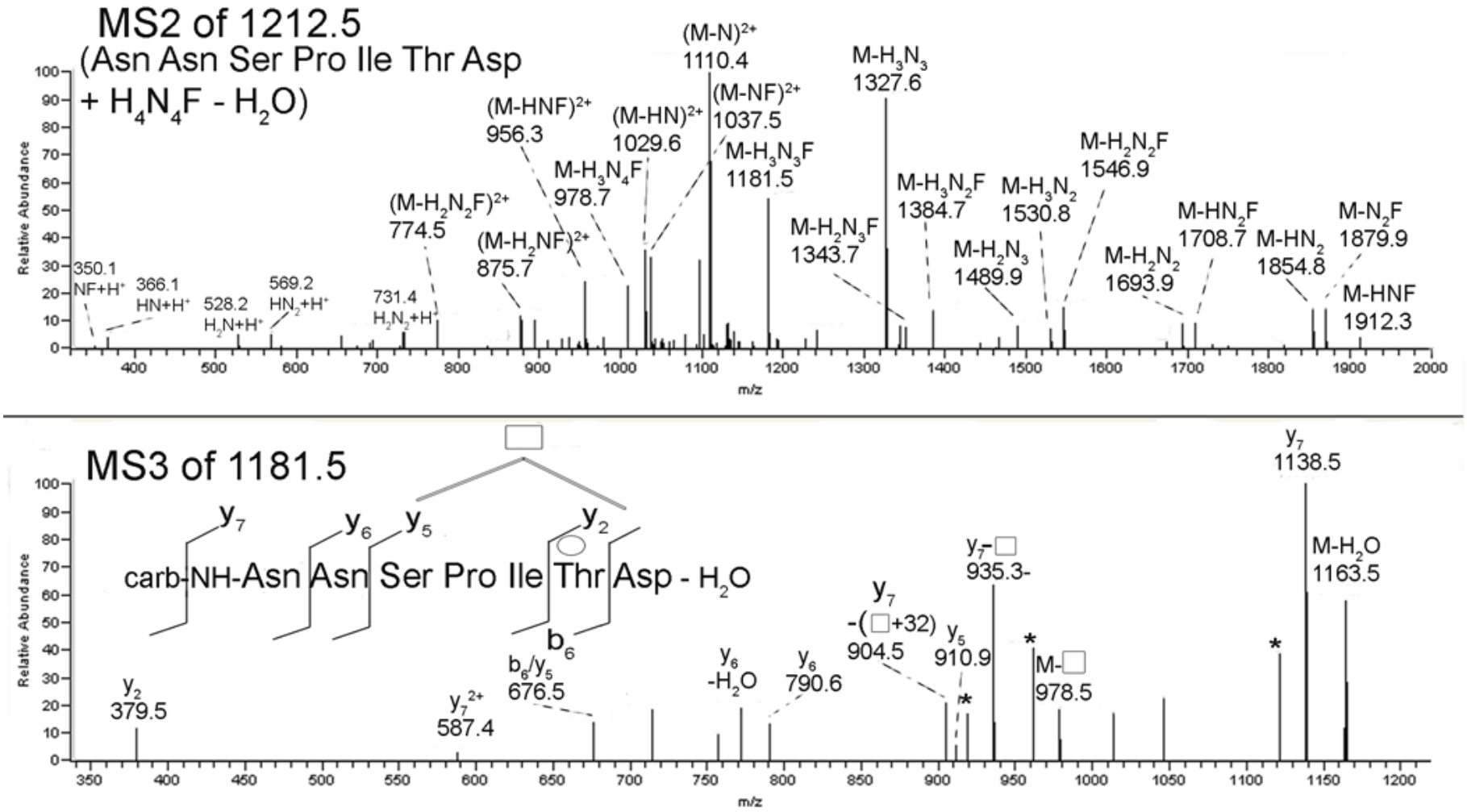

Figure 16: ESI-MS3 of the *O*-mannosylated and mucin-type *O*-glycosylated glycopeptide NNSPITD from neurofascin. The peptide is modified with $Hex_4HexNAc_4F$ (m/z = 2424.0), N-terminally carbamylated and dehydrated. In addition a double oxidation (+32 Da) at an unidentified region was observed. The fragmentation pattern revealed a mucin-type *O*-glycosylation at the serine residue and an *O*-mannosyl glycosylation at the threonine residue (abbreviations: H: Hex, N: HexNAc, F: Fuc, M: peptide, square: HexNAc, circle: Hex).

Three other *O*-mannosyl glycopeptides of neurofascin could be identified using this approach (see appendix Figure 34 for second example). The peptide RSGTLVINFR (amino acids 95-104 of NF, m/z = 1163.6 modified by carbamylation) was shown to be modified with the typical *O*-mannosyl tetrasaccharide $NeuAcHex_2HexNAc$ as indicated by the glycopeptide signals with the stepwise loss of the saccharide moieties. The peptide was identified by its naked mass (m/z = 1229.5) and partial fragmentation observed in the MS/MS spectrum. The other two peptides were FSLARTQVGSGE (amino acids 898-910 of NF, modified by $Hex_3HexNAc_2$ corresponding to a branched O-mannose glycan) and RPRDLELTD (amino acids 630-638 of NF, modified with $NeuAcHex_3HexNAc_2$ corresponding to mucin-type and O-mannose-based glycans).

3.2.4 Conclusion

In this part was shown that neurofascin from mouse brain is *O*-mannosylated. NF isoform 186 was isolated using the combined fractionation approach with only minor amounts of contaminating proteins. The *O*-glycan analysis revealed that NF186 is modified with fucosylated, sialylated and in minor amounts also branched *O*-mannose glycans. Also high amounts of several mucin-type glycans were found whereby the disialylated core 1 structure resembles the predominant modification.
The glycopeptide analysis of endogenous protein proved to be challenging because of the following reasons: First, it was not possible to completely purify NF without any contaminating proteins so that all glycopeptide spectra had to be checked closely regarding the origin of the peptide. NCAM1 was a typical contaminant present in the NF186 fractions. *O*-Glycan analysis of purified NCAM1 showed that this protein is not modified by *O*-mannosylation. Instead, mainly fragments of *N*-glycosidically bound polysialic acid were detected which is possible since *N*-glycan fragmentation sometimes occurs during β-elimination. Indeed, NCAM1 was the first protein shown to be modified by the rare polysialic acid modification of *N*-glycans (Hoffman *et al.*, 1982). Second, the heterogeneity of glycosylation causes a low abundance of one specific glycopeptide species compared to a non-glycosylated peptide. Third, during LC-ESI-MS the presence of non-glycosylated peptides leads to a suppression of glycopeptide signals (Morelle *et al.*, 2006) which results in an even further decrease in sensitivity. Therefore, only a few glycopeptides could be detected in each sample and from those only a fraction was modified with *O*-mannose.

So far, no reliable method for the efficient enrichment of *O*-glycosylated peptides in the presence of non-glycosylated peptides exists. Several methods described for the enrichment of *N*-glycopeptides were tested (data not shown) but none proved to be suitable for *O*-glycosylated peptides. The reason for this might be that the methods mainly rely on the hydrophilicity change caused by the attachment of an *N*-glycan to a peptide. But *O*-glycans are much smaller than *N*-glycans and therefore their hydrophilic properties do not dominate the overall hydrophilicity of an *O*-glycopeptide. The glycopeptide analysis led to the identification of several neurofascin-derived peptides modified by *O*-mannosylation. Surprisingly, the identified peptides did not originate from the mucin domain of NF186 as in the case of α-DG. Instead, *O*-mannose glycans were detected on fibronectin type-III and Ig-like domains (see Figure 17). These domains do not contain a region similar to the *cis*-controlling peptide of α-DG. Therefore, the signals leading to an *O*-mannosylation in these domains are unknown. The reason why no *O*-mannosylated peptides from the mucin domain were detected might be that the enzymatic digestion is hindered by the extensive glycosylation present in this region. In addition generated peptides would have been highly glycosylated and therefore hard to be analyzed by LC-MS. A glycopeptide analysis of the recombinantly expressed mucin domain of NF186 revealed the presence of *O*-mannosyl glycans on several peptides (Pacharra *et al.*, 2012). Together, these results suggest that neurofascin is *O*-mannosylated in the mucin domain, possibly initiated by the *cis*-located determinant identified in the BLAST search, and outside of the mucin domain where the initiation mechanism remains unclear.

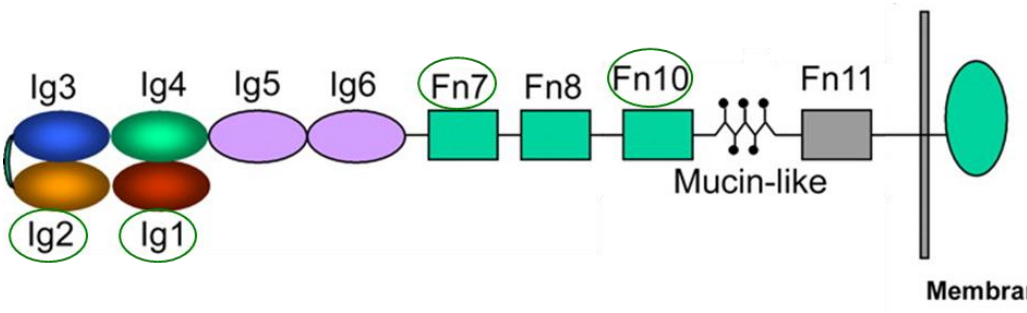

Figure 17: Schematic view of the domain composition of neurofascin 186. Green circles indicate domains that were found to be *O*-mannosylated in mouse brain (Ig-like domains 1 and 2 and fibronectin type-III domains 7 and 10). Modified from (Liu *et al.*, 2011).

3.3 *O*-Mannosylation of lecticans

3.3.1 *O*-Glycan analysis of lecticans from mouse brain

Apart from the analysis of neurofascin-containing fractions other mouse brain fractions were and analyzed regarding their *O*-glycosylation and protein content generated (see appendix Figure 35 for a gel of fractions from GPC (A) and preparative SDS-PAGE (B), see Figure 11 for fractionation scheme). Many of the higher molecular weight fractions (> 150 kDa) containing high amounts of *O*-mannosyl glycans were found to comprise brevican or neurocan or both of these proteins. An exemplary MALDI-MS result of one of these fractions (F24) is shown in Figure 36 (appendix). The *O*-mannose glycans at m/z ratios of 912.5, 1099.6 and 1910.0 were confirmed by fragmentation analysis, which is depicted in Figure 37 (appendix) for the branched structure (m/z = 1910.0). The protein identification revealed the presence of brevican and neurocan (see appendix insert in Figure 36) in this fraction but also other secreted glycoproteins were present such as tenascin-R which had not been analyzed regarding potential *O*-mannosylation.

In an attempt to purify tenascin-R from mouse brain by immunoaffinity chromatography (kindly provided by Prof. Dr. Faissner from Ruhr University Bochum) a sample comprising the fucosylated and sialylated *O*-mannosyl glycans was obtained (see appendix Figure 38). However, the protein identification (see appendix Table 11) revealed that the lecticans neurocan, brevican and versican had been copurified. The reason for a copurification might be based on the fact that tenascin-R is a binding partner of all lecticans. The result shows that at least one member of this group of proteins (lecticans and tenascin-R) is *O*-mannosylated.

In an attempt to generate a tenascin-R-free lectican sample the hyaluronic acid-binding lecticans were purified by hyaluronan affinity chromatography of mouse brain lysate. The eluate showed a very high content of *O*-mannosyl glycans (see Figure 18), especially the sialylated structure which exhibited a higher signal than any mucin-type glycan. Protein identification revealed neurocan as the only *O*-glycoprotein (see Table 3). This shows that neurocan from mouse brain is indeed *O*-mannosylated whereby the sialylated *O*-mannose glycan seems to be the prevalent *O*-glycan. The other copurified proteins, for example the tubulin chains, mostly originate from the cytoplasm and presumably bind in an unspecific manner to the sepharose matrix. The only secreted protein beside neurocan that could be

detected in the hyaluronan eluate was hyaluronan and proteoglycan link protein 1, which is a small protein that binds hyaluronan and the lecticans. It is responsible for the stabilization of the link between these molecules and therefore it is easily copurified together with them.

Table 3: Protein identification of hyaluronan affinity-isolated mouse brain proteins. Shown are the Mascot scores.

Protein (mouse)	**Score**
Tubulin β-2A chain	1152
other tubulin chains	1113-764
60S ribosomal protein L7a	388
other ribosomal proteins	298-99
Myelin basic protein	277
Histone H4	202
Neurocan core protein	155
Hyaluronan and proteoglycan link protein 1	132
Calcium/calmodulin-dependent protein kinase type II subunit α	122
Glyceraldehyde-3-phosphate dehydrogenase	94

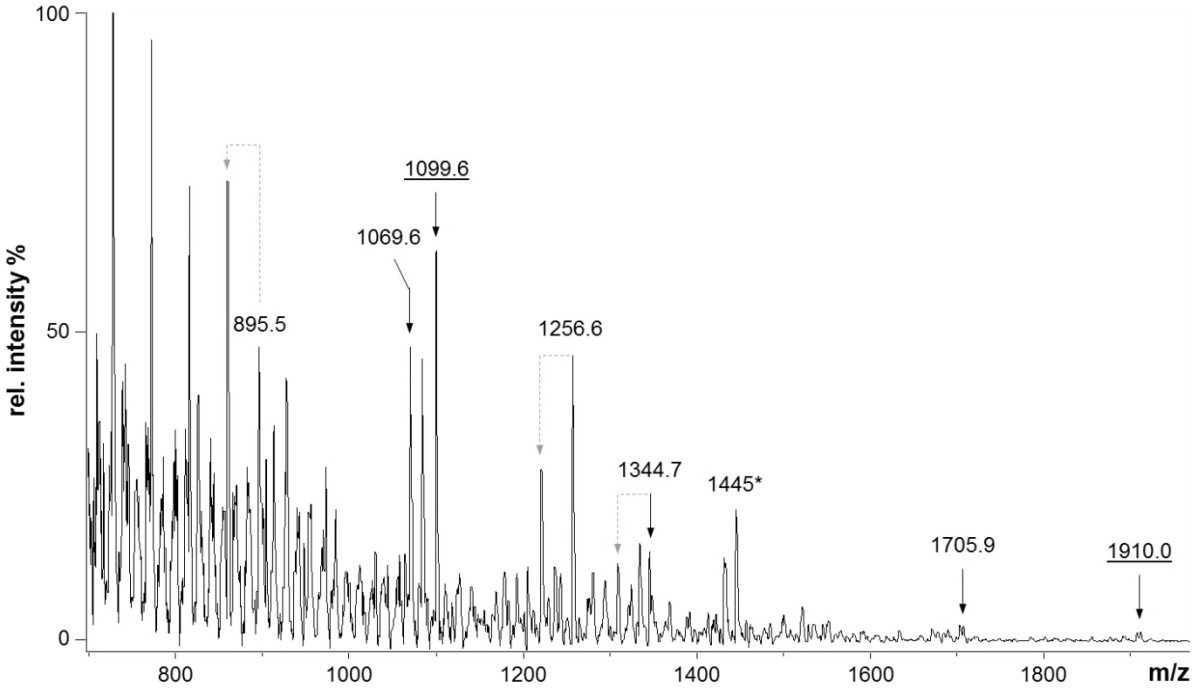

Figure 18: *O*-Glycoprofile of hyaluronan affinity-isolated mouse brain proteins. The MALDI mass spectrum shows permethylated *O*-glycan alditols. Monoisotopic masses corresponding to *O*-mannosyl glycans are underlined. Glycan fragments without a reduced end are indicated with an asterisk, arrows indicate signals derived by a loss of a methyl group and sodium (-36 Da).

3.3.2 Recombinant expression of neurocan

For further analyses of the functions of *O*-mannosylation a relatively high amount of almost pure protein would be needed. Therefore, the *O*-mannosylated protein neurocan should be expressed recombinantly in HEK293 cells. It was assumed that these cells are capable of *O*-mannosylation because Lommel *et al.* showed that POMT1 and 2 are expressed in kidney cells and show even higher mannose transferase activity than enzymes derived from muscle or nerve tissues (Lommel *et al.*, 2008). Also, the mucin domains of α-DG and neurofascin had been successfully expressed in these cells and were shown to be *O*-mannosylated (Breloy *et al.*, 2008; Pacharra *et al.*, 2012) although to lesser degrees than the endogenous proteins.
HEK293-EBNA cells expressing full length rat neurocan (kindly provided by Prof. Rauch from Lund University, Sweden) were cultivated and neurocan was purified from the cell supernatant using hyaluronan affinity chromatography (see Figure 19A for a silver-stained SDS-PAGE gel of the HA purification). The purity of the recombinant neurocan preparation was demonstrated by protein identification (see insert in Figure 20). The purified neurocan was treated with chondroitinase ABC in order to remove glycosaminoglycan chains (see Figure 19B) and was then subjected to *O*-glycan analysis. The *O*-glycan profile of recombinantly expressed neurocan (see Figure 20) revealed the presence of many different mucin-type glycans but no signals of *O*-mannose glycans were observed. The typical high modification with glycosaminoglycans was shown to be present by Western blot analysis of neurocan before and after digestion with chondroitinase ABC.

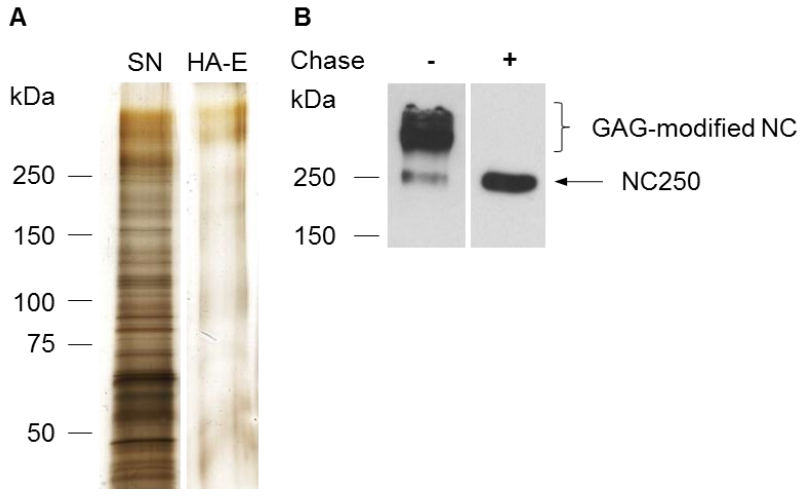

Figure 19: Purification of recombinant Neurocan. (A) Silver-stained SDS-PAGE gel of the crude cell supernatant (SN) of HEK293-EBNA cells expressing rat neurocan and the hyaluronan affinity purified neurocan (HA-E). (B) The Western blot shows the recombinant neurocan prior to (-) and after (+) Chondroitinase ABC (Chase) digestion.

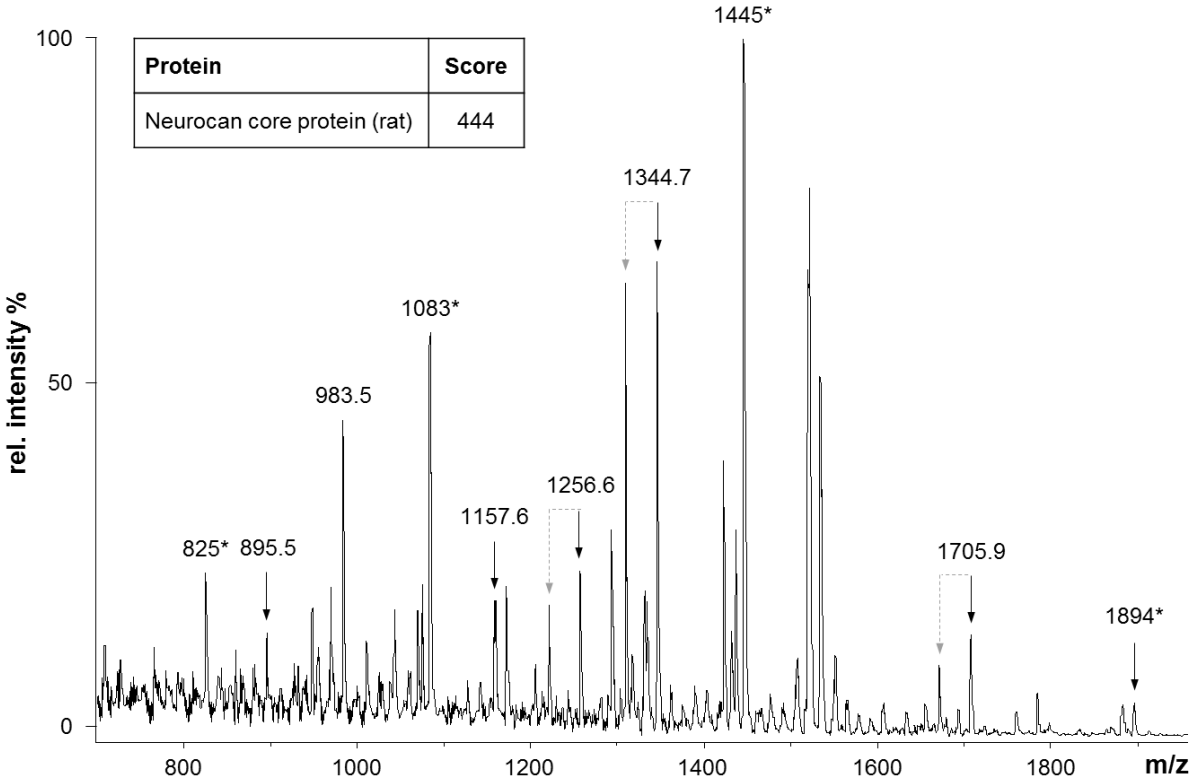

Figure 20: Analysis of recombinant neurocan. MALDI-MS of permethylated glycan alditols reveals only mucin-type *O*-glycans. Signals derived from nonreduced *N*-glycan fragments are indicated with an asterisk, dashed arrows indicate the loss of methyl and sodium (-36). The insert shows the protein identification by LC-MS/MS (Mascot score).

3.3.3 *O*-Glycan analysis of calf brain lecticans

In order to see if the lecticans were also *O*-mannosylated in another mammalian species and to upscale the purification procedure calf brain was applied instead of mouse brain. As the approach to purify the lecticans by hyaluronan affinity chromatography was not successful a multistep fractionation approach specific for the enrichment and fractionation of the lecticans from calf brain was developed (see appendix Figure 39 for fractionation scheme). Calf brain glycoproteins were enriched using WGA affinity chromatography as described for mouse brain. Because of the acidic isoelectric points of the lecticans and the acidic nature of the attached CS-GAG chains the glycoproteins from calf brain were then subjected to preparative free-flow isoelectric focusing (IEF). During free-flow IEF the proteins are separated into ten fractions according to their isoelectric points. As expected the majority of the proteoglycans could be recovered in the first, most acidic fraction F1 (see Table 4 for the protein identification). The lecticans neurocan, brevican and versican are the prominent components although other glycoproteins are also present. The known *O*-mannosylated proteins dystroglycan and phosphacan (also called RPTPζ) were

identified just as the glycoproteins that have not been analyzed regarding potential *O*-mannosylation (myelin-associated glycoprotein (MAG), seizure 6-like protein 2, contactin-1, chondroitin sulfate proteoglycan 5 and CD44). The hyaluronate-binding protein is a proteolytic product originating from versican and NCAM1 was already shown not to carry *O*-mannosyl glycans. *O*-Glycan analysis of this IEF fraction showed a high content of *O*-mannosyl glycans (see Figure 21) in addition to several mucin-type glycans.

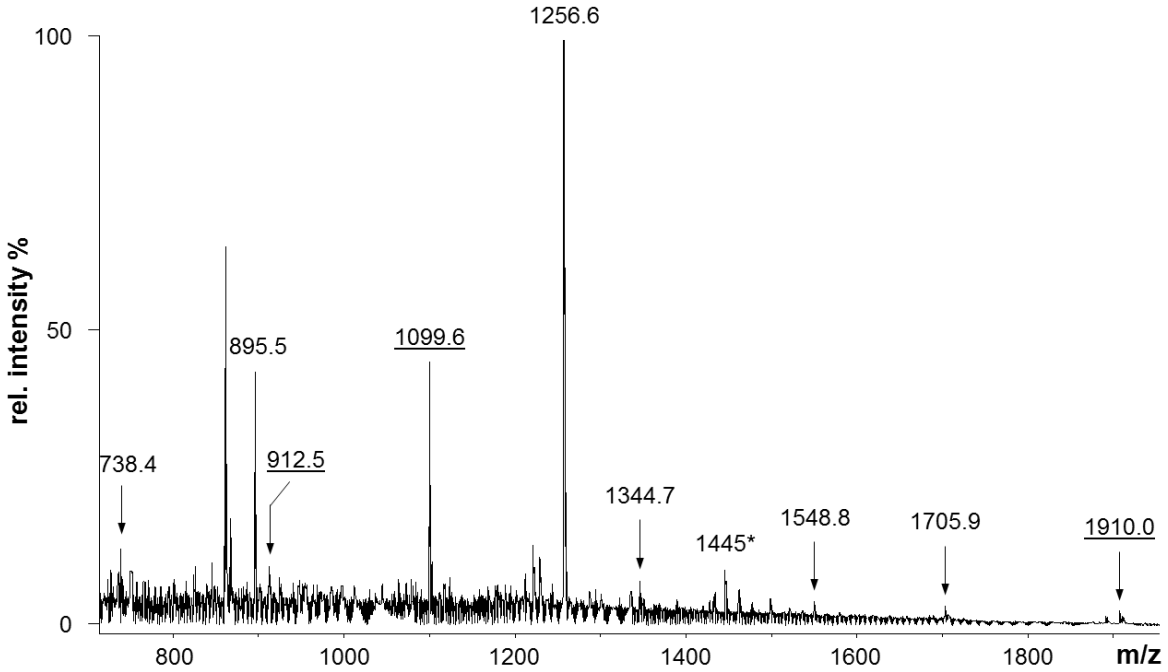

Figure 21: MALDI-MS of permethylated glycan alditols derived from isoelectric focusing fraction F1 of calf brain glycoproteins. Monoisotopic masses corresponding to *O*-mannosyl glycans are underlined. Signals derived from nonreduced *N*-glycan fragments are indicated with an asterisk.

Table 4: Protein identification of isoelectric focusing fraction F1 of calf brain glycoproteins. Shown are the Mascot scores.

Protein (bovine)	Score
Neurocan core protein	1194
Brevican core protein	1084
Versican core protein	794
Myelin-associated glycoprotein	660
Myelin basic protein	401
Seizure 6-like protein 2	318
Contactin-1	272
Dystroglycan	260
Tenascin-R	207
Receptor-type tyrosine-protein phosphatase ζ	199
Neural cell adhesion molecule 1	194
Chondroitin sulfate proteoglycan 5	155
Myelin-proteolipid protein	146
Hyaluronate-binding protein	138
CD44 antigen	131
L1 cell adhesion molecule	119

The lectican-rich IEF fractions F1 and F2 were combined and subjected to further fractionation by preparative gel electrophoresis. The whole fractionation process was performed twice with one difference: in experiment (A) the GAG chains were eliminated using chondroitinase ABC (Chase) digestion prior to preparative SDS-PAGE while in experiment (B) no digestion was performed. Due to the GAG digestion the proteoglycans in experiment (A) have reduced molecular weights and were thought to show less heterogeneity. This effect can be seen in Figure 40A (appendix) using the example of neurocan. While native neurocan from calf brain shows a broad band between 150 and 250 kDa in the Western blot its molecular weight is reduced to 120 kDa following Chase digestion and a distinct band can be observed indicating reduced heterogeneity. The silver-stained gels of the resulting SDS-PAGE fractions from both experiments are depicted in Figure 40B and C (appendix). From all presumably lectican-positive fractions the *O*-glycans were analyzed by MALDI-MS and proteins were identified using LC-ESI-MS/MS (results summarized in appendix Table 12).

Subsequentially, the results of the most important fractions shall be described in detail. In experiment (B) a fraction was identified that contained proteins with apparent molecular masses of 150 to 200 kDa (fraction F18 in appendix Figure 40C), a high content of *O*-mannose glycans (see Figure 22) and the lecticans versican and neurocan as major components. These findings indicate that at least one of these two lecticans from calf brain is modified by *O*-mannosylation. NCAM1 had already been shown not to carry *O*-mannose based oligosaccharides. MAG glycosylation was analyzed in fraction F14 from experiment (A) which contained MAG together with minor amounts of cadherin-13. *O*-Glycan analysis of this sample revealed that only a few mucin-type glycans and no *O*-mannosyl glycans were present (see appendix Figure 41). Thus, cadherin-13 and MAG were shown not to be *O*-mannosylated.

The confirmation that neurocan from calf brain is indeed *O*-mannosylated was achieved with a fraction from experiment (A). Fraction F11 in which neurocan was found to be the only glycoprotein component (see appendix Table 13) comprised the sialylated *O*-mannose glycan with an m/z ratio of 1099.6 (see appendix Figure 42). Another fraction (F13) from experiment (A) contained brevican and versican among other proteins not relevant in this context (see insert in appendix Figure 43) and could be identified to harbor the sialylated *O*-mannose-based glycan (see appendix Figure 43). This shows that at least one of these lecticans (brevican or versican) is modified by *O*-mannosylation.

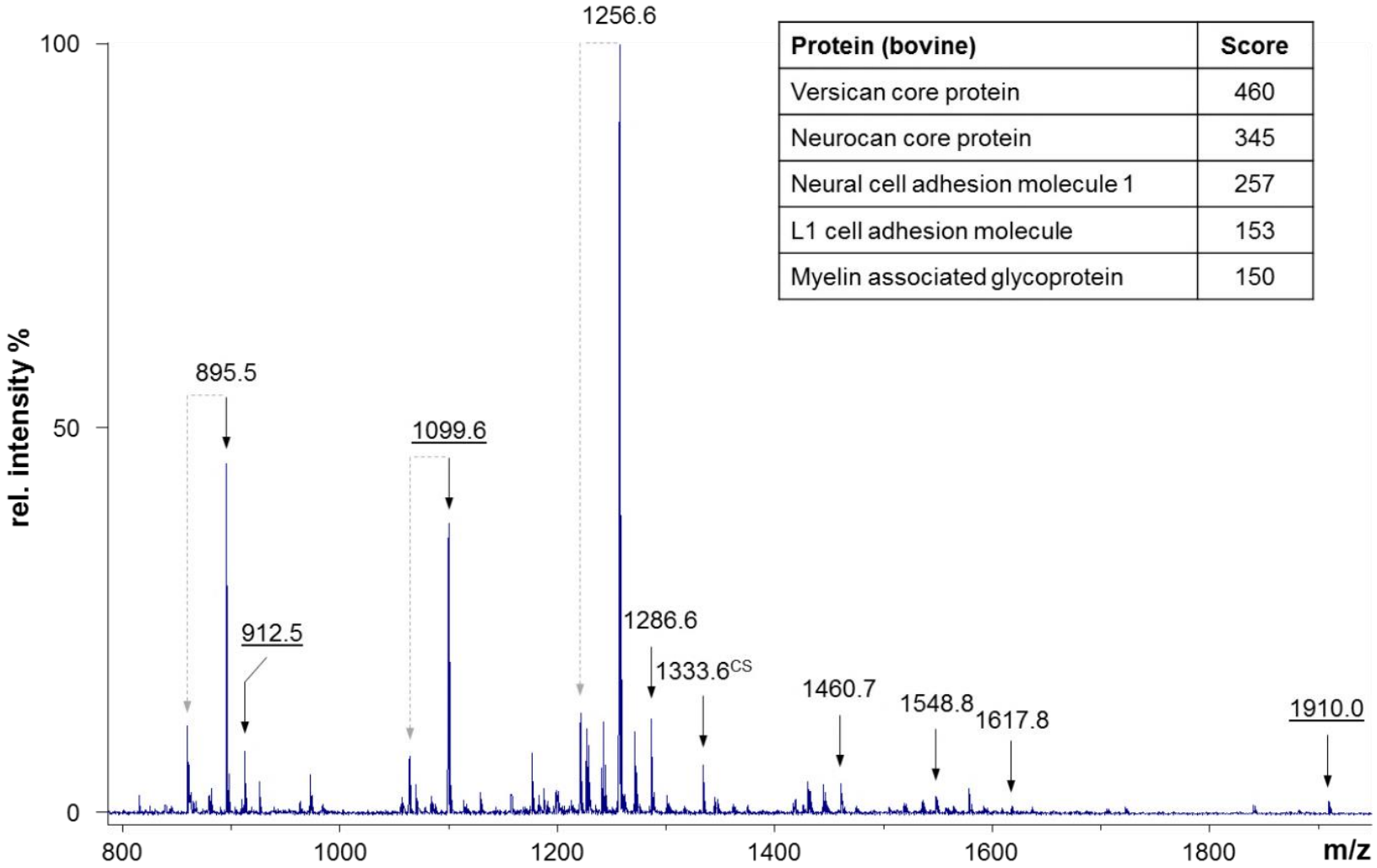

Protein (bovine)	Score
Versican core protein	460
Neurocan core protein	345
Neural cell adhesion molecule 1	257
L1 cell adhesion molecule	153
Myelin associated glycoprotein	150

Figure 22: Analysis of the lectican-containing fraction F18 from experiment (B). The MALDI-MS spectrum shows the permethylated glycan alditols. Monoisotopic masses corresponding to *O*-mannosyl glycans are underlined. Glycan fragments without a reduced end are indicated with an asterisk, arrows indicate signals derived by a loss of a methyl group and sodium (-36 Da). Signals marked by CS are a result of unspecific cleavage of chondroitin sulfate chains. The insert shows the Mascot results of protein identification in the respective fraction by ESI-MS/MS.

In order to get more information on the *O*-mannosylation present in calf brain fraction F16 from experiment (B), which contained several *O*-mannosylated proteins (neurocan, versican, neurofascin and phosphacan (RPTPζ), see Table 5), was analyzed in more detail (in cooperation with Dr. Lefeber from the Radboud University Nijmegen, the Netherlands). The antibody IIH6 recognizes the laminin-binding epitope on α-DG (Ervasti & Campbell, 1993). A Western blot using this antibody revealed many signals in samples originating from muscle cells but no signal was detected in the calf brain derived sample (see Figure 23A). In addition, a laminin overlay assay was performed (see Figure 23B) which shows if the containing proteins bind laminin. But again no signal could be detected in the sample originating from calf brain. These findings indicate that the brain derived *O*-mannosylated proteins do not bind to laminin and accordingly that they are not modified with the laminin-binding glycan epitope present on α-DG from muscle.

Table 5: Protein identification based on Mascot results of protein fraction F16 (experiment B).

Protein (bovine)	**Score**
Neurocan core protein	1138
Versican core protein	705
Neural cell adhesion molecule 1	431
Neurofascin	301
Myelin-associated glycoprotein	270
Hyaluronate-binding protein	251
Excitatory amino acid transporter 1	227
Receptor-type tyrosine-protein phosphatase ζ	227
Tenascin-R	171
L1 cell adhesion molecule	145
Seizure protein 6 homolog	138
Sodium/potassium-transporting ATPase subunit α-1	136
Microtubule-associated protein 1B	108
Actin, cytoplasmic 1	97

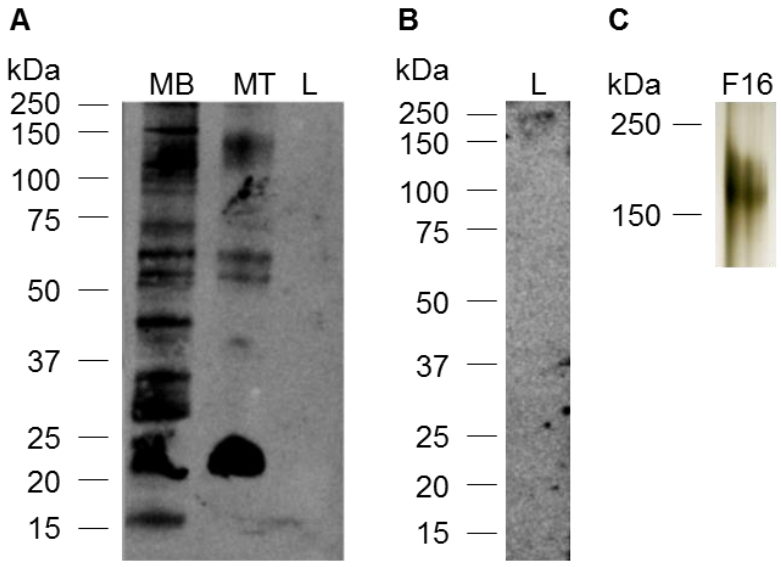

Figure 23: Analysis of fraction F16 from experiment (B). (A) Western blot against an *O*-mannose-based glycan epitope using the IIH6 antibody. MB: myoblast, MT: myotube, L: lectican fraction F16. (B) Laminin overlay assay using muscle tissue (M) and the lectican fraction F16 (L). (C) Silver-stained SDS-PGE gel of fraction F16.

3.3.4 Conclusion

In this part I could show that the lecticans of mouse and of calf brain are modified with *O*-linked mannose. Neurocan from mouse brain and presumably also brevican were shown to harbor this modification. In addition, the lecticans neurocan, brevican and versican were found to be *O*-mannosylated in another mammalian species, in bovine brain. The fourth lectican, aggrecan, was not detected, presumably because it is mainly expressed in a later developmental stage (Zimmermann & Dours-Zimmermann, 2008).

The myelin-associated glycoprotein was shown not to be modified with *O*-mannose glycans. Together with NCAM1 and NCAM L1 it belongs to the group of closely related immunoglobulin-like cell adhesion molecules (Walmod *et al.*, 2004). Since NCAM1 also was shown not to be *O*-mannosylated it is likely that NCAM L1 as well does not carry *O*-mannose based oligosaccharides.

The recombinant expression of neurocan in HEK293-EBNA cells generated a protein that was modified by mucin-type but not with *O*-mannose glycans. This finding was unexpected since *O*-mannosyl glycans were observed on the recombinantly expressed mucin domains of neurofascin and α-DG (Breloy *et al.*, 2008; Pacharra *et al.*, 2012). However, it was also observed that recombinant glycoproteins expressed in kidney-derived cells are less modified with *O*-mannosylation than the respective endogenous proteins. The complete lack of *O*-mannosyl oligosaccharides on the

brain-specific protein neurocan expressed in kidney cells could potentially indicate the existence of a distinct control mechanism for *O*-mannosylation in brain. This might explain the lack of the previously described *cis*-controlling peptide in all lecticans identified as *O*-mannosylated.

In order to get further insights into the lectican *O*-mannosylation a site-specific glycopeptide analysis was tried but hardly any glycopeptides were detected and no definite assignment of the peptides was possible (data not shown). Therefore, a different approach was applied to a lectican-containing sample. The IIH6 antibody specifically binds the mannosyl-glycan epitope on α-DG which was also shown to be responsible for the interaction with laminin (Ervasti & Campbell, 1993). A Western blot using the IIH6 antibody together with a laminin overlay assay showed that this specific laminin binding epitope is absent in the lecticans as well as in neurofascin and phosphacan. These findings indicate that the *O*-mannosylation of brain proteins plays a different role than the modification in the muscle.

4 Discussion and outlook

In this study I could identify the mammalian brain protein neurofascin 186 and the lecticans brevican, neurocan and versican to be modified with *O*-mannosyl glycans. The lecticans are major constituents of the brain extracellular matrix (Howell & Gottschall, 2012) and neurofascin was shown to account for up to 0.25 percent of the total protein amount in brain (Kriebel *et al.*, 2012). Together with the other known *O*-mannosylated proteins phosphacan, CD24, RPTPβ and α-DG, finally the high prevalence of *O*-mannose glycans in mammalian brain (Chai *et al.*, 1999) can be explained. Figure 24 shows a schematic overview of the localization of *O*-mannosylated proteins on a neuron thereby illustrating that *O*-mannose-modified proteins are present in every functional part of the neuron.

Indirect evidence for the *O*-mannosylation of the lecticans had already been provided before: Not otherwise specified proteoglycans from rat brain were found to be *O*-mannosylated in 1979 (Finne *et al.*, 1979) and in 1991 Rauch *et al.* found mannose originating from rat brain chondroitin sulfate proteoglycans (Rauch *et al.*, 1991). Although the authors did not analyze the nature of their isolates in detail they might have contained the chondroitin sulfate modified lecticans and/or phosphacan and RPTPβ.

4.1 Comparability of murine and bovine *O*-mannosylation to human protein modification

The experiments presented here were performed using murine and bovine tissues. So the question is to what extent these results are transferable to human. The *O*-mannosylation of all mammals analyzed so far was found to be comparable in muscle and in brain (Endo, 1999) with the exception of human brain tissue which has not been analyzed in this context. However, the severe CNS phenotype of dystroglycanopathies suggests a high grade of modification in human brain. Also, knockout models of mice lacking enzymes of the *O*-mannosylation pathway (Hewitt, 2009) share many symptoms with patients who suffer from dystroglycanopathies (Dobson *et al.*, 2012) as is summarized in Table 14. The knockout mice exhibit muscle weakness as well as nerve and retinal defects whereby the POMT1 knockout is the severest form resulting in embryonic lethality. Likewise, humans suffering from dystroglycanopathy have severe muscular dystrophy and brain and eye

malformations of varying severity. WWS patients with mutations in the *POMT1* gene possess the most serious phenotype with life expectancies of only up to 12 months. These similarities suggest that the structures and functions of the *O*-mannosyl modifications are akin among all mammals. Thus, it is likely that the identified proteins in this study are also *O*-mannosylated in humans. Further evidence for the high grade of conservation of this biosynthetic pathway is given by the fact that the laminin-binding *O*-mannosyl glycan present on muscle α-dystroglycan – as visualized by IIH6 staining and laminin overlay – is also present in other vertebrates, for example in chicken (Saito *et al.*, 2005).

4.2 Implications for dystroglycanopathy

With the now identified *O*-mannosylated proteins the brain phenotype of patients with dystroglycanopathy finally becomes more allegeable. Since the loss of *O*-mannosyl oligosaccharides leads to severe brain symptoms it can be assumed that the *O*-mannose glycans at least partially affect the functions of these proteins.

Neurofascin is crucial in the formation of the nodes of Ranvier and the axon initial segment. A knockout of neurofascin in mice (see Table 16 for a summary) resulted in a disorganization of the nodes leading to a drastically reduced conduction velocity of myelinated axons (Sherman *et al.*, 2005). In addition, Thaxton and coworkers could recently show with a neuron-specific knockout model that NF186 plays a vital role in the organization and demarcation of nodes of Ranvier in myelinated axons (Thaxton *et al.*, 2011). Although function and binding specificities of the *O*-glycans on neurofascin are still unknown we can assume that a loss of the *O*-mannosyl glycans on this protein might lead to disturbed nerve functionality.

The lecticans play an important role in the stabilization of the brain ECM mainly by forming the perineuronal nets together with hyaluronan and tenascin-R. The lecticans were found to be interchangeable since mice lacking neurocan or brevican (see Table 16) were shown to be viable and fertile, and exhibited no gross anatomical alterations of the central nervous system (Zhou *et al.*, 2001; Brakebusch *et al.*, 2002). Even a combined knockout of the two lecticans neurocan and brevican together with tenascin-R and tenascin-C did not result in an obvious phenotype. Only the versican V2 deficiency showed a mild effect resulting in a disorganized ECM at the nodes of

Ranvier (Dours-Zimmermann *et al.*, 2009). It remains to be elucidated what would be the result of a complete loss of CNS lecticans.

The deletion of CD24, phosphacan or RPTPβ in mice (see Table 15) did not lead to obvious brain phenotypes (Nielsen *et al.*, 1997; Harroch *et al.*, 2000) indicating that these proteins also show replaceability with other ECM components. In contrast, the complete knockout of dystroglycan was shown to be embryonically lethal (Williamson *et al.*, 1997) because of its widespread expression. A brain-specific deficiency led to abnormalities in nerve structure such as disorganized microvilli, changes in nodal composition and abnormal myelin sheath folding (Saito *et al.*, 2003).

These findings indicate that the *O*-mannosyl glycans in brain tissue are essential for development and function while the underlying protein core is replaceable to some degree.

4.3 Initiation of mammalian *O*-mannosylation

α-Dystroglycan was shown to be *O*-mannosylated at the mucin domain and the initiation of this modification was found to be dependent on the direct periphery of the *O*-mannosylation site and a *cis*-located peptide region (Breloy *et al.*, 2008). It was assumed first that neurofascin would also be *O*-mannosylated exclusively at the mucin domain which harbors a peptide similar to the *cis*-controlling determinant of α-DG. Upon the recombinant expression of the NF186 mucin domain in HEK293-EBNA cells this domain was indeed identified to carry *O*-mannosyl glycans (Pacharra *et al.*, 2012). Peptides from the mucin domain of endogenous neurofascin from mouse brain were not detected by LC-MS/MS, but the protein was shown to be *O*-mannosylated on fibronectin type-III (FNIII) and Ig-like domains. These domains are neither rich in Ser or Thr nor do they contain a *cis*-controlling peptide indicating a completely different and yet unknown initiation mechanism. The *O*-mannosylation of an Ig domain was first shown for a recombinantly expressed immunoglobulin (Martinez *et al.*, 2007). Although the sites of their *O*-mannosyl modification were not analyzed so far, phosphacan and RPTPβ contain FNIII domains and might therefore be *O*-mannosylated there. For the lecticans the exact sites of *O*-mannosylation could not be determined in this study. But they harbor Ig-like domains at their globular termini similar to those of neurofascin and therefore might be *O*-mannosylated there. All these proteins harbor no mucin domain comparable to α-DG confirming that the

O-mannosylation is not restricted to a mucin domain as was a common view among experts until recently.

The lack of *O*-mannosyl glycans on the brain-specific protein neurocan when expressed in kidney derived cells (HEK) indicates a distinct control mechanism for *O*-mannosylation in brain. Further evidence for a difference in the initiation of brain and muscle *O*-mannosylation was given by the IIH6 staining and laminin overlay. A neurofascin, lectican and phosphacan containing sample derived from calf brain did not harbor the laminin-binding glycan epitope observed on muscle α-DG. This phosphorylated *O*-mannose structure was never observed in the present study which might show the absence of this glycan in brain. But the phosphate group is instable during the chemical release of *O*-glycans and therefore cannot be detected in MALDI-MS.

4.4 Unresolved questions

Although the high amount of *O*-mannosyl glycans in brain can finally be explained and the phenotype of dystroglycanopathy is better understood, some questions remain to be answered. The functions of *O*-mannosylation in the brain remain to be elucidated. Do *O*-mannose glycans confer a binding activity to the core protein as in the case of muscle α-DG? This question might be answered by binding studies such as overlay assays, ELISA or co-immunoprecipitation. The overlay assay is an easy way to get a first impression of potential binding. The assay was shown to be reliable in the binding analysis of α-DG to its laminin G-domain containing binding partners (Michele *et al.*, 2002). Also, crude protein mixtures can be used, only the potential binding partner needs to be purified. So, the binding partner could be recombinantly expressed and purified while the *O*-mannosylated protein of interest can be partially purified from endogenous material. Using this strategy the interaction of neurofascin (before and after treatment with glycosidases) with its interaction partners neuronal cell adhesion molecule (NrCAM) and gliomedin could be assessed (Zonta *et al.*, 2008). Recently, a binding of NF to brevican and versican V2 was suggested (Dours-Zimmermann *et al.*, 2009; Frischknecht & Seidenbecher, 2012) which would be especially interesting to analyze regarding the influence of the *O*-mannosylation. The most important binding partners of the lecticans are the link proteins and tenascins. Here, the binding characteristics of mucin-type *O*-glycosylated neurocan expressed

in HEK293-EBNA cells could be compared to binding properties of endogenous neurocan purified from mammalian brain.

The initiation of brain-specific *O*-mannosylation is also to be investigated. To address this question we plan to use a “click chemistry”-based *in vitro* model in which azide-linked mannose is transferred to the target proteins. After the “click-coupling” of an alkyne-bound label *O*-mannosylated proteins can be purified and the *O*-mannosylation sites can be analyzed by glycopeptide analysis. Different enzyme preparations can be used which contain the enzymes that are needed for the transfer of the mannose onto Ser or Thr of the target protein. Here, the glycosylation efficiency of HEK cell-derived enzyme mixtures can be compared with neuronal preparations. Differences in the *O*-mannosylation pattern of the analyzed proteins might lead to new insights regarding the exact sites of the *O*-mannosyl modification in nervous tissue. Similarities in the direct periphery of the identified modification sites might help to identify new structural elements required for brain-specific *O*-mannosylation.

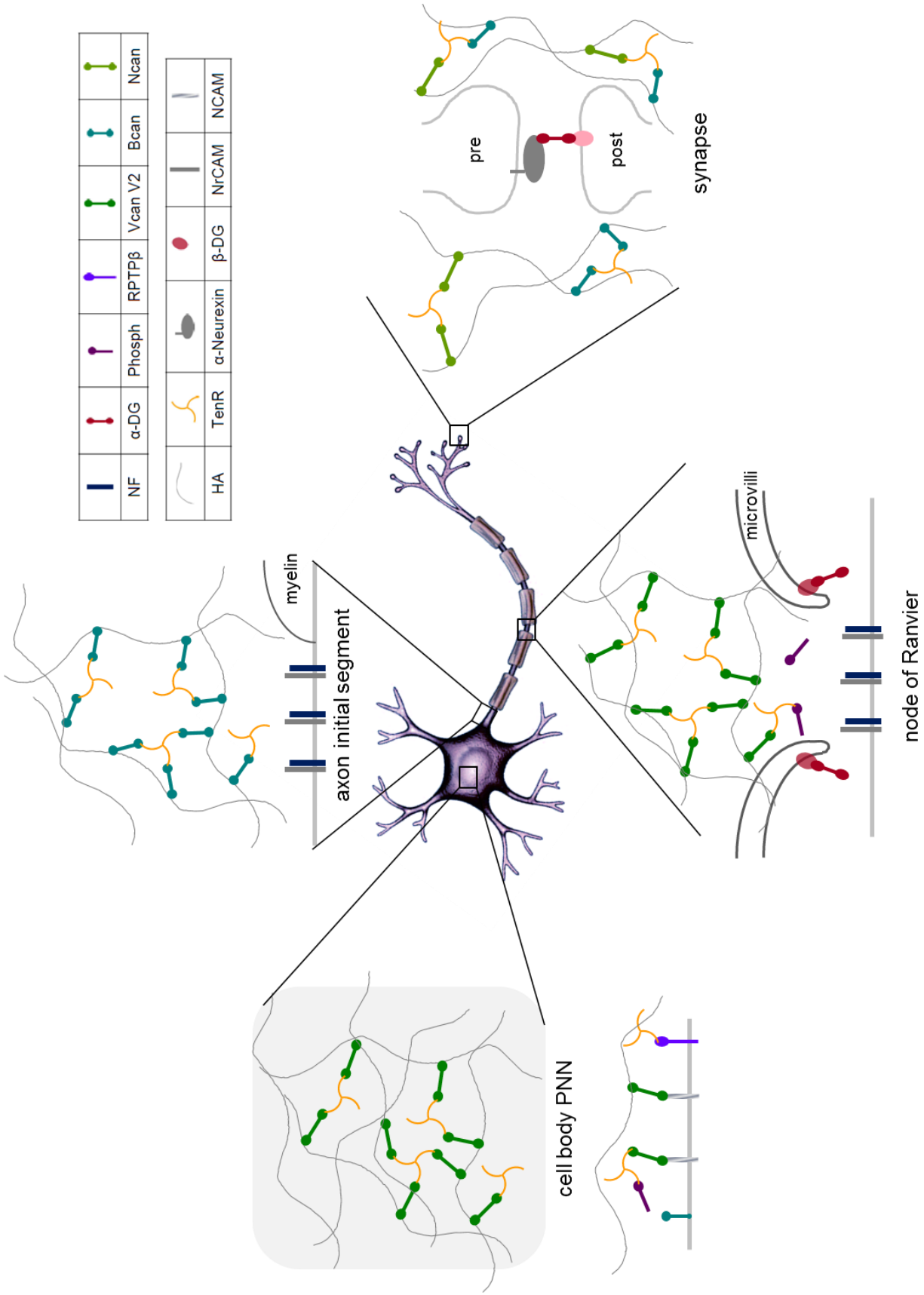

Figure 24: Schematic view of the localization of *O*-mannosylated proteins on a neuron. *O*-mannosylated proteins are: NF, α-DG, phosphacan, RPTPβ, versican V2, brevican and neurocan. Depicted binding partners: HA, tenascin-R, α-neurexin, β-DG, NrCAM and NCAM.

5 References

Abbott, K.L., Matthews, R.T. & Pierce, M. (2008) Receptor tyrosine phosphatase beta (RPTPbeta) activity and signaling are attenuated by glycosylation and subsequent cell surface galectin-1 binding. *J Biol Chem*, **283**, 33026-33035.

Akasaka-Manya, K., Manya, H., Nakajima, A., Kawakita, M. & Endo, T. (2006) Physical and functional association of human protein O-mannosyltransferases 1 and 2. *J Biol Chem*, **281**, 19339-19345.

Apweiler, R., Hermjakob, H. & Sharon, N. (1999) On the frequency of protein glycosylation, as deduced from analysis of the SWISS-PROT database. *Biochim Biophys Acta*, **1473**, 4-8.

Aspberg, A., Miura, R., Bourdoulous, S., Shimonaka, M., Heinegârd, D., Schachner, M., Ruoslahti, E. & Yamaguchi, Y. (1997) The C-type lectin domains of lecticans, a family of aggregating chondroitin sulfate proteoglycans, bind tenascin-R by protein-protein interactions independent of carbohydrate moiety. *Proc Natl Acad Sci U S A*, **94**, 10116-10121.

Bandtlow, C.E. & Zimmermann, D.R. (2000) Proteoglycans in the developing brain: new conceptual insights for old proteins. *Physiol Rev*, **80**, 1267-1290.

Barone, R., Aiello, C., Race, V., Morava, E., Foulquier, F., Riemersma, M., Passarelli, C., Concolino, D., Carella, M., Santorelli, F., Vleugels, W., Mercuri, E., Garozzo, D., Sturiale, L., Messina, S., Jaeken, J., Fiumara, A., Wevers, R.A., Bertini, E., Matthijs, G. & Lefeber, D.J. (2012) DPM2-CDG: a muscular dystrophy-dystroglycanopathy syndrome with severe epilepsy. *Ann Neurol*, **72**, 550-558.

Barresi, R. & Campbell, K.P. (2006) Dystroglycan: from biosynthesis to pathogenesis of human disease. *J Cell Sci*, **119**, 199-207.

Bartus, K., James, N.D., Bosch, K.D. & Bradbury, E.J. (2012) Chondroitin sulphate proteoglycans: key modulators of spinal cord and brain plasticity. *Exp Neurol*, **235**, 5-17.

Bekku, Y., Vargová, L., Goto, Y., Vorísek, I., Dmytrenko, L., Narasaki, M., Ohtsuka, A., Fässler, R., Ninomiya, Y., Syková, E. & Oohashi, T. (2010) Bral1: its role in diffusion barrier formation and conduction velocity in the CNS. *J Neurosci*, **30**, 3113-3123.

Beltrán-Valero de Bernabé, D., Currier, S., Steinbrecher, A., Celli, J., van Beusekom, E., van der Zwaag, B., Kayserili, H., Merlini, L., Chitayat, D., Dobyns, W.B., Cormand, B., Lehesjoki, A.E., Cruces, J., Voit, T., Walsh, C.A., van Bokhoven, H. & Brunner, H.G. (2002) Mutations in the O-mannosyltransferase gene POMT1 give rise to the severe neuronal migration disorder Walker-Warburg syndrome. *Am J Hum Genet*, **71**, 1033-1043.

Bleckmann, C., Geyer, H., Lieberoth, A., Splittstoesser, F., Liu, Y., Feizi, T., Schachner, M., Kleene, R., Reinhold, V. & Geyer, R. (2009) O-glycosylation pattern of CD24 from mouse brain. *Biol Chem*, **390**, 627-645.

Brakebusch, C., Seidenbecher, C.I., Asztely, F., Rauch, U., Matthies, H., Meyer, H., Krug, M., Böckers, T.M., Zhou, X., Kreutz, M.R., Montag, D., Gundelfinger, E.D. & Fässler, R. (2002) Brevican-deficient mice display impaired hippocampal CA1 long-term potentiation but show no obvious deficits in learning and memory. *Mol Cell Biol*, **22**, 7417-7427.

Breloy, I., Schwientek, T., Gries, B., Razawi, H., Macht, M., Albers, C. & Hanisch, F.G. (2008) Initiation of mammalian O-mannosylation in vivo is independent of a consensus sequence and controlled by peptide regions within and upstream of the alpha-dystroglycan mucin domain. *J Biol Chem*, **283**, 18832-18840.

Brockhausen, I., Schachter, H. & Stanley, P. (2009) O-GalNAc Glycans. In Varki, A., Cummings, R., Esko, J., Freeze, H.H., Stanley, P., Bertozzi, C.R., Hart, G.W., Etzler, M.E. (eds) *Essentials of Glycobiology*. Cold Spring Harbor Laboratory Press, Cold Spring Harbor (NY).

Brooks, S.A. (2004) Appropriate glycosylation of recombinant proteins for human use: implications of choice of expression system. *Mol Biotechnol*, **28**, 241-255.

Brooks, S.A. (2009) Strategies for analysis of the glycosylation of proteins: current status and future perspectives. *Mol Biotechnol*, **43**, 76-88.

Burda, P. & Aebi, M. (1999) The dolichol pathway of N-linked glycosylation. *Biochim Biophys Acta*, **1426**, 239-257.

Campbell, K.P. (1995) Three muscular dystrophies: loss of cytoskeleton-extracellular matrix linkage. *Cell*, **80**, 675-679.

Cao, W., Henry, M.D., Borrow, P., Yamada, H., Elder, J.H., Ravkov, E.V., Nichol, S.T., Compans, R.W., Campbell, K.P. & Oldstone, M.B. (1998) Identification of alpha-dystroglycan as a receptor for lymphocytic choriomeningitis virus and Lassa fever virus. *Science*, **282**, 2079-2081.

Chai, W., Yuen, C.T., Kogelberg, H., Carruthers, R.A., Margolis, R.U., Feizi, T. & Lawson, A.M. (1999) High prevalence of 2-mono- and 2,6-di-substituted manol-terminating sequences among O-glycans released from brain glycopeptides by reductive alkaline hydrolysis. *Eur J Biochem*, **263**, 879-888.

Chan, L.L., Lo, S.C. & Hodgkiss, I.J. (2002) Proteomic study of a model causative agent of harmful red tide, Prorocentrum triestinum I: Optimization of sample preparation methodologies for analyzing with two-dimensional electrophoresis. *Proteomics*, **2**, 1169-1186.

Chiba, A., Matsumura, K., Yamada, H., Inazu, T., Shimizu, T., Kusunoki, S., Kanazawa, I., Kobata, A. & Endo, T. (1997) Structures of sialylated O-linked oligosaccharides of bovine peripheral nerve alpha-dystroglycan. The role of a novel O-mannosyl-type oligosaccharide in the binding of alpha-dystroglycan with laminin. *J Biol Chem*, **272**, 2156-2162.

Ciucanu, I. & Kerek, F. (1984) A Simple and Rapid Method for the Permethylation of Carbohydrates. *Carbohydrate Research*, **131**, 209-217.

Cohn, R.D. (2005) Dystroglycan: important player in skeletal muscle and beyond. *Neuromuscul Disord*, **15**, 207-217.

Dityatev, A., Brückner, G., Dityateva, G., Grosche, J., Kleene, R. & Schachner, M. (2007) Activity-dependent formation and functions of chondroitin sulfate-rich extracellular matrix of perineuronal nets. *Dev Neurobiol*, **67**, 570-588.

Dityatev, A., Seidenbecher, C.I. & Schachner, M. (2010) Compartmentalization from the outside: the extracellular matrix and functional microdomains in the brain. *Trends Neurosci*, **33**, 503-512.

Dobson, C.M., Hempel, S.J., Stalnaker, S.H., Stuart, R. & Wells, L. (2012) O-Mannosylation and human disease. *Cell Mol Life Sci*.

Domon, B. & Costello, C.E. (1988) A systematic nomenclature for carbohydrate fragmentations in FAB-MS/MS spectra of glycoconjugates. *Glycoconjugate Journal*, **5**, 397-409.

Dours-Zimmermann, M.T., Maurer, K., Rauch, U., Stoffel, W., Fässler, R. & Zimmermann, D.R. (2009) Versican V2 assembles the extracellular matrix surrounding the nodes of ranvier in the CNS. *J Neurosci*, **29**, 7731-7742.

Dwyer, C.A., Baker, E., Hu, H. & Matthews, R.T. (2012) RPTPζ/phosphacan is abnormally glycosylated in a model of muscle-eye-brain disease lacking functional POMGnT1. *Neuroscience*, **220**, 47-61.

Endo, T. (1999) O-mannosyl glycans in mammals. *Biochim Biophys Acta*, **1473**, 237-246.

Ervasti, J.M. & Campbell, K.P. (1993) A role for the dystrophin-glycoprotein complex as a transmembrane linker between laminin and actin. *J Cell Biol*, **122**, 809-823.

Esko, J., Kimata, K. & Lindahl, U. (2009) Proteoglycans and Sulfated Glycosaminoglycans. In Varki, A., Cummings, R., Esko, J., Freeze, H.H., Stanley, P., Bertozzi, C.R., Hart, G.W., Etzler, M.E. (eds) *Essentials of Glycobiology*. Cold Spring Harbor Laboratory Press, Cold Spring Harbor (NY).

Finne, J., Krusius, T., Margolis, R.K. & Margolis, R.U. (1979) Novel mannitol-containing oligosaccharides obtained by mild alkaline borohydride treatment of a chondroitin sulfate proteoglycan from brain. *J Biol Chem*, **254**, 10295-10300.

Frischknecht, R. & Seidenbecher, C.I. (2012) Brevican: a key proteoglycan in the perisynaptic extracellular matrix of the brain. *Int J Biochem Cell Biol*, **44**, 1051-1054.

Galtrey, C.M. & Fawcett, J.W. (2007) The role of chondroitin sulfate proteoglycans in regeneration and plasticity in the central nervous system. *Brain Res Rev*, **54**, 1-18.

Gentzsch, M., Immervoll, T. & Tanner, W. (1995a) Protein O-glycosylation in Saccharomyces cerevisiae: the protein O-mannosyltransferases Pmt1p and Pmt2p function as heterodimer. *FEBS Lett*, **377**, 128-130.

Gentzsch, M., Strahl-Bolsinger, S. & Tanner, W. (1995b) A new Dol-P-Man:protein O-D-mannosyltransferase activity from Saccharomyces cerevisiae. *Glycobiology*, **5**, 77-82.

Gentzsch, M. & Tanner, W. (1996) The PMT gene family: protein O-glycosylation in Saccharomyces cerevisiae is vital. *EMBO J*, **15**, 5752-5759.

Godfrey, C., Foley, A.R., Clement, E. & Muntoni, F. (2011) Dystroglycanopathies: coming into focus. *Curr Opin Genet Dev*, **21**, 278-285.

Grewal, P.K., Holzfeind, P.J., Bittner, R.E. & Hewitt, J.E. (2001) Mutant glycosyltransferase and altered glycosylation of alpha-dystroglycan in the myodystrophy mouse. *Nat Genet*, **28**, 151-154.

Hang, H.C. & Bertozzi, C.R. (2005) The chemistry and biology of mucin-type O-linked glycosylation. *Bioorg Med Chem*, **13**, 5021-5034.

Harroch, S., Palmeri, M., Rosenbluth, J., Custer, A., Okigaki, M., Shrager, P., Blum, M., Buxbaum, J.D. & Schlessinger, J. (2000) No obvious abnormality in mice deficient in receptor protein tyrosine phosphatase beta. *Mol Cell Biol*, **20**, 7706-7715.

Hart, G.W. (1997) Dynamic O-linked glycosylation of nuclear and cytoskeletal proteins. *Annu Rev Biochem*, **66**, 315-335.

Hascall, V. & Esko, J. (2009) Hyaluronan. In Varki, A., Cummings, R., Esko, J., Freeze, H.H., Stanley, P., Bertozzi, C.R., Hart, G.W., Etzler, M.E. (eds) *Essentials of Glycobiology*. Cold Spring Harbor Laboratory Press, Cold Spring Harbor (NY).

Haselbeck, A. & Tanner, W. (1983) O-glycosylation in Saccharomyces cerevisiae is initiated at the endoplasmic reticulum. *FEBS Lett*, **158**, 335-338.

Hedstrom, K.L., Xu, X., Ogawa, Y., Frischknecht, R., Seidenbecher, C.I., Shrager, P. & Rasband, M.N. (2007) Neurofascin assembles a specialized extracellular matrix at the axon initial segment. *J Cell Biol*, **178**, 875-886.

Hewitt, J.E. (2009) Abnormal glycosylation of dystroglycan in human genetic disease. *Biochim Biophys Acta*, **1792**, 853-861.

Hoffman, S., Sorkin, B.C., White, P.C., Brackenbury, R., Mailhammer, R., Rutishauser, U., Cunningham, B.A. & Edelman, G.M. (1982) Chemical characterization of a neural cell adhesion molecule purified from embryonic brain membranes. *J Biol Chem*, **257**, 7720-7729.

Howell, M.D. & Gottschall, P.E. (2012) Lectican proteoglycans, their cleaving metalloproteinases, and plasticity in the central nervous system extracellular microenvironment. *Neuroscience*, **217**, 6-18.

Ibraghimov-Beskrovnaya, O., Ervasti, J.M., Leveille, C.J., Slaughter, C.A., Sernett, S.W. & Campbell, K.P. (1992) Primary structure of dystrophin-associated glycoproteins linking dystrophin to the extracellular matrix. *Nature*, **355**, 696-702.

Ibraghimov-Beskrovnaya, O., Milatovich, A., Ozcelik, T., Yang, B., Koepnick, K., Francke, U. & Campbell, K.P. (1993) Human dystroglycan: skeletal muscle cDNA, genomic structure, origin of tissue specific isoforms and chromosomal localization. *Hum Mol Genet*, **2**, 1651-1657.

Imperiali, M., Thoma, C., Pavoni, E., Brancaccio, A., Callewaert, N. & Oxenius, A. (2005) O Mannosylation of alpha-dystroglycan is essential for lymphocytic choriomeningitis virus receptor function. *J Virol*, **79**, 14297-14308.

Inamori, K., Endo, T., Gu, J., Matsuo, I., Ito, Y., Fujii, S., Iwasaki, H., Narimatsu, H., Miyoshi, E., Honke, K. & Taniguchi, N. (2004) N-Acetylglucosaminyltransferase IX acts on the GlcNAc beta 1,2-Man alpha 1-Ser/Thr moiety, forming a 2,6-branched structure in brain O-mannosyl glycan. *J Biol Chem*, **279**, 2337-2340.

Inamori, K., Yoshida-Moriguchi, T., Hara, Y., Anderson, M.E., Yu, L. & Campbell, K.P. (2012a) Dystroglycan function requires xylosyl- and glucuronyltransferase activities of LARGE. *Science*, **335**, 93-96.

Inamori, K.I., Hara, Y., Willer, T., Anderson, M.E., Zhu, Z., Yoshida-Moriguchi, T. & Campbell, K.P. (2012b) Xylosyl- and glucuronyltransferase functions of LARGE in α-dystroglycan modification are conserved in LARGE2. *Glycobiology*.

Jensen, P.H., Kolarich, D. & Packer, N.H. (2010) Mucin-type O-glycosylation--putting the pieces together. *FEBS J*, **277**, 81-94.

Johansen, P.G., Marshall, R.D. & Neuberger, A. (1961) Carbohydrates in protein. 3 The preparation and some of the properties of a glycopeptide from hen's-egg albumin. *Biochem J*, **78**, 518-527.

Jurado, L.A., Coloma, A. & Cruces, J. (1999) Identification of a human homolog of the Drosophila rotated abdomen gene (POMT1) encoding a putative protein O-mannosyl-transferase, and assignment to human chromosome 9q34.1. *Genomics*, **58**, 171-180.

Kriebel, M., Metzger, J., Trinks, S., Chugh, D., Harvey, R.J., Harvey, K. & Volkmer, H. (2011) The cell adhesion molecule neurofascin stabilizes axo-axonic GABAergic terminals at the axon initial segment. *J Biol Chem*, **286**, 24385-24393.

Kriebel, M., Wuchter, J., Trinks, S. & Volkmer, H. (2012) Neurofascin: a switch between neuronal plasticity and stability. *Int J Biochem Cell Biol*, **44**, 694-697.

Laemmli, U.K. (1970) Cleavage of structural proteins during the assembly of the head of bacteriophage T4. *Nature*, **227**, 680-685.

Lefeber, D.J., Schönberger, J., Morava, E., Guillard, M., Huyben, K.M., Verrijp, K., Grafakou, O., Evangeliou, A., Preijers, F.W., Manta, P., Yildiz, J., Grünewald, S., Spilioti, M., van den Elzen, C., Klein, D., Hess, D., Ashida, H., Hofsteenge, J., Maeda, Y., van den Heuvel, L., Lammens, M., Lehle, L. & Wevers, R.A. (2009) Deficiency of Dol-P-Man synthase subunit DPM3 bridges the congenital disorders of glycosylation with the dystroglycanopathies. *Am J Hum Genet*, **85**, 76-86.

Lehle, L., Strahl, S. & Tanner, W. (2006) Protein glycosylation, conserved from yeast to man: a model organism helps elucidate congenital human diseases. *Angew Chem Int Ed Engl*, **45**, 6802-6818.

Liu, H., Focia, P.J. & He, X. (2011) Homophilic adhesion mechanism of neurofascin, a member of the L1 family of neural cell adhesion molecules. *J Biol Chem*, **286**, 797-805.

Lommel, M. & Strahl, S. (2009) Protein O-mannosylation: conserved from bacteria to humans. *Glycobiology*, **19**, 816-828.

Lommel, M., Willer, T. & Strahl, S. (2008) POMT2, a key enzyme in Walker-Warburg syndrome: somatic sPOMT2, but not testis-specific tPOMT2, is crucial for mannosyltransferase activity in vivo. *Glycobiology*, **18**, 615-625.

Longman, C., Brockington, M., Torelli, S., Jimenez-Mallebrera, C., Kennedy, C., Khalil, N., Feng, L., Saran, R.K., Voit, T., Merlini, L., Sewry, C.A., Brown, S.C. & Muntoni, F. (2003) Mutations in the human LARGE gene cause MDC1D, a novel form of congenital muscular dystrophy with severe mental retardation and abnormal glycosylation of alpha-dystroglycan. *Hum Mol Genet*, **12**, 2853-2861.

Löffler, A., Doucey, M.A., Jansson, A.M., Müller, D.R., de Beer, T., Hess, D., Meldal, M., Richter, W.J., Vliegenthart, J.F. & Hofsteenge, J. (1996) Spectroscopic and protein chemical analyses demonstrate the presence of C-mannosylated tryptophan in intact human RNase 2 and its isoforms. *Biochemistry*, **35**, 12005-12014.

Manya, H., Suzuki, T., Akasaka-Manya, K., Ishida, H.K., Mizuno, M., Suzuki, Y., Inazu, T., Dohmae, N. & Endo, T. (2007) Regulation of mammalian protein O-mannosylation: preferential amino acid sequence for O-mannose modification. *J Biol Chem*, **282**, 20200-20206.

Marshall, R.D. (1974) The nature and metabolism of the carbohydrate-peptide linkages of glycoproteins. *Biochem Soc Symp*, 17-26.

Martin, P.T. (2007) Congenital muscular dystrophies involving the O-mannose pathway. *Curr Mol Med*, **7**, 417-425.

Martinez, T., Pace, D., Brady, L., Gerhart, M. & Balland, A. (2007) Characterization of a novel modification on IgG2 light chain. Evidence for the presence of O-linked mannosylation. *J Chromatogr A*, **1156**, 183-187.

Michele, D.E., Barresi, R., Kanagawa, M., Saito, F., Cohn, R.D., Satz, J.S., Dollar, J., Nishino, I., Kelley, R.I., Somer, H., Straub, V., Mathews, K.D., Moore, S.A. & Campbell, K.P. (2002) Post-translational disruption of dystroglycan-ligand interactions in congenital muscular dystrophies. *Nature*, **418**, 417-422.

Miura, R., Aspberg, A., Ethell, I.M., Hagihara, K., Schnaar, R.L., Ruoslahti, E. & Yamaguchi, Y. (1999) The proteoglycan lectin domain binds sulfated cell surface glycolipids and promotes cell adhesion. *J Biol Chem*, **274**, 11431-11438.

Molloy, M.P., Herbert, B.R., Walsh, B.J., Tyler, M.I., Traini, M., Sanchez, J.C., Hochstrasser, D.F., Williams, K.L. & Gooley, A.A. (1998) Extraction of membrane proteins by differential solubilization for separation using two-dimensional gel electrophoresis. *Electrophoresis*, **19**, 837-844.

Morawski, M., Brückner, M.K., Riederer, P., Brückner, G. & Arendt, T. (2004) Perineuronal nets potentially protect against oxidative stress. *Exp Neurol*, **188**, 309-315.

Morelle, W., Canis, K., Chirat, F., Faid, V. & Michalski, J.C. (2006) The use of mass spectrometry for the proteomic analysis of glycosylation. *Proteomics*, **6**, 3993-4015.

Moremen, K.W., Tiemeyer, M. & Nairn, A.V. (2012) Vertebrate protein glycosylation: diversity, synthesis and function. *Nat Rev Mol Cell Biol*, **13**, 448-462.

Muntoni, F., Brockington, M., Torelli, S. & Brown, S.C. (2004) Defective glycosylation in congenital muscular dystrophies. *Curr Opin Neurol*, **17**, 205-209.

Nakamura, N., Lyalin, D. & Panin, V.M. (2010) Protein O-mannosylation in animal development and physiology: from human disorders to Drosophila phenotypes. *Semin Cell Dev Biol*, **21**, 622-630.

Nicholson, C. & Syková, E. (1998) Extracellular space structure revealed by diffusion analysis. *Trends Neurosci*, **21**, 207-215.

Nielsen, P.J., Lorenz, B., Müller, A.M., Wenger, R.H., Brombacher, F., Simon, M., von der Weid, T., Langhorne, W.J., Mossmann, H. & Köhler, G. (1997) Altered erythrocytes and a leaky block in B-cell development in CD24/HSA-deficient mice. *Blood*, **89**, 1058-1067.

Nizet, V. & Esko, J. (2009) Bacterial and Viral Infections. In Varki, A., Cummings, R., Esko, J., Freeze, H.H., Stanley, P., Bertozzi, C.R., Hart, G.W., Etzler, M.E. (eds) *Essentials of Glycobiology*. Cold Spring Harbor Laboratory Press, Cold Spring Harbor (NY).

O'Connell, B.C., Hagen, F.K. & Tabak, L.A. (1992) The influence of flanking sequence on the O-glycosylation of threonine in vitro. *J Biol Chem*, **267**, 25010-25018.

Olin, A.I., Mörgelin, M., Sasaki, T., Timpl, R., Heinegård, D. & Aspberg, A. (2001) The proteoglycans aggrecan and Versican form networks with fibulin-2 through their lectin domain binding. *J Biol Chem*, **276**, 1253-1261.

Pacharra, S., Hanisch, F.G. & Breloy, I. (2012) Neurofascin 186 Is O-Mannosylated within and Outside of the Mucin Domain. *J Proteome Res*, **11**, 3955-3964.

Perez-Vilar, J. & Hill, R.L. (1999) The structure and assembly of secreted mucins. *J Biol Chem*, **274**, 31751-31754.

Preston, M. & Sherman, L.S. (2011) Neural stem cell niches: roles for the hyaluronan-based extracellular matrix. *Front Biosci (Schol Ed)*, **3**, 1165-1179.

Rambukkana, A., Yamada, H., Zanazzi, G., Mathus, T., Salzer, J.L., Yurchenco, P.D., Campbell, K.P. & Fischetti, V.A. (1998) Role of alpha-dystroglycan as a Schwann cell receptor for Mycobacterium leprae. *Science*, **282**, 2076-2079.

Rauch, U. (2007) Brain matrix: structure, turnover and necessity. *Biochem Soc Trans*, **35**, 656-660.

Rauch, U., Gao, P., Janetzko, A., Flaccus, A., Hilgenberg, L., Tekotte, H., Margolis, R.K. & Margolis, R.U. (1991) Isolation and characterization of developmentally regulated chondroitin sulfate and chondroitin/keratan sulfate proteoglycans of brain identified with monoclonal antibodies. *J Biol Chem*, **266**, 14785-14801.

Roscioli, T., Kamsteeg, E.J., Buysse, K., Maystadt, I., van Reeuwijk, J., van den Elzen, C., van Beusekom, E., Riemersma, M., Pfundt, R., Vissers, L.E., Schraders, M., Altunoglu, U., Buckley, M.F., Brunner, H.G., Grisart, B., Zhou, H., Veltman, J.A., Gilissen, C., Mancini, G.M., Delrée, P., Willemsen, M.A., Ramadža, D.P., Chitayat, D., Bennett, C., Sheridan, E., Peeters, E.A., Tan-Sindhunata, G.M., de Die-Smulders, C.E., Devriendt, K., Kayserili, H., El-Hashash, O.A., Stemple, D.L., Lefeber, D.J., Lin, Y.Y. & van Bokhoven, H. (2012) Mutations in ISPD cause Walker-Warburg syndrome and defective glycosylation of α-dystroglycan. *Nat Genet*, **44**, 581-585.

Saito, F., Blank, M., Schröder, J., Manya, H., Shimizu, T., Campbell, K.P., Endo, T., Mizutani, M., Kröger, S. & Matsumura, K. (2005) Aberrant glycosylation of alpha-dystroglycan causes defective binding of laminin in the muscle of chicken muscular dystrophy. *FEBS Lett*, **579**, 2359-2363.

Saito, F., Moore, S.A., Barresi, R., Henry, M.D., Messing, A., Ross-Barta, S.E., Cohn, R.D., Williamson, R.A., Sluka, K.A., Sherman, D.L., Brophy, P.J., Schmelzer, J.D., Low, P.A., Wrabetz, L., Feltri, M.L. & Campbell, K.P. (2003) Unique role of dystroglycan in peripheral nerve myelination, nodal structure, and sodium channel stabilization. *Neuron*, **38**, 747-758.

Sasaki, T., Yamada, H., Matsumura, K., Shimizu, T., Kobata, A. & Endo, T. (1998) Detection of O-mannosyl glycans in rabbit skeletal muscle alpha-dystroglycan. *Biochim Biophys Acta*, **1425**, 599-606.

Schachter, H., Vajsar, J. & Zhang, W. (2004) The role of defective glycosylation in congenital muscular dystrophy. *Glycoconj J*, **20**, 291-300.

Schessl, J., Zou, Y. & Bönnemann, C.G. (2006) Congenital muscular dystrophies and the extracellular matrix. *Semin Pediatr Neurol*, **13**, 80-89.

Sentandreu, R. & Northcote, D.H. (1968) The structure of a glycopeptide isolated from the yeast cell wall. *Biochem J*, **109**, 419-432.

Sherman, D.L., Tait, S., Melrose, S., Johnson, R., Zonta, B., Court, F.A., Macklin, W.B., Meek, S., Smith, A.J., Cottrell, D.F. & Brophy, P.J. (2005) Neurofascins are required to establish axonal domains for saltatory conduction. *Neuron*, **48**, 737-742.

Smalheiser, N.R., Haslam, S.M., Sutton-Smith, M., Morris, H.R. & Dell, A. (1998) Structural analysis of sequences O-linked to mannose reveals a novel Lewis X structure in cranin (dystroglycan) purified from sheep brain. *J Biol Chem*, **273**, 23698-23703.

Sparks, S., Quijano-Roy, S., Harper, A. & al., e. (2001 [Updated 2012]) Congenital Muscular Dystrophy Overview. In Pagon, R., Bird, T., Dolan, C., al., e. (eds) *GeneReviews™*. University of Washington, Seattle, Seattle (WA).

Spiro, R.G. (2002) Protein glycosylation: nature, distribution, enzymatic formation, and disease implications of glycopeptide bonds. *Glycobiology*, **12**, 43R-56R.

Stalnaker, S.H., Aoki, K., Lim, J.M., Porterfield, M., Liu, M., Satz, J.S., Buskirk, S., Xiong, Y., Zhang, P., Campbell, K.P., Hu, H., Live, D., Tiemeyer, M. & Wells, L. (2011a) Glycomic analyses of mouse models of congenital muscular dystrophy. *J Biol Chem*, **286**, 21180-21190.

Stalnaker, S.H., Stuart, R. & Wells, L. (2011b) Mammalian O-mannosylation: unsolved questions of structure/function. *Curr Opin Struct Biol*, **21**, 603-609.

Sugita, S., Saito, F., Tang, J., Satz, J., Campbell, K. & Südhof, T.C. (2001) A stoichiometric complex of neurexins and dystroglycan in brain. *J Cell Biol*, **154**, 435-445.

Sugiyama, J., Bowen, D.C. & Hall, Z.W. (1994) Dystroglycan binds nerve and muscle agrin. *Neuron*, **13**, 103-115.

Susuki, K. & Rasband, M.N. (2008) Molecular mechanisms of node of Ranvier formation. *Curr Opin Cell Biol*, **20**, 616-623.

Takahashi, S., Sasaki, T., Manya, H., Chiba, Y., Yoshida, A., Mizuno, M., Ishida, H., Ito, F., Inazu, T., Kotani, N., Takasaki, S., Takeuchi, M. & Endo, T. (2001) A new beta-1,2-N-acetylglucosaminyltransferase that may play a role in the biosynthesis of mammalian O-mannosyl glycans. *Glycobiology*, **11**, 37-45.

Talts, J.F., Andac, Z., Göhring, W., Brancaccio, A. & Timpl, R. (1999) Binding of the G domains of laminin alpha1 and alpha2 chains and perlecan to heparin, sulfatides, alpha-dystroglycan and several extracellular matrix proteins. *EMBO J*, **18**, 863-870.

Ten Hagen, K.G., Fritz, T.A. & Tabak, L.A. (2003) All in the family: the UDP-GalNAc:polypeptide N-acetylgalactosaminyltransferases. *Glycobiology*, **13**, 1R-16R.

Thaxton, C., Pillai, A.M., Pribisko, A.L., Dupree, J.L. & Bhat, M.A. (2011) Nodes of Ranvier act as barriers to restrict invasion of flanking paranodal domains in myelinated axons. *Neuron*, **69**, 244-257.

van Reeuwijk, J., Janssen, M., van den Elzen, C., Beltran-Valero de Bernabé, D., Sabatelli, P., Merlini, L., Boon, M., Scheffer, H., Brockington, M., Muntoni, F., Huynen, M.A., Verrips, A., Walsh, C.A., Barth, P.G., Brunner, H.G. & van Bokhoven, H. (2005) POMT2 mutations cause alpha-dystroglycan hypoglycosylation and Walker-Warburg syndrome. *J Med Genet*, **42**, 907-912.

Varki, A. & Lowe, J. (2009) Biological Roles of Glycans. In Varki, A., Cummings, R., Esko, J., Freeze, H.H., Stanley, P., Bertozzi, C.R., Hart, G.W., Etzler, M.E. (eds) *Essentials of Glycobiology*. Cold Spring Harbor Laboratory Press, Cold Spring Harbor (NY).

Vorum, H., Østergaard, M., Hensechke, P., Enghild, J.J., Riazati, M. & Rice, G.E. (2004) Proteomic analysis of hyperoxia-induced responses in the human choriocarcinoma cell line JEG-3. *Proteomics*, **4**, 861-867.

Walmod, P.S., Kolkova, K., Berezin, V. & Bock, E. (2004) Zippers make signals: NCAM-mediated molecular interactions and signal transduction. *Neurochem Res*, **29**, 2015-2035.

Willer, T., Amselgruber, W., Deutzmann, R. & Strahl, S. (2002) Characterization of POMT2, a novel member of the PMT protein O-mannosyltransferase family specifically localized to the acrosome of mammalian spermatids. *Glycobiology*, **12**, 771-783.

Willer, T., Lee, H., Lommel, M., Yoshida-Moriguchi, T., de Bernabe, D.B., Venzke, D., Cirak, S., Schachter, H., Vajsar, J., Voit, T., Muntoni, F., Loder, A.S., Dobyns, W.B., Winder, T.L., Strahl, S., Mathews, K.D., Nelson, S.F., Moore, S.A. & Campbell, K.P. (2012) ISPD loss-of-function mutations disrupt dystroglycan O-mannosylation and cause Walker-Warburg syndrome. *Nat Genet*, **44**, 575-580.

Willer, T., Valero, M.C., Tanner, W., Cruces, J. & Strahl, S. (2003) O-mannosyl glycans: from yeast to novel associations with human disease. *Curr Opin Struct Biol*, **13**, 621-630.

Williamson, R.A., Henry, M.D., Daniels, K.J., Hrstka, R.F., Lee, J.C., Sunada, Y., Ibraghimov-Beskrovnaya, O. & Campbell, K.P. (1997) Dystroglycan is essential for early embryonic development: disruption of Reichert's membrane in Dag1-null mice. *Hum Mol Genet*, **6**, 831-841.

Wopereis, S., Lefeber, D.J., Morava, E. & Wevers, R.A. (2006) Mechanisms in protein O-glycan biosynthesis and clinical and molecular aspects of protein O-glycan biosynthesis defects: a review. *Clin Chem*, **52**, 574-600.

Yoshida, A., Kobayashi, K., Manya, H., Taniguchi, K., Kano, H., Mizuno, M., Inazu, T., Mitsuhashi, H., Takahashi, S., Takeuchi, M., Herrmann, R., Straub, V., Talim, B., Voit, T., Topaloglu, H., Toda, T. & Endo, T. (2001) Muscular dystrophy and neuronal migration disorder caused by mutations in a glycosyltransferase, POMGnT1. *Dev Cell*, **1**, 717-724.

Yoshida-Moriguchi, T., Yu, L., Stalnaker, S.H., Davis, S., Kunz, S., Madson, M., Oldstone, M.B., Schachter, H., Wells, L. & Campbell, K.P. (2010) O-mannosyl phosphorylation of alpha-dystroglycan is required for laminin binding. *Science*, **327**, 88-92.

Yuen, C.T., Chai, W., Loveless, R.W., Lawson, A.M., Margolis, R.U. & Feizi, T. (1997) Brain contains HNK-1 immunoreactive O-glycans of the sulfoglucuronyl lactosamine series that terminate in 2-linked or 2,6-linked hexose (mannose). *J Biol Chem*, **272**, 8924-8931.

Zhou, X.H., Brakebusch, C., Matthies, H., Oohashi, T., Hirsch, E., Moser, M., Krug, M., Seidenbecher, C.I., Boeckers, T.M., Rauch, U., Buettner, R., Gundelfinger, E.D. & Fässler, R. (2001) Neurocan is dispensable for brain development. *Mol Cell Biol*, **21**, 5970-5978.

Zimmermann, D.R. & Dours-Zimmermann, M.T. (2008) Extracellular matrix of the central nervous system: from neglect to challenge. *Histochem Cell Biol*, **130**, 635-653.

Zonta, B., Tait, S., Melrose, S., Anderson, H., Harroch, S., Higginson, J., Sherman, D.L. & Brophy, P.J. (2008) Glial and neuronal isoforms of Neurofascin have distinct roles in the assembly of nodes of Ranvier in the central nervous system. *J Cell Biol*, **181**, 1169-1177.

6 Appendix

Table 6: Summary of all mass-to-charge (m/z) values and their corresponding *O*-glycan composition observed by MALDI-MS analysis of permethylated oligosaccharides.

m/z	Composition	Type
738.4	$Hex_2HexNAc\text{-}ol\ Na^+$	*O*-GalNAc/*O*-Man
895.5	$NeuAcHexHexNAc\text{-}ol\ Na^+$	*O*-GalNAc
912.5	$FucHex_2HexNAc\text{-}ol\ Na^+$	*O*-Man
983.5	$Hex_2HexNAc_2\text{-}ol\ Na^+$	*O*-GalNAc
1069.6	$NeuAcFucHexHexNAc\text{-}ol\ Na^+$	*O*-GalNAc
1099.6	$NeuAcHex_2HexNAc\text{-}ol\ Na^+$	*O*-Man
1157.6	$FucHex_2HexNAc_2\text{-}ol\ Na^+$	*O*-GalNAc
1256.6	$NeuAc_2HexHexNAc\text{-}ol\ Na^+$	*O*-GalNAc
1286.6	$NeuAcNeuGcHexHexNAc\text{-}ol\ Na^+$	*O*-GalNAc
1344.7	$NeuAcHex_2HexNAc_2\text{-}ol\ Na^+$	*O*-GalNAc/*O*-Man
1432.7	$Hex_3HexNAc_3\text{-}ol\ Na^+$	*O*-GalNAc
1460.7	$NeuAc_2Hex_2HexNAc\text{-}ol\ Na^+$	*O*-GalNAc
1548.8	$NeuAcHex_3HexNAc_2\text{-}ol\ Na^+$	*O*-GalNAc/*O*-Man
1595.8	$Hex_5HexNAc_2\text{-}ol\ Na^+$	*O*-GalNAc
1617.8	$NeuAc_3HexHexNAc\text{-}ol\ Na^+$	*O*-GalNAc
1705.9	$NeuAc_2Hex_2HexNAc_2\text{-}ol\ Na^+$	*O*-GalNAc
1722.9	$NeuAcFucHex_3HexNAc_2\text{-}ol\ Na^+$	*O*-Man
1910.0	$NeuAc_2Hex_3HexNAc_2\text{-}ol\ Na^+$	*O*-Man

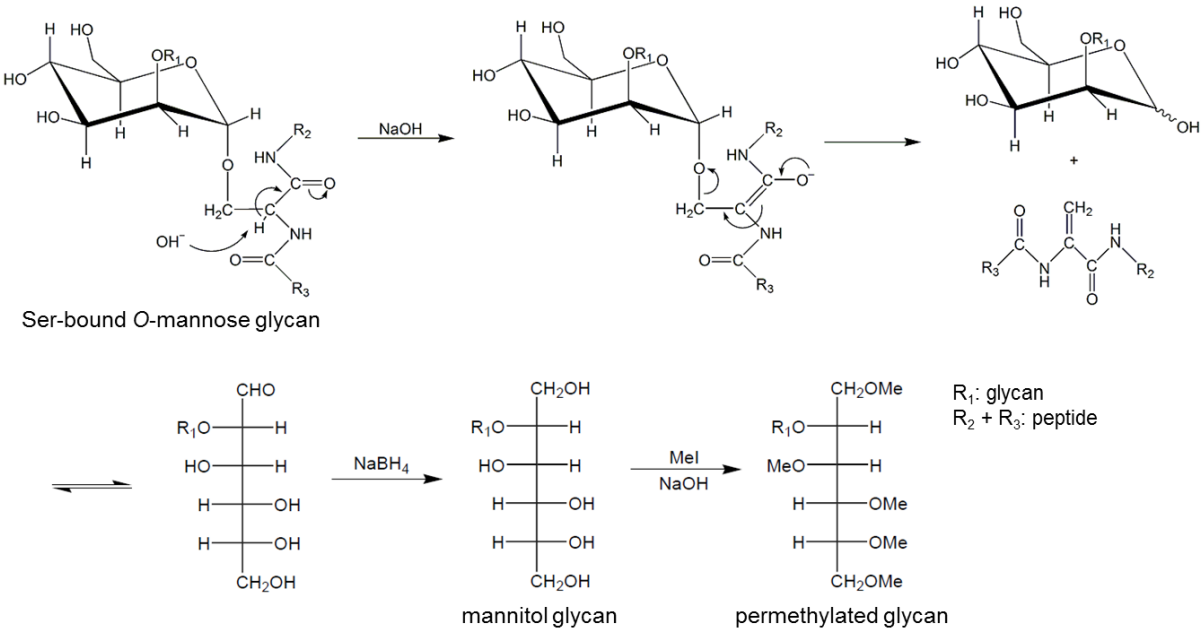

Figure 25: Reaction scheme for the release of *O*-glycans by β-elimination. A serine-bound *O*-mannosyl glycan is used as example. After its release the glycan is permethylated.

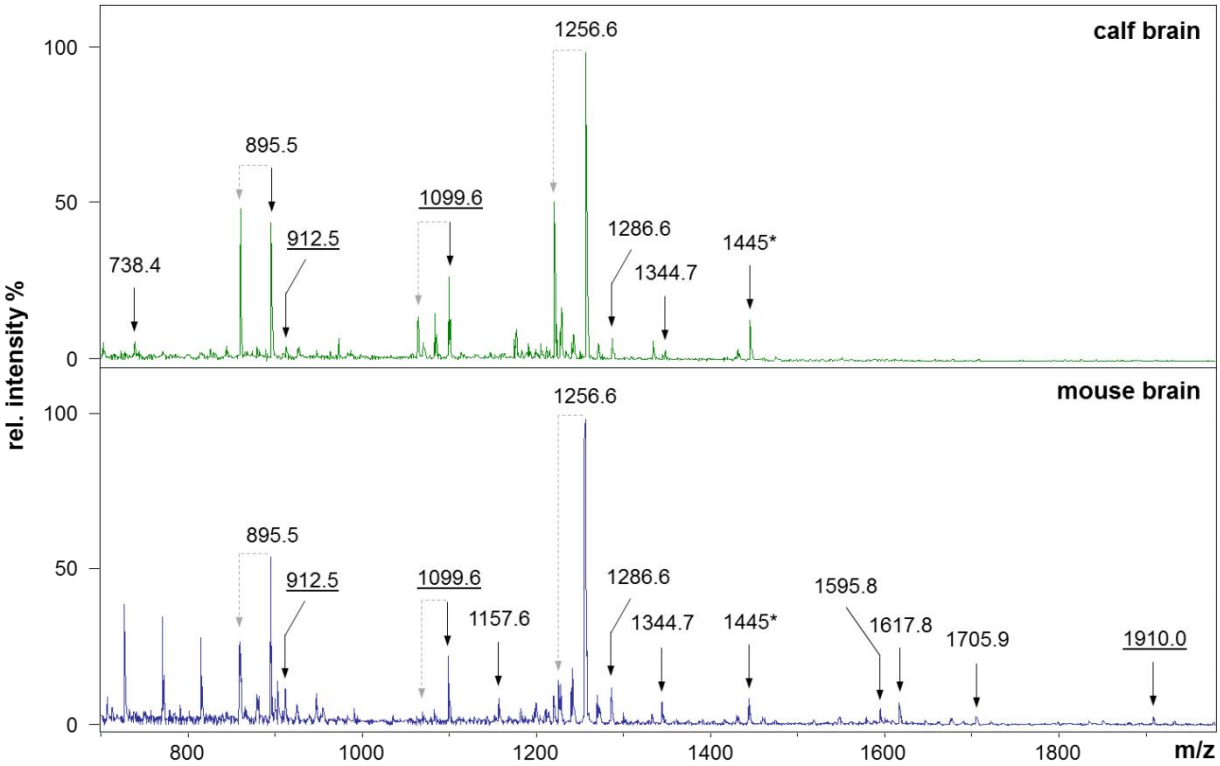

Figure 26: Comparison between the *O*-glycome of calf (upper panel) and mouse brain (lower panel). The MALDI-MS spectra show permethylated glycan alditols. Monoisotopic masses corresponding to *O*-mannosyl glycans are underlined. Signals derived from nonreduced *N*-glycan fragments are indicated with an asterisk, dashed arrows indicate the loss of methyl and sodium (-36).

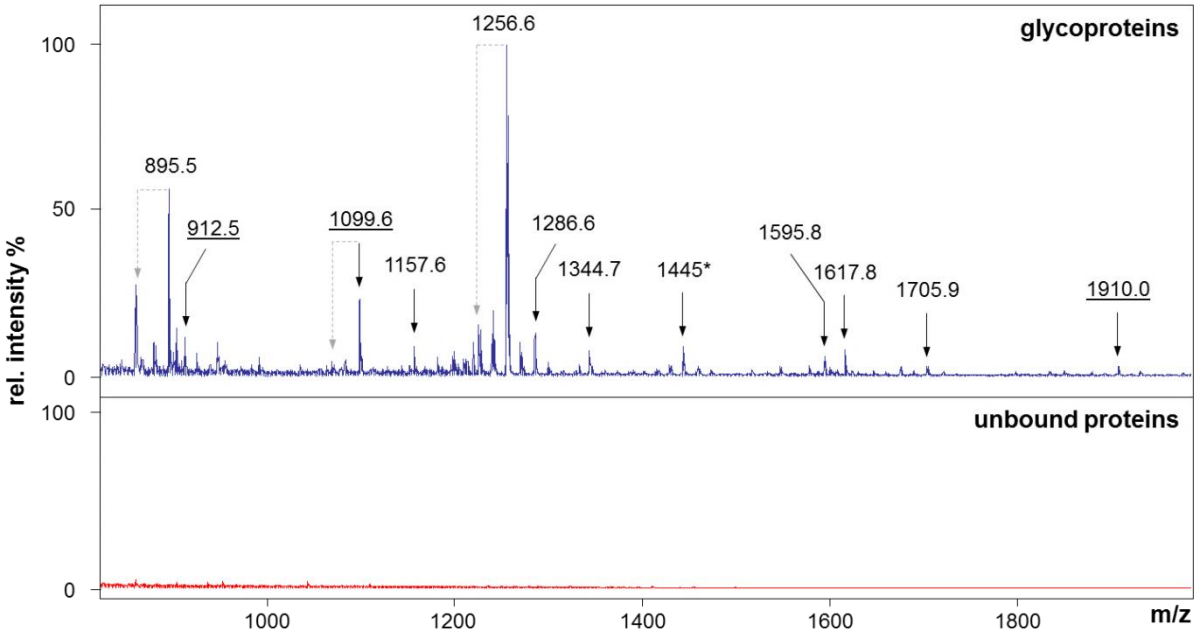

Figure 27: Comparison between the *O*-glycans present in the WGA flow-through (unbound proteins, lower panel) and the eluted glycoproteins (upper panel). The MALDI-MS spectra show permethylated glycan alditols. Monoisotopic masses corresponding to *O*-mannosyl glycans are underlined. Signals derived from nonreduced *N*-glycan fragments are indicated with an asterisk, dashed arrows indicate the loss of methyl and sodium (-36).

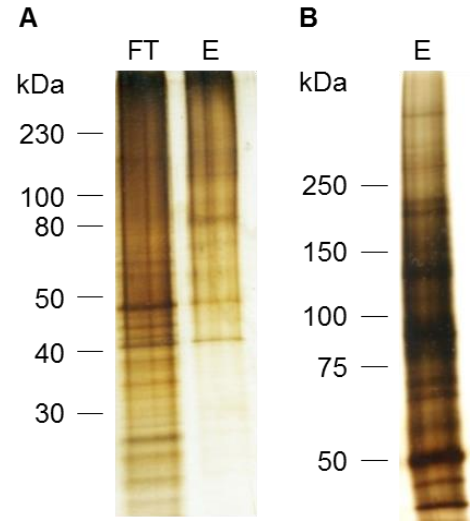

Figure 28: Silver-stained SDS-PAGE gels of WGA flow-through (FT) and eluate (E). (A) 5-15 % gel is used to visualize smaller proteins. (B) 3.5-10 % gel is used to visualize the whole range of mouse glycoproteins.

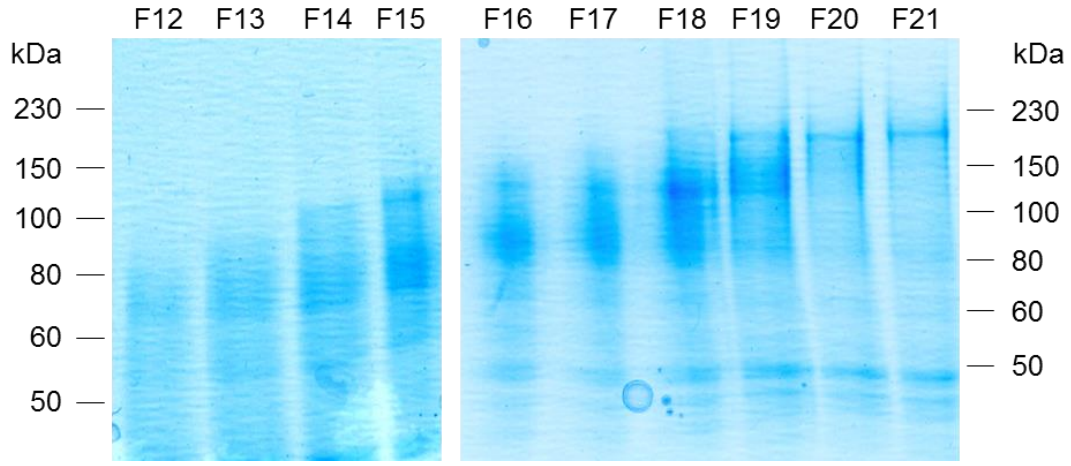

Figure 29: SDS-PAGE gel of several protein fractions generated by preparative SDS-PAGE (stained with Coomassie Brilliant Blue).

Table 7: Summary of protein size and *O*-mannose content of the fractions generated by preparative SDS-PAGE. Abbreviations: n. d.: not determined.

Fraction	Protein size / kDa	O-man?
F9	-55	no
F10	-70	no
F11	-90	no
F12	-95	little
F13	-100	little
F14	60-120	little
F15	60-135	little
F16	60-160	yes
F17	60-160	n. d.
F18	60-200	yes
F19	80-210	yes
F20	80-210	yes
F21	140-215	yes

Table 8: Protein identification of the gel band at 190 kDa originating from F21. Shown are the Mascot scores.

Protein (mouse)	**Score**
Neurofascin	1589
Tenascin-R	571
Neural cell adhesion molecule 1	523
Sodium/potassium-transporting ATPase subunit α-3	399
Sodium/potassium-transporting ATPase subunit α-1	395
Sodium/potassium-transporting ATPase subunit α-2	327
Plexin-A4	216
Plexin-A1	172
Neurocan core protein	136
Plexin-B1	131
ADP/ATP translocase 1	91
Neural cell adhesion molecule L1	91

Table 9: BLAST search for peptides similar to the *cis*-controlling peptide of α-DG. Shown here are the results except for neurofascin which can be seen in Figure 12.

prokineticin receptor 2 [Homo sapiens]	α-DG		LGPIQP-TRVSEAGTTVP
			L P+ P TRVS AG TVP
	Sbjct	100	LPPL-PGTRVSAAGATVP 116
mucin 5AC, oligomeric mucus [Homo sapiens]	α-DG		TPTLG-PIQPT-RVSEA----GTTVPGQIRPT
			TP L P P+ R +E+ GTT PG R T
	Sbjct	3389	TPALSSP-HPSSRTTESPPSPGTTTPGHTRAT 3419
mucin 5B, oligomeric mucus [Homo sapiens]	α-DG		TPTLG-PIQPT-RVSEA----GTTVPGQIRPT
			TP L P P+ R +E+ GTT PG R T
	Sbjct	2809	TPALSSP-HPSSRTTESPPSPGTTTPGHTRAT 2839
protein tyrosine phosphatase, receptor type, F [Homo sapiens]	α-DG		TT--VPGQIRPTMTI
			TT VPG RPTM I
	Sbjct	816	TTGAVPG--RPTMMI 828

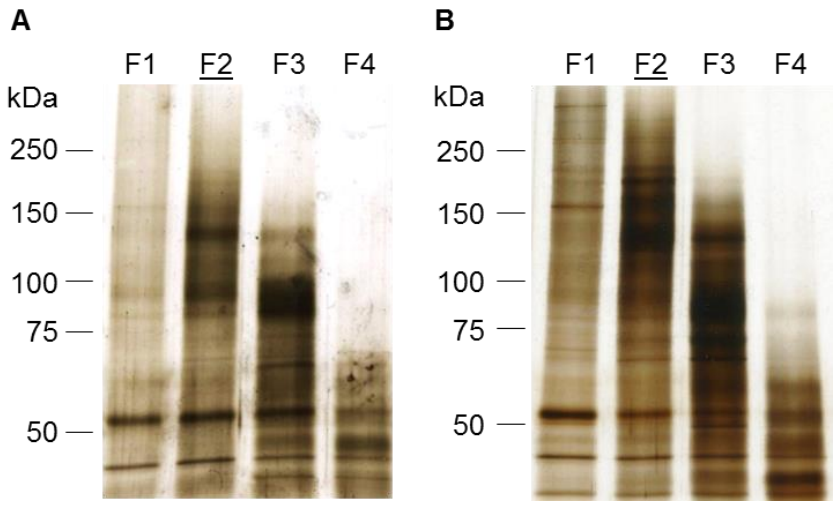

Figure 30: GPC fractionation of mouse brain glycoproteins. The four protein-containing fractions of experiment (A) and (B) are depicted in silver-stained gels. The fraction F2 (underlined) was used for preparative SDS-PAGE.

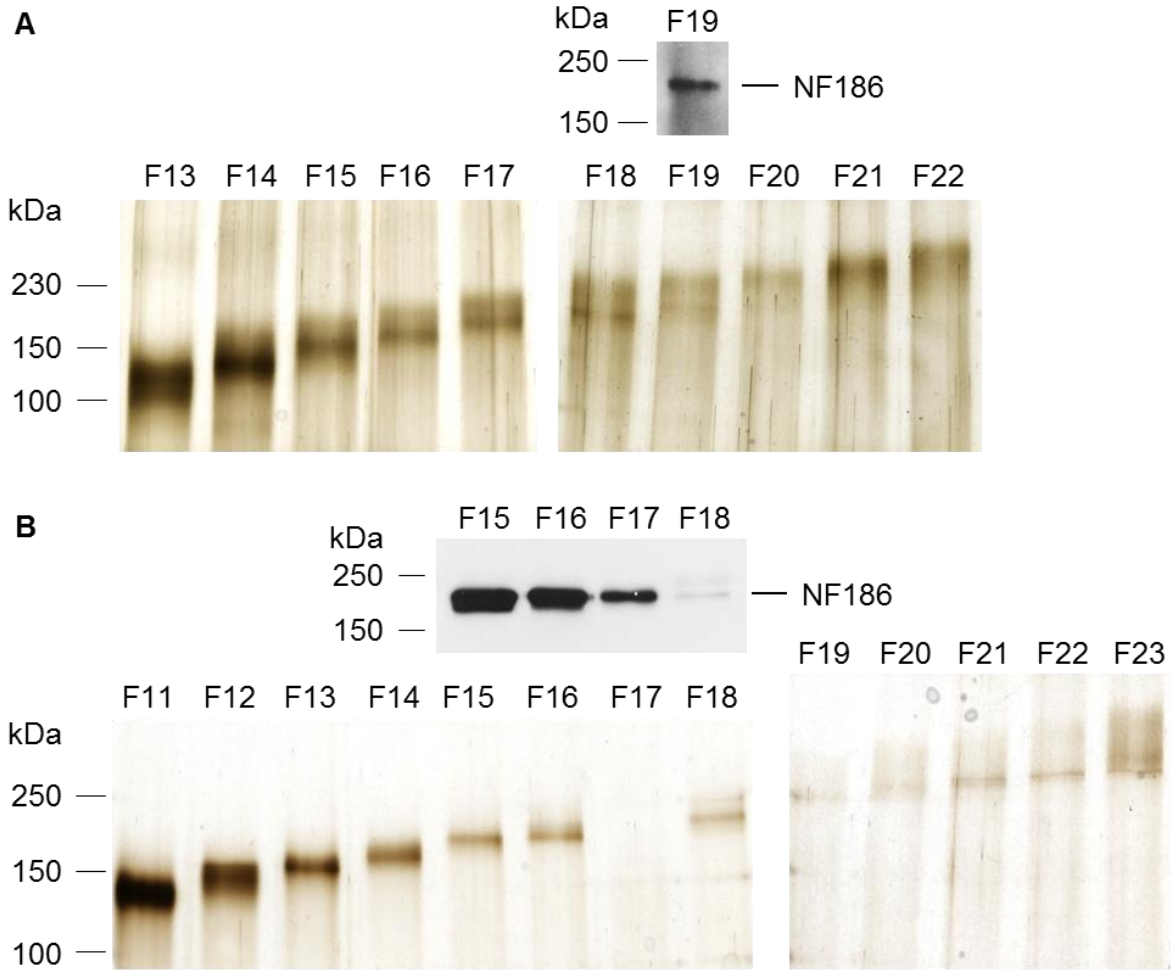

Figure 31: Protein fractions generated by preparative SDS-PAGE of mouse brain glycoproteins after GPC. Some of the protein-containing fractions of experiments (A) and (B) are depicted in silver-stained gels. Western blots against neurofascin show the presence of NF186 in F19 (A) and F15 to F17 (B).

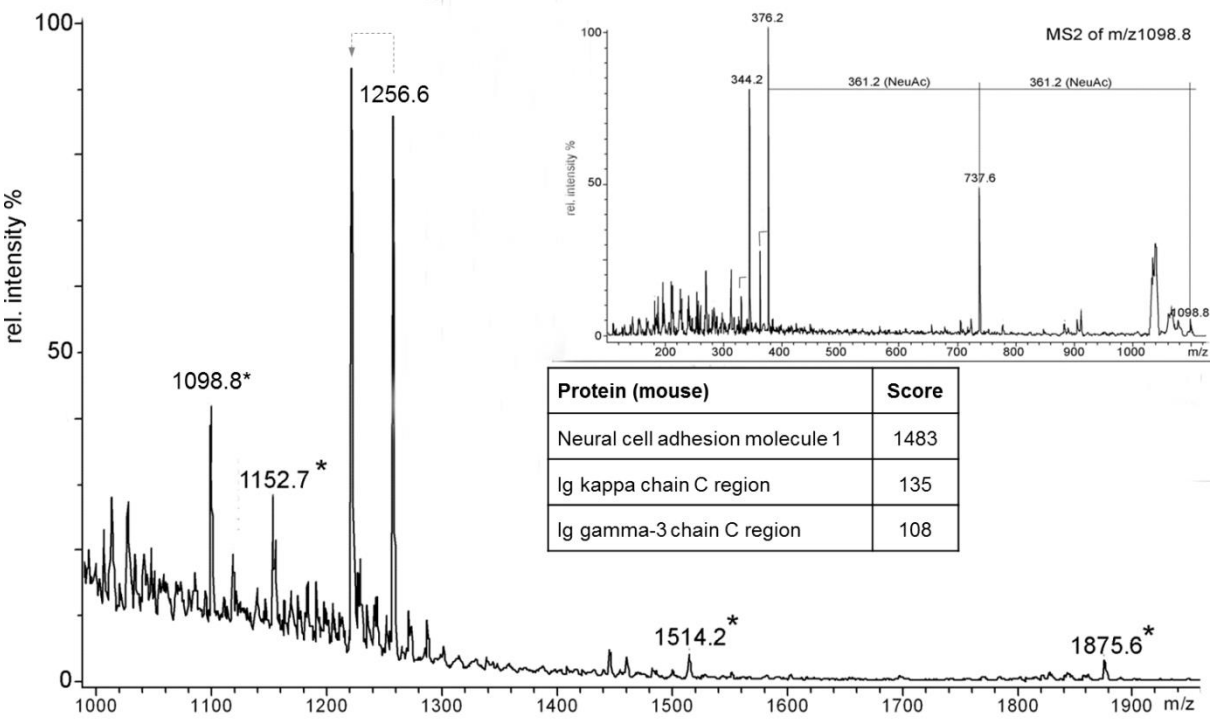

Figure 32: *O*-Glycan analysis of permethylated *O*-glycan alditols from mouse NCAM1. Dashed arrows indicate the loss of methyl and sodium (-36) and fragments of polysialic acid are indicated with a star. The monoisotopic signal at 1098.8 Da (see upper insert for MS/MS) corresponds to three neuraminic acid residues without a reduced end. The lower insert shows the Mascot results from the protein identification of this NCAM1 preparation.

Table 10: Protein identification of the neurofascin-containing fraction used for ESI-MS/MS of the CID mode. Shown are the Mascot scores.

Protein (mouse)	Score
Neurofascin	176
Neurocan core protein	152
Sodium/potassium-transporting ATPase subunit α-3	114
Neural cell adhesion molecule 1	114
Tenascin-R	90

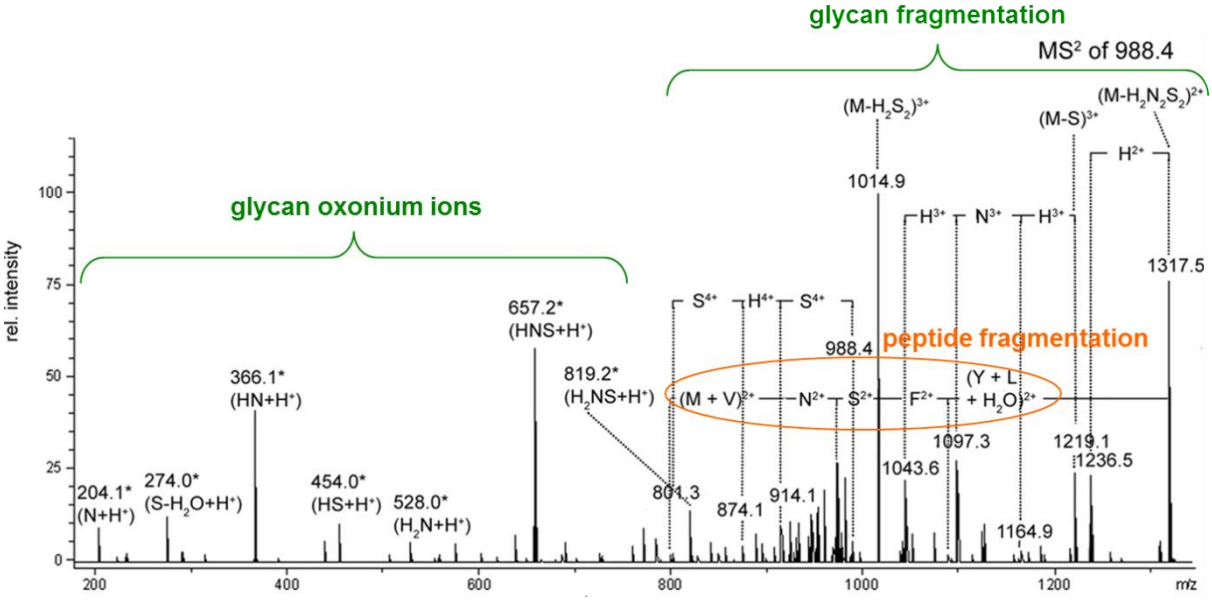

Figure 33: ESI-MS/MS (CID mode) of a glycopeptide from neurofascin. The *O*-mannosylated and mucin-type *O*-glycosylated glycopeptide LYFSNVMLQDMQTDYSCNAR is modified with NeuAcHexHexNAc and NeuAcHex$_2$HexNAc (m/z = 3950.6). Oxonium ions arising from glycan fragmentation are indicated with an asterisk. (H: hexose; N: HexNAc, S: Sialic acid).

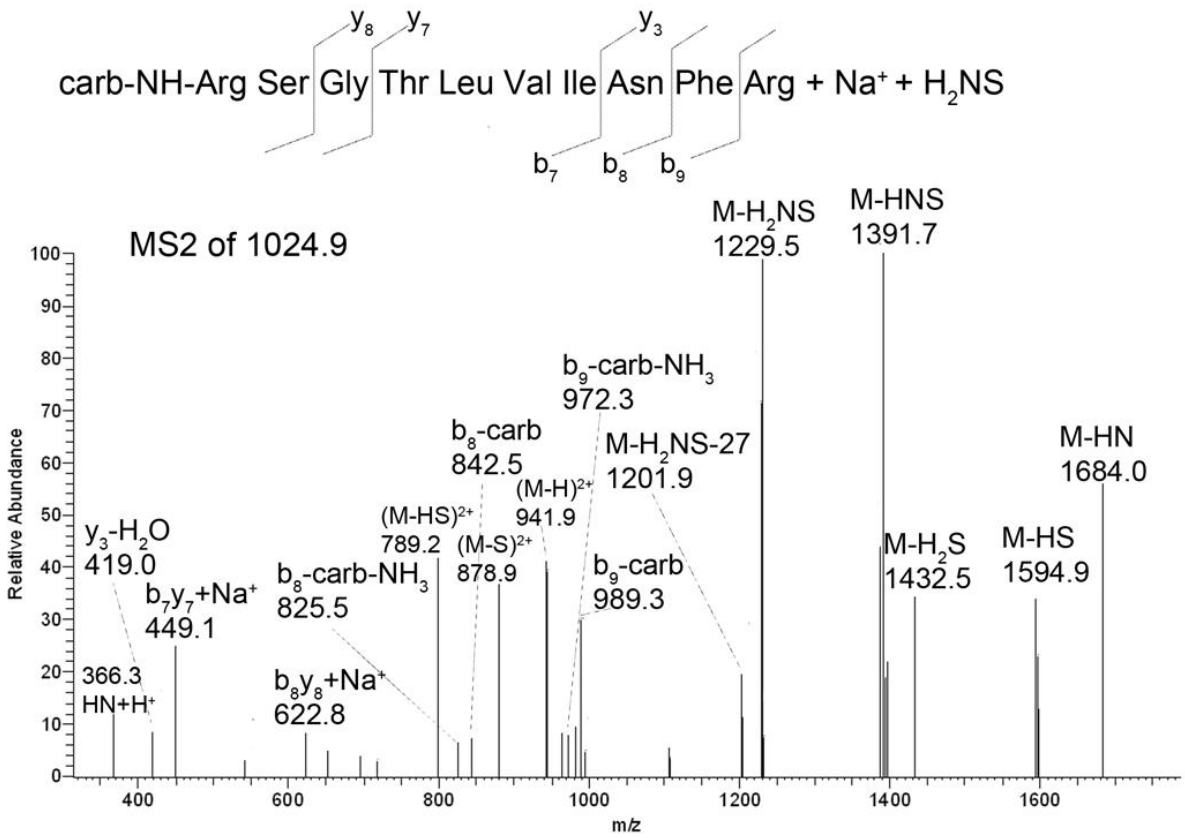

Figure 34: ESI-MS/MS of the *O*-mannosylated glycopeptide RSGTLVINFR from neurofascin modified with NeuAcHex$_2$HexNAc (m/z 2048.8). Several amino acid fragmentations can be observed within the MS/MS spectrum (H: hexose; N: HexNAc, S: Sialic acid).

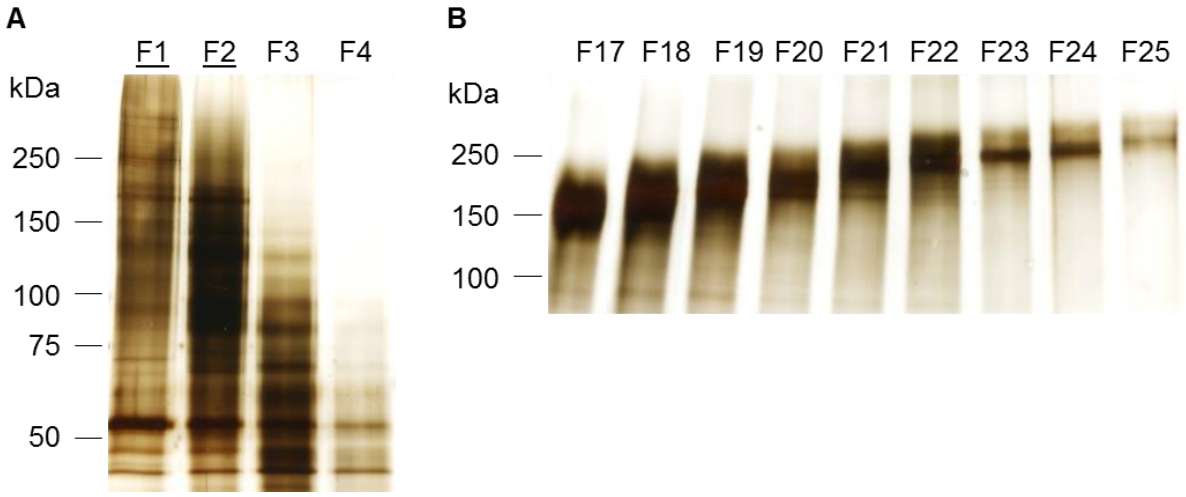

Figure 35: Silver-stained SDS-PAGE gels of the mouse brain glycoprotein fractionation. Depicted are the protein fractions after GPC (A) and after preparative gel electrophoresis (B). GPC fractions F1 and F2 (underlined) were subjected to preparative SDS-PAGE.

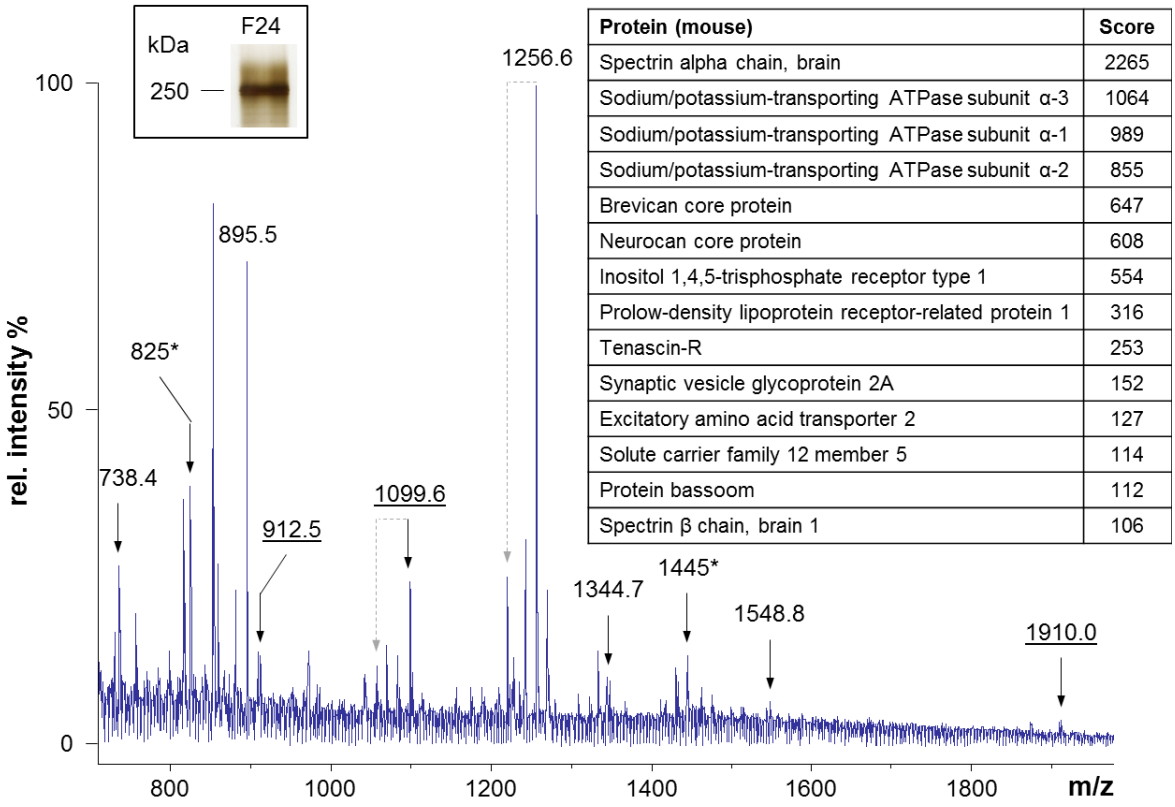

Protein (mouse)	Score
Spectrin alpha chain, brain	2265
Sodium/potassium-transporting ATPase subunit α-3	1064
Sodium/potassium-transporting ATPase subunit α-1	989
Sodium/potassium-transporting ATPase subunit α-2	855
Brevican core protein	647
Neurocan core protein	608
Inositol 1,4,5-trisphosphate receptor type 1	554
Prolow-density lipoprotein receptor-related protein 1	316
Tenascin-R	253
Synaptic vesicle glycoprotein 2A	152
Excitatory amino acid transporter 2	127
Solute carrier family 12 member 5	114
Protein bassoom	112
Spectrin β chain, brain 1	106

Figure 36: Analysis of fraction F24 from preparative gel electrophoresis of mouse brain glycoproteins. The MALDI-MS spectrum shows permethylated glycan alditols. Monoisotopic masses corresponding to *O*-mannosyl glycans are underlined. Signals derived from nonreduced *N*-glycan fragments are indicated with an asterisk, dashed arrows indicate the loss of methyl and sodium (-36).The left insert shows the silver stained SDS-PAGE of the fraction. The right insert shows the Mascot results of the protein identification by ESI-MS/MS.

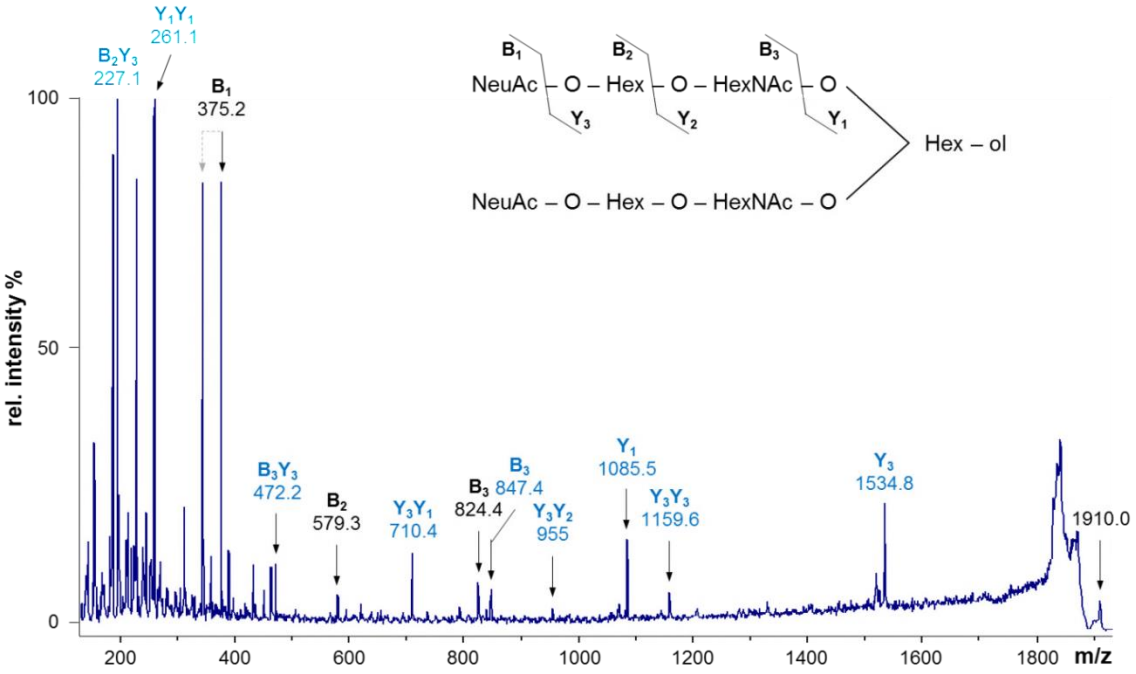

Figure 37: MALDI-MS/MS of the permethylated oligosaccharide with a precursor mass of 1910.0. The mass corresponds to the glycan composition $NeuAc_2Hex_3HexNAc_2$-ol + Na^+. The fragmentation pattern reveals a branched structure with a reduced core-hexose, indicating an *O*-mannosylated glycan. Signals superscripted in black resemble proton adducts while signals inscribed in blue are sodium adducts. The dashed arrow indicates a signal derived by a loss of 32 Da.

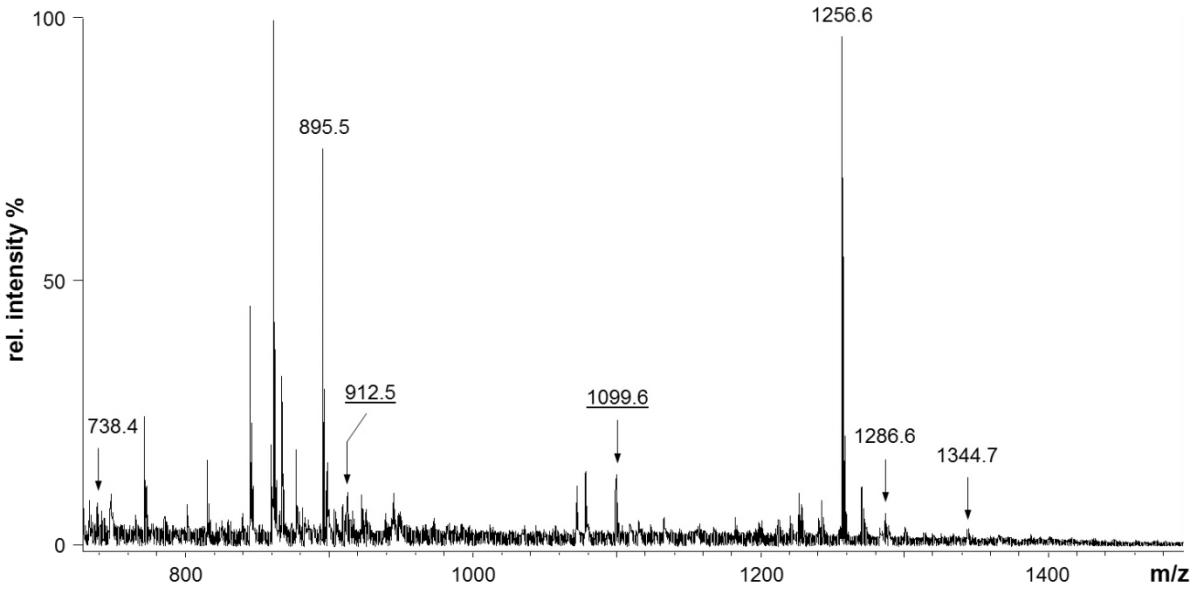

Figure 38: Analysis of the eluate from tenascin-R specific affinity chromatography. The MALDI-MS spectrum shows the permethylated glycan alditols. Monoisotopic masses corresponding to *O*-mannosyl glycans are underlined.

Table 11: Protein identification of the eluate from tenascin-R specific affinity chromatography. Shown are the Mascot scores.

Protein (mouse)	**Score**
Tenascin-R	2029
Brevican core protein	1078
Serine/arginine-rich splicing factor 4	357
Actin, aortic smooth muscle	322
Versican core protein	311
Neurocan core protein	304
Dihydropyrimidinase-related protein 2	234
Synapsin-1	217
Hemoglobin subunit β-1	163
Serine/arginine-rich splicing factor 2	163
Heat shock protein HSP 90-α	127
L-lactate dehydrogenase B chain	118
Pyruvate kinase isozymes M1/M2	113
Brain acid soluble protein 1	109
Tubulin α-1A	100

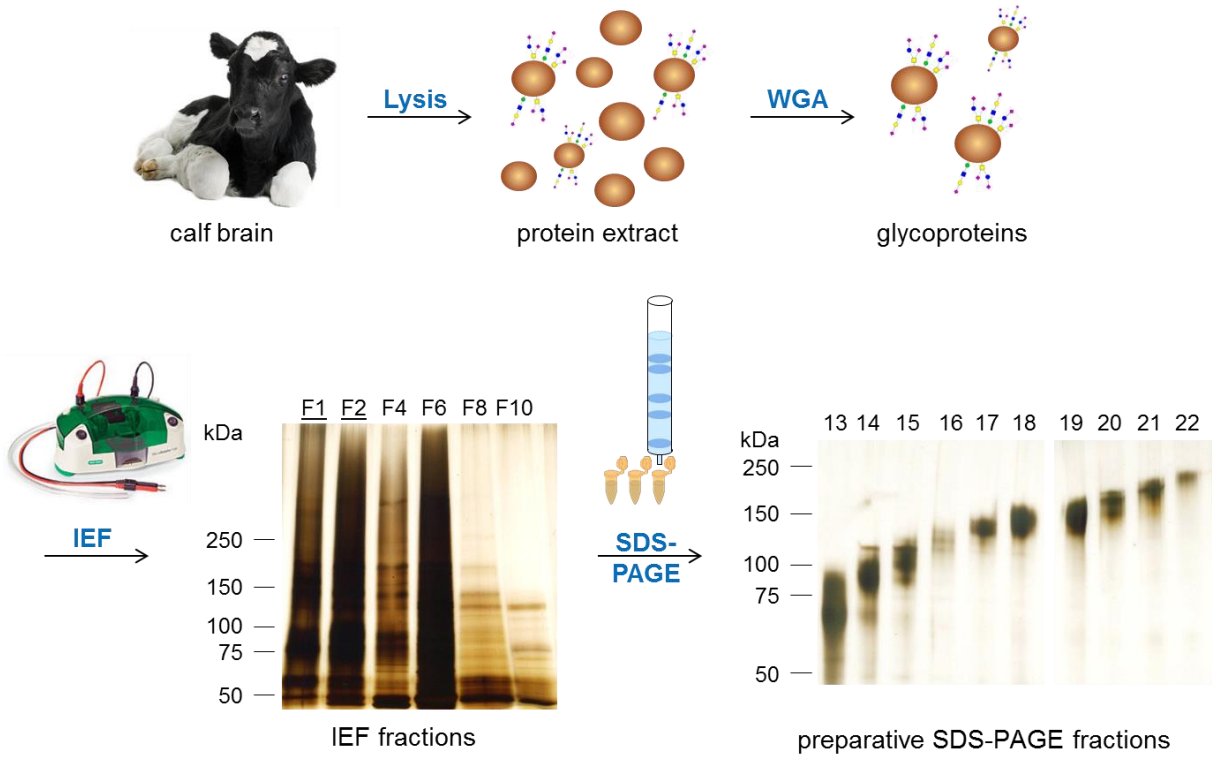

Figure 39: Fractionation scheme for calf brain. After the lysis of calf brain the glycoproteins are enriched using WGA affinity chromatography. These are prefractionated using free flow isoelectric focusing (IEF) and the proteins from IEF fractions F1 and F2 (underlined) are further fractionated by preparative SDS-PAGE. Exemplary SDS-PAGE gels (silver-stained) of the some IEF and some preparative SDS-PAGE fractions are shown.

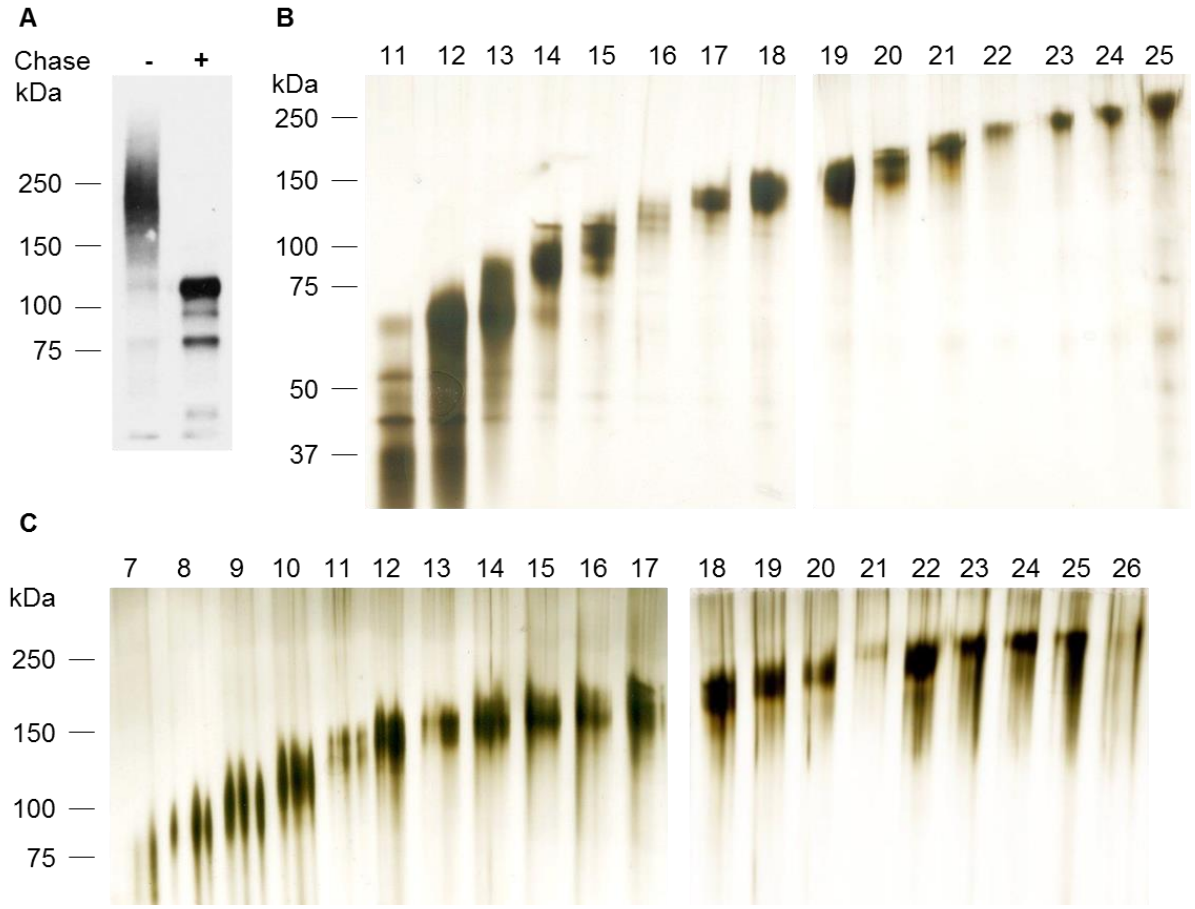

Figure 40: Calf brain-derived protein fractions generated by preparative gel electrophoresis. (A) Western blot of the WGA eluate from calf brain lysate with anti-neurocan antibody before (-) and after (+) treatment with chondroitinase ABC (Chase). (B) Silver-stained SDS-PAGE of the preparative gel electrophoresis fractions after isoelectric focusing (experiment A). (C) Silver-stained SDS-PAGE of the preparative gel electrophoresis fractions after isoelectric focusing (experiment B).

Table 12: Summary of lectican-containing calf brain fractions from experiments (A) and (B). Presence of lecticans, other known *O*-mannosylated proteins, other glycoproteins that have not been analyzed regarding potential *O*-mannosylation and other non-glycosylated proteins indicated. Abbreviations: B: brevican, N: neurocan, V, versican, D: dystroglycan, NF: neurofascin, P: phosphacan, Ra: RPTPα.

A	**F11**	**F12**	**F13**	**F17**	**F19**	**F20**
Lecticans	N	B, V	B, V	N	B, N, V	N, V
O-Mannosylated proteins	no	no	no	no	NF, P	NF, P
Glycoproteins	no	yes	no	no	yes	no
Other proteins	yes	yes	yes	yes	yes	yes
O-Mannosylation	yes	yes	yes	yes	yes	yes

B	**F8**	**F10**	**F11**	**F13**	**F14**	**F16**	**F18**
Lecticans	B, N, V	B, N, V	B, N, V	B, N, V	B, N, V	N, V	N, V
O-Mannosylated proteins	no	D	P, Ra	NF	NF	NF	no
Glycoproteins	yes	yes	yes	yes	yes	yes	no
Other proteins	yes	yes	yes	yes	yes	yes	yes
O-Mannosylation	yes	yes	yes	yes	yes	yes	yes

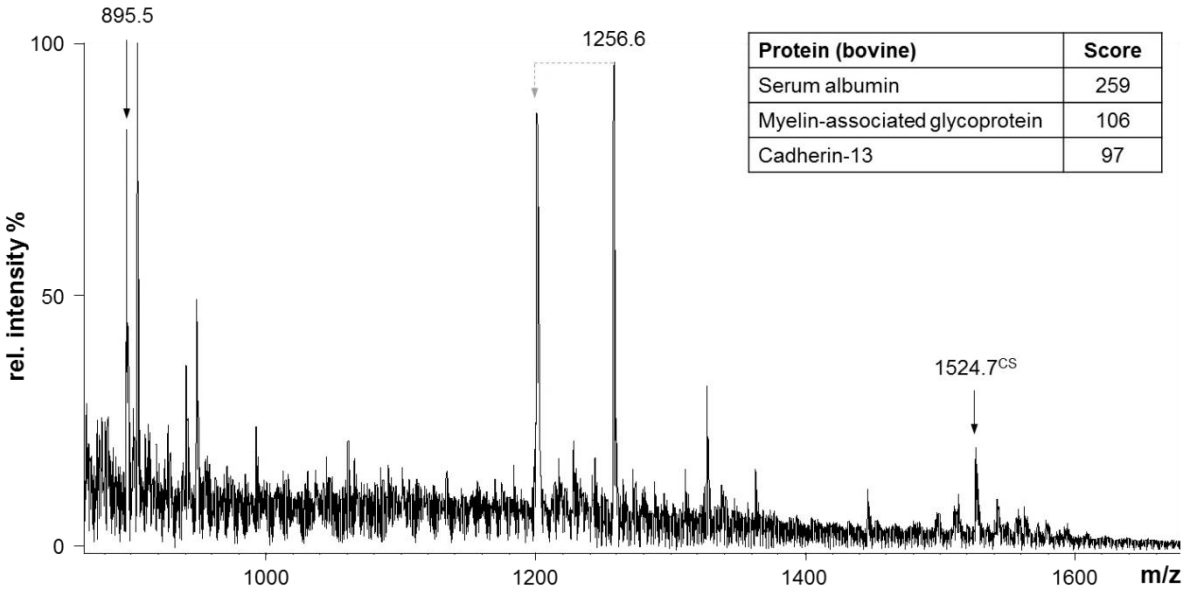

Figure 41: Analysis of the MAG-containing fraction F14 from experiment (A). The MALDI-MS spectrum shows the permethylated glycan alditols. Arrows indicate signals derived by a loss of a methyl group and sodium (-36 Da). Signals marked by CS are a result of unspecific cleavage of chondroitin sulfate chains. The insert shows the results of protein identification in the respective fraction by ESI-MS/MS.

Table 13: Protein identification based on Mascot score of the lectican-containing fraction F11 from experiment (A).

Protein (bovine)	Score
Serum albumin	996
Clusterin	709
Actin, cytoplasmic 1	401
Tubulin α-1B chain	217
Calmodulin	198
α-1-Acid glycoprotein	130
Apolipoprotein D	121
Neurocan core protein	102
Myelin basic protein	96
ATP synthase subunit δ, mitochondrial	93
CD99 antigen-like protein 2	92

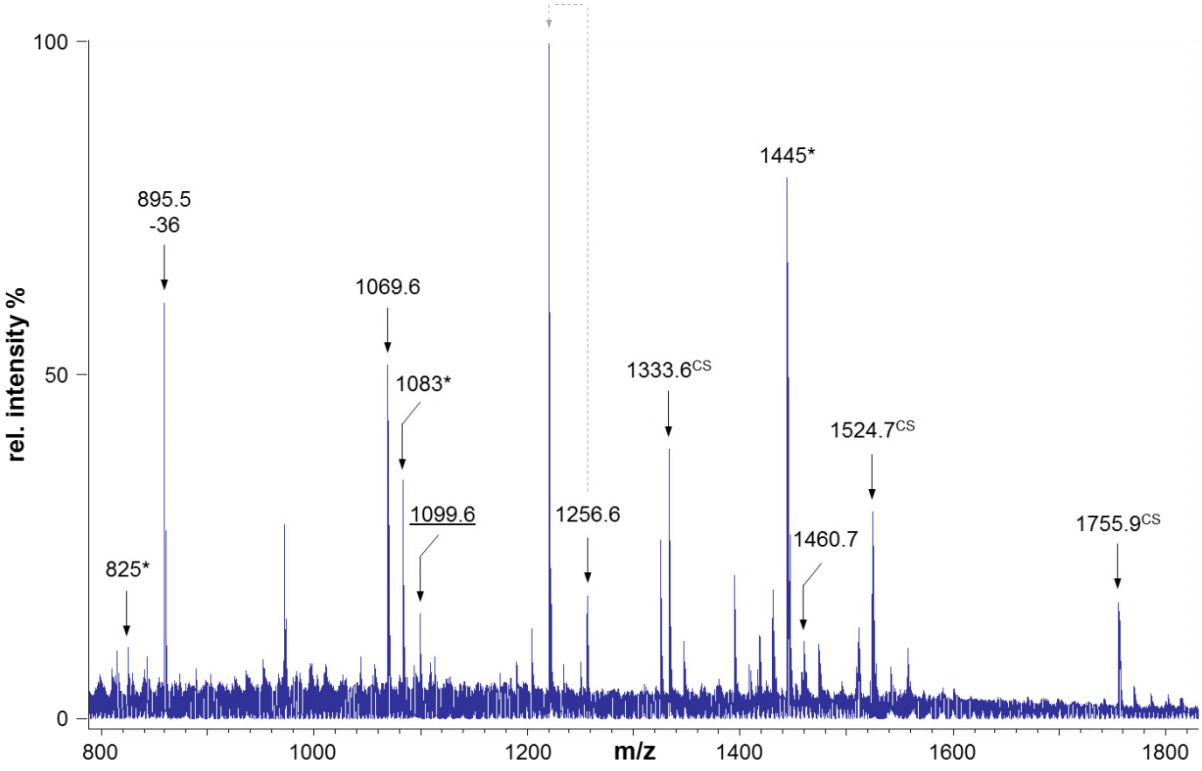

Figure 42: Analysis of the lectican-containing fraction F11 from experiment (A). The MALDI-MS spectrum shows the permethylated glycan alditols. Monoisotopic masses corresponding to *O*-mannosyl glycans are underlined. Glycan fragments without a reduced end are indicated with an asterisk, arrows indicate signals derived by a loss of a methyl group and sodium (-36 Da). Signals marked by CS are a result of unspecific cleavage of chondroitin sulfate chains.

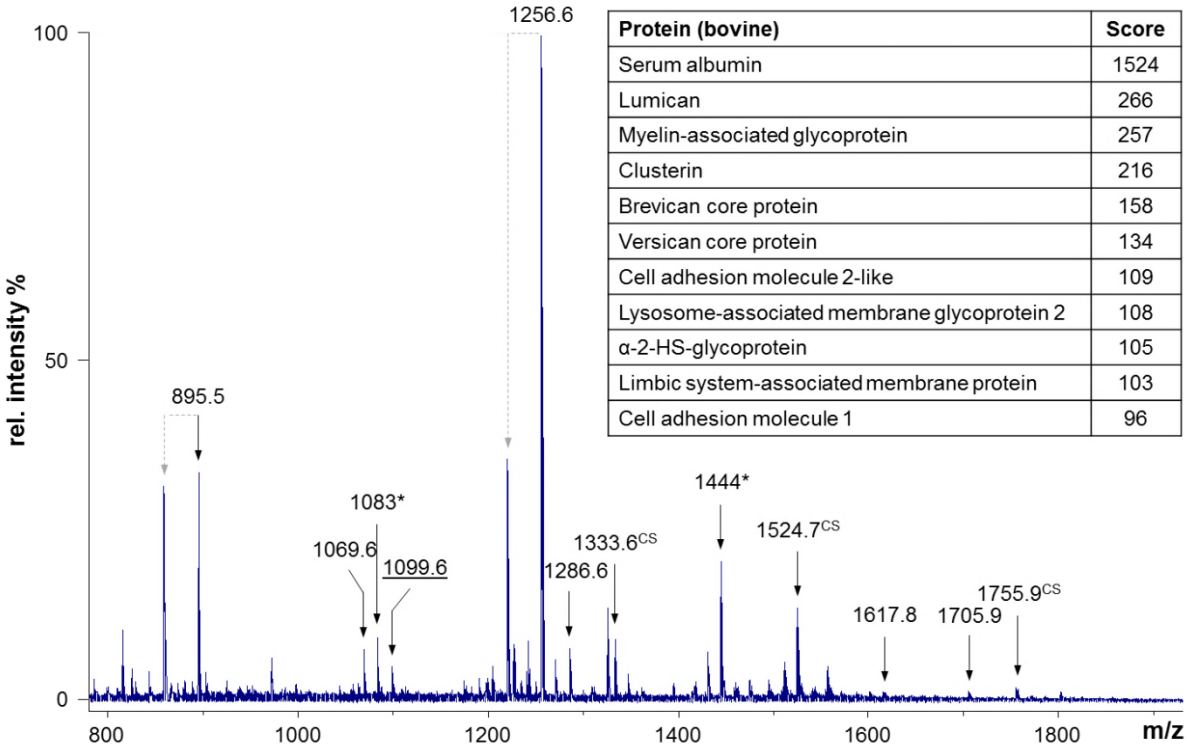

Protein (bovine)	Score
Serum albumin	1524
Lumican	266
Myelin-associated glycoprotein	257
Clusterin	216
Brevican core protein	158
Versican core protein	134
Cell adhesion molecule 2-like	109
Lysosome-associated membrane glycoprotein 2	108
α-2-HS-glycoprotein	105
Limbic system-associated membrane protein	103
Cell adhesion molecule 1	96

Figure 43: Analysis of the lectican-containing fraction F13 from experiment (A). The MALDI-MS spectrum shows the permethylated glycan alditols. Monoisotopic masses corresponding to *O*-mannosyl glycans are underlined. Glycan fragments without a reduced end are indicated with an asterisk, arrows indicate signals derived by a loss of a methyl group and sodium (-36 Da). Signals marked by CS are a result of unspecific cleavage of chondroitin sulfate chains. The insert shows the results of protein identification in the respective fraction by ESI-MS/MS.

Table 14: Summary of human phenotypes of dystroglycanopathies and phenotypes of the respective knockout in mice.

Protein	POMT1	POMGnT1	LARGE	Fukutin	FKRP
Human phenotype	early death (12 months), MD, severe eye and brain malformations	early death (12 years), MD, eye and brain malformations	MD, eye malformations, abnormal neuronal migration	wide range of phenotypes, MD, eye malformations, mental retardation	wide range of phenotypes, milder MD, brain malformations
Disease	WWS	MEB	MDC1D, WWS	FCMD, WWS, MEB	LGMD, MDC1C
Phenotype of knockout mice	embryonic lethality	viable, MD, CNS abnormalities, neuronal migration abnormalities	reduced lifespan, MD, neuronal migration abnormalities, retinal and peripheral nerve defects	embryonic lethality	reduced lifespan, neuronal migration abnormalities

Table 15: Summary of characteristics of previously known *O*-mannosylated proteins.

Protein	CD24	α-DG	Phosphacan	RPTPβ
Expression	widely expressed (blood cells, brain, muscle)	widely expressed (skin, brain, muscle)	CNS	CNS
Localization	membrane (GPI)	secreted	secreted	membrane (single pass)
Glycosylation	extensive *O*-gl	*O*- and *N*-gl	CS-GAG, *N*- and *O*-gl	CS-GAG, *N*- and *O*-gl
Domains	rich in Ser and Thr	mucin	α-carbonic anhydrase, FNIII	α-carbonic anhydrase, FNIII
Phenotype of knockout mice	mild phenotype	full KO: embryonic lethality brain-specific KO: abnormalities in nerve and muscle structure	no phenotype observed	

Table 16: Summary of characteristics of newly identified *O*-mannosylated proteins.

Protein	Neurofascin 186	Aggrecan	Brevican	Neurocan	Versican
Expression	CNS (neurons)	mainly in cartilage	brain	brain	widely expressed V2 only in brain
Localization	membrane (single pass)	secreted	secreted or membrane (GPI)	secreted	secreted
Glycosylation	*O*- and *N*-gl	CS- and KS-GAG, *N*- and *O*-gl	CS-GAG, *N*- and *O*-gl	CS-GAG, *N*- and *O*-gl	CS-GAG, *N*- and *O*-gl
Domains	Ig-like, FNIII, mucin	Ig-like, C-type lectin, Link, Sushi	Ig-like, EGF, C-type lectin, Link, Sushi	Ig-like, EGF, C-type lectin, Link, Sushi	Ig-like, EGF, C-type lectin, Link, Sushi
Phenotype of knockout mice	reduced life span, drastically reduced conduction velocities	embryonic lethality, dwarfism	no phenotype	no phenotype	full KO: embryonic lethality V2 KO: altered ECM at nodes of Ranvier

Erklärung

Ich versichere, dass ich die von mir vorgelegte Dissertation selbständig angefertigt, die benutzten Quellen und Hilfsmittel vollständig angegeben und die Stellen der Arbeit − einschließlich Tabellen, Karten und Abbildungen −, die anderen Werken im Wortlaut oder dem Sinn nach entnommen sind, in jedem Einzelfall als Entlehnung kenntlich gemacht habe; dass diese Dissertation noch keiner anderen Fakultät oder Universität zur Prüfung vorgelegen hat; dass sie − abgesehen von unten angegebenen Teilpublikationen − noch nicht veröffentlicht worden ist sowie, dass ich eine solche Veröffentlichung vor Abschluss des Promotionsverfahrens nicht vornehmen werde. Die Bestimmungen der Promotionsordnung sind mir bekannt. Die von mir vorgelegte Dissertation ist von Dr. Isabelle Breloy und Prof. Dr. Mats Paulsson betreut worden.

Nachfolgend genannte Teilpublikationen liegen vor:

Pacharra S, Hanisch FG, Breloy I (2012): Neurofascin 186 is O-mannosylated within and outside of the mucin domain. *J. Proteome Res.* **11**, 3955-64.

Pacharra S, Hanisch FG, Mühlenhoff M, Faissner A, Rauch U, Breloy I (2013):The lecticans of mammalian brain perineural net are O-mannosylated. *J. Proteome Res.* **12**, 1764-71.

Sandra Pacharra